UNIVERSITY OF GAZIANTEP
GRADUATE SCHOOL OF
NATURAL & APPLIED SCIENCES

IMPROVING THE DUCTILITY PROPERTIES OF
LIGHTWEIGHT CONCRETES BY STEEL FIBER ADDITION

M.Sc. THESIS
IN
CIVIL ENGINEERING

BY

SÜLEYMAN İPEK

JANUARY 2013

Improving the Ductility Properties of Lightweight Concretes by Steel Fiber Addition

M.Sc. Thesis

in

Civil Engineering

University of Gaziantep

Supervisor

Assoc. Prof. Dr. Erhan GÜNEYİSİ

by

Süleyman İPEK

January 2013

REPUBLIC OF TURKEY
UNIVERSITY OF GAZİANTEP
GRADUATE SCHOOL OF NATURAL & APPLIED SCIENCES
CIVIL ENGINEERING DEPARTMENT

Name of the thesis: Improving the Ductility Properties of Lightweight Concretes by Steel Fiber Addition

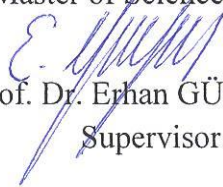Name of the student: Süleyman İPEK

Exam date: January 22, 2013

Approval of the Graduate School of Natural and Applied Sciences

Assoc. Prof. Dr. Metin BEDİR
Director

I certify that this thesis satisfies all the requirements as a thesis for the degree of Master of Science.

Prof. Dr. Mustafa GÜNAL
Head of Department

This is to certify that we have read this thesis and that in our opinion it is fully adequate, in scope and quality, as a thesis for the degree of Master of Science.

Assoc. Prof. Dr. Erhan GÜNEYİSİ
Supervisor

Examining Committee Members	Signature
Prof. Dr. Turan ÖZTURAN	
Assoc. Prof. Dr. Mehmet GESOĞLU	
Assoc. Prof. Dr. Erhan GÜNEYİSİ	

I hereby declare that all information in this document has been obtained and presented in accordance with academic rules and ethical conduct. I also declare that, as required by these rules and conduct, I have fully cited and referenced all material and results that are not original to this work.

Süleyman İPEK

ABSTRACT

Improving the Ductility Properties of Lightweight Concretes by Steel Fiber Addition

İPEK, Süleyman

M.Sc. in Civil Engineering

Supervisor: Assoc. Prof. Dr. Erhan GÜNEYİSİ

January 2013, 103

In this study, the mechanical and fracture properties of the cold bonded fly ash lightweight aggregate concretes (LWACs) with and without steel fiber were experimentally investigated. The LWAC with a constant water-to-cement ratio of 0.40 and 400 kg/m^3 cement content were produced with two different volume fraction of artificial fly ash lightweight aggregates. Three types of hooked-end steel fibers with the aspect ratios of 55, 65, and 80 were utilized with four different volume fractions of 0.35, 0.70, 1.00, and 1.50% of concrete volume. The effectiveness of aspect ratio, steel fiber volume fraction, and lightweight aggregate volume fraction on the compressive, splitting tensile, flexural and bond strengths, modulus of elasticity, fracture energy and characteristic length of concrete were investigated at the end of 28-days of water curing. The results have revealed that utilization of steel fiber enhanced splitting tensile, flexural, bond strengths of LWACs. The compressive strength, however, were not affected significantly by the steel fiber addition. The utilization of steel fiber considerably increased the fracture energy and characteristic length. Moreover, the compressive, splitting tensile, flexural and bond strengths, fracture energy, and characteristic length were significantly influenced by the artificial fly ash lightweight aggregate content.

Keywords: Concrete; Fracture properties; Lightweight cold-bonded fly ash aggregate; Mechanical properties; Steel fiber.

ÖZET

Çelik lif kullanılarak hafif betonların süneklik özelliklerinin iyileştirilmesi

İPEK, Süleyman

Yüksek lisans tezi, İnşaat Mühendisliği

Danışman: Doç. Dr. Erhan GÜNEYİSİ

Ocak 2013, 103

Bu çalışmada, çelik lifsiz ve çelik lifli soğuk bağlama yöntemi ile üretilmiş uçucu kül hafif agregası içeren betonların mekanik ve kırılma özellikleri deneysel olarak incelenmiştir. Hafif agregalı betonlar, iki farklı yapay hafif agrega hacimsel oranı ile 0.40 su çimento oranı ve 400 kg/m^3 çimento dozajında üretilmiştir. Üç farklı narinlik oranına sahip (L/d); 55, 65 ve 80, kanca uçlu çelik lifler beton hacminin yüzdece 0.35, 0.70, 1.0 ve 1.5'i olmak üzere dört farklı hacimsel oranda betonlara katılmıştır. 28 günlük su kürü sonrası, hafif agrega hacim oranının, çelik lif narinlik ve hacim oranlarının betonun basınç, yarmada çekme, eğilmede çekme ve beton ile donatı arasındaki aderans dayanımları, elastisite modülü, kırılma enerjisi ve karakteristik boyu üzerindeki etkisi incelenmiştir. Sonuçlar çelik lif kullanımının betonun yarmada çekme, eğilmede çekme ve beton ile donatı arasındaki aderans dayanımlarını iyileştirdiğini göstermiştir. Ancak basınç dayanımı çelik lif kullanımından çok fazla etkilenmemiştir. Karakteristik boy ve kırılma enerjisi çelik lif kullanımından önemli bir şekilde etkilenmiştir. Ayrıca, basınç, yarmada çekme, eğilmede çekme, ve beton ile donatı arasındaki aderans dayanımları, kırılma enerjisi ve karakteristik boy hafif agrega hacimsel oranından önemli bir ölçüde etkilenmiştir.

Anahtar Kelimeler: Beton; Kırılma özellikleri; Soğuk bağlanmış hafif uçucu kül agregası; Mekanik özellikler; Çelik lif.

To my beloved cousin,

Vedat Aydın IPEK

ACKNOWLEDGEMENTS

CONTENTS

LIST OF FIGURES

xi

LIST OF TABLES

LIST OF SYMBOLS

K_{IC}^{S}	Critical stress intensity factor
f_t'	Direct tensile strength
ACI	American Concrete Institute
ASTM	American Society for Testing and Materials
CLA	Crushed limestone aggregate
$CTOD_c$	Critical crack tip opening displacement
E	Modulus of elasticity
ECM	Effective crack model
FA	Fly ash
f_c	Compressive strength
FCM	Fictitious crack model
FPZ	Fracture process zone
f_{st}	Splitting tensile strength
f_t	Tensile strength
G_F	Fracture energy
l_{ch}	Characteristic length
LEFM	Linear elastic fracture mechanics
LVDT	Linear variable displacement transducer
LWA	Lightweight aggregate
LWAC	Lightweight aggregate concrete
NWC	Normal weight concrete
SSD	Saturated surface dry
TPM	Two parameter model
V_f	Steel fiber volume fraction
τ	Bond strength

CHAPTER 1

1. INTRODUCTION

1.1.   General

Concrete has been used all over the world as a construction material for over a century and in everyday utilization areas are increasing and becoming more common. Concrete industry, evolving day by day, started construction life by the manufacturing of Portland cement. The biggest weakness of the concrete is low enough of tensile strength to be neglected. Besides, different performances are expected from concrete according to utilization field and structure. These expectations, however, can be met with special concretes. Special concretes are produced by different methods because of different needs. Concrete tensile strength increases by the addition of certain proportion of fibers into concrete, light and heavy weight concretes are produced by changing type, quantity and kind of aggregate, high-strength concretes are produced by using high-strength cement or pozzolans (Taşdemir et al., 2002).

Since the 1990s, lightweight concrete, which has a quite superior characteristics especially in terms of thermal insulation and unit weight compared to normal concrete, has begun to find using area with a rising trend (Gesoğlu, 2004). In the construction industry, versatile utilization of lightweight concrete produced mostly by variety of natural or artificial lightweight aggregate is becoming increasingly important. Weight of the structure is directly proportional to the loads of the building during earthquakes. In this context, earthquake resistance taking in terms of material; carrier structural elements with high strength, non-bearing structural elements with lightweight in terms of reduction the total weight of structure are aimed (ACI 213R, 2003). Namely, as the weight of structure decreases, the load acted during the earthquake will reduce. Fill and partition walls and slabs should be made of lightweight materials as possible to get lightweight reinforced concrete structure (Bayulke, 1998). Due to being directly proportional of the horizontal forces which

are effective in the construction of building with the collected mass arisen from slabs of building, the weight reduction in the slabs is quite important. In order to decrease the weight of slabs, unit weight of the concrete used in these slabs should be decreased. Concrete consists of cement, aggregate, water and sometimes chemical and mineral additives and mostly it is considered as two-phase composite materials consisting of aggregate and cement mortar. However, the mechanical behavior of this composite is strongly influenced by the interface of the micro-structure occurred between coarse aggregate particles and cement mortar (Alexander et al., 1992; Taşdemir et al., 1998). Adherence cracks formation in the interface between aggregate and mortar is an important factor that determines the non-elastic deformation and fracture behavior of concrete (Hsu et al., 1963; Shah and Winter, 1966; Büyüköztürk et al., 1971). During the collapse, the progression of adherence cracks in the normal strength concrete occur mostly the interface between aggregate and significant energy is absorbed. In the high strength concrete, however, the interface between mortar and aggregate is more intense and powerful than normal strength concrete and the cracks generally spread by cutting the weaker aggregate grains (Lee et al., 1992; Trende and Büyüköztürk, 1998). The interface is the weakest link in the ternary system consisting of aggregate-interface-cement mortar. However, the micro-structure strengthening and intensifying with the use of silica fume in this region is said (Taşdemir and Taşdemir, 1996; Taşdemir et al., 1999). On the other hand, coarse aggregate type and surface roughness of aggregate utilized in the concrete significantly effects the interfacial properties and therefore the mechanical properties and fracture behavior of concrete (Lee and Büyüköztürk, 1995)

The understanding the mechanism of crack progress in the interface between aggregate and mortar has a great importance for the examination of mechanical behavior and fracture process in concrete. Two different crack propagation scenarios can occur depending on the strength of mortar and aggregate properties in the interface. If the aggregate particle is weaker than adhesion strength in the interface, the crack will proceed through the aggregate and the effect of interfacial features to the fracture behavior will be very little. But otherwise the crack will go on changing direction from the surface of aggregate or will spread into the mortar. In both cases, a higher energy will be absorbed.

In the researches, natural aggregates with different physical and mineralogical characteristics were utilized with normal and high strength mortars. In the studies conducted on lightweight concrete has shown that the strength and microscopic structure of aggregate are an important factor affecting the mechanical properties of concrete (Zang and Gjory, 1991; Wasserman and Bentur, 1997). When the artificial aggregate with higher strength and more intensive than mortar phase is used in the lightweight aggregate concretes, the behavior of these concretes resemble to the normal strength concrete, but when the aggregate with weaker and more permeable condition is used, the concretes behave like high strength concrete and the aggregates become the weakest link (Zang and Gjory, 1990). The studies investigating the fracture parameters of lightweight aggregate concretes are very limited (Chang and Shieh, 1996). It is specified that lightweight concretes are usually broken within aggregate in the experiments carried out by size effect method and to improve the ductility the use of steel fiber is recommended (Chang and Shieh, 1996). Some materials are added to concrete in order to improve the weak mechanical properties of concrete. Fibers are one of these materials. The main aim of the producing fiber reinforced concretes is that increasing the toughness, resistance against impact loads, flexural strength, etc. of material.

Adherence behavior between concrete and reinforcement steel needs to be well understood for more commonly utilization of lightweight concrete as structural purpose. Despite this reality, the necessary interest is not shown on the adherence properties in this type of concretes and the studies are limited (Mayfield and Loutai, 1990; Mor, 1992). It is indicated in previous study, deterioration of engagement between concrete and reinforcement steel is due to generally weakness of aggregate (Robins and Austin, 1986). While the ideal behavior of reinforced concrete elements is showing limited stress-strain behavior, it is suggested that does not exceed the adhesion capacity between concrete and reinforcement steel. However, due to the above mentioned results, the use of this type of concrete in the reinforced concrete elements is limited and providing the longer clamping length than normal concretes is obliged.

1.2.   Research Significance

In this thesis, the mechanical and fracture properties of concretes produced with cold bonded fly ash lightweight aggregate were investigated. The modulus of elasticity, compressive, splitting tensile, and flexural strengths are studied for mechanical properties of concrete. Fracture mechanic parameters such as fracture energy and characteristic length are determined for fracture properties. Moreover, the adherence between concrete and reinforcement steel were examined to utilize of this type of concrete for structural purposes. To improve the mechanical behavior and fracture properties of lightweight concretes manufactured by two different volume fractions (45% and 60%) of lightweight aggregates, steel fibers were added to lightweight concretes with 3 different aspect ratios (55, 65, and 80) and 4 different volume fractions (0.35%, 0.70%, 1.00%, and 1.50%) of concrete volume. Totally, 26 concrete mixtures with constant water-to-cement ratio (w/c) of 0.40 were produced to investigate for mentioned properties at the end of 28-day water curing period.

1.3.   Outline of the thesis

Chapter 1-Introduction: Aim and objectives of the thesis are introduced.

Chapter 2-Literature review: A literature survey was conducted on cold bonded fly ash lightweight aggregates and steel fiber. The previous studies on the use of lightweight aggregates and steel fiber in concrete are presented.

Chapter 3-Experimental study: Materials, mixtures, casting, curing conditions, and test methods are described.

Chapter 4-Test results and discussions: Indication, evaluation, and discussion of the test results are presented.

Chapter 5-Conclusion: Conclusion of the thesis and recommendation for future studies are given.

CHAPTER 2

2. LITERATURE REVIEW AND BACKGROUND

2.1. Fly Ash

Fly ash (FA), occurred as a result of combustion of pulverized coal at thermal power plants, is an important by-product and the most widely supplementary cementitious material in concrete. When the coal is thrown in the furnace, due to ignition, most of the volatile matter and carbon are burned off. During combustion, the impurities in the coal fuse and by the moving of flue gases they are carried away from the combustion chamber. FA firms completely or partially spherical-shaped ash particles with the gas flowing of cooled molten material resulting from the combustion of coal at high temperatures. It is then collected at the cyclone and electro-filters by the moving with exhaust gases (Figure 2.1). FA is a finely divided powder resembling Portland cement (Pandey et al., 2011).
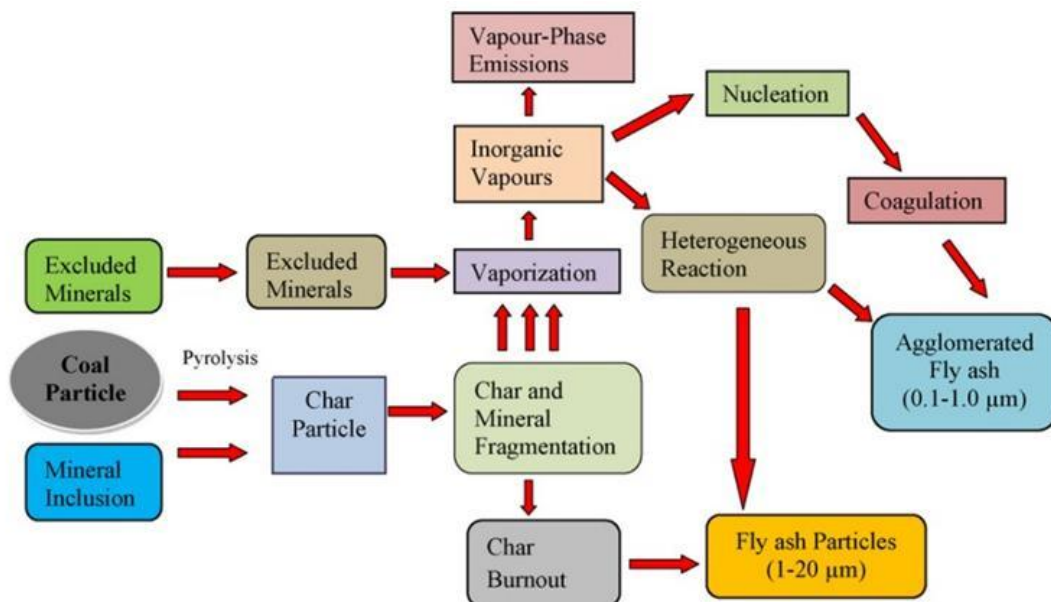
Figure 2.1 A schematic diagram of fly ash formation (reproduced from Pandey et al., 2011)

2.1.1. Classification of Fly Ash

Fly ash is classified with respect to ASTM C 618 according to its chemical compositions. In accordance with ASTM C 618, FA is divided into two class; Class F and Class C. Fly ashes produced from bituminous coal and having more than 70% of total $SiO_2+Al_2O_3+Fe_2O_3$ content fall in Class F. At the same time, this type of ashes is also known as low calcareous ash due to having less than 10% of CaO. Class F fly ashes have pozzolanic property. Class C fly ash is an ash, which produced from lignite or semi-bituminous coal and they have more than 50% of total $SiO_2+Al_2O_3+Fe_2O_3$ amount. These ashes are also named as calcareous fly ash because of having more than 10% of CaO. Class C fly ashes have binding character in addition to pozzolanic property (ASTM C 618, 2000).

2.1.2. Mineralogical Properties of Fly Ash

The sizes of fly ashes usually range between 0.5 and 200 microns and they are particles of glassy and mostly spherical character (Görhan et al., 2009). Although surface area of fly ashes generally range between 3000 and 5000 g/cm^2, some fly ashes have surfaces are as low as 2000 g/cm^2 as high as 7000 g/cm^2. The range of relative density (specific gravity) can be 1.9 to 2.8 (UM, 2012).
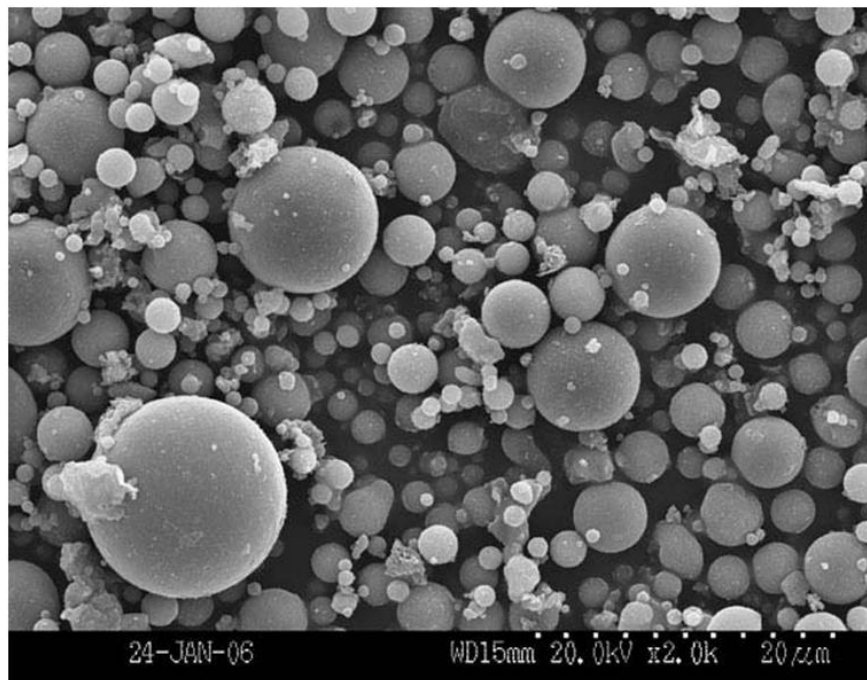
Figure 2.2 Fly ash particles (Kutahya Cement, 2012)

Morphology and structure of FA is variable and complex, and particle shape is spherical due to surface tension. Grain shape and size are affected by the cooling rate. Common type of FA is usually occurred in crystal compounds (such as quartz, mullite and hematite), glassy compounds (such as silica glass) and other oxides (Matsunaga et al., 2001).

Production and characteristics of FA depend on the power plant type, operating format, type of burned coal, the combustion format, the coal composition and combustion system (Xu, 1997; Güler et al., 2005). Properties of FA may vary even in the same plant due to download (Gikuno, 2004). The most obvious common feature of physical, chemical, mineralogical and pozzolanic properties of FA is that they can vary from region to region, even if they show variability in the same region (Güler et al., 2005).

2.1.3. Chemical Properties of Fly Ash

The main components of FA are silica (SiO_2), alumina (Al_2O_3), iron oxide (Fe_2O_3) and calcium oxide (CaO) and the amount of these components varies according to type of fly ash (Türker et al., 2003; Gikunoo, 2004). The amount of carbon contained in the fly ash shows variability according to coal type and combustion process (Güler et al., 2005). In addition, alkali oxides such as MgO and SO_3 are available in the fly ash as a minot component. There are basic oxides in the fly ash as rates of 25-60% SiO_2, 10-30% Al_2O_3, 1-15% Fe_2O_3 and 1-40% CaO. These different values characterize the type of FA (Türker et al., 2003), nevertheless the chemical structure of FA shows differentness due to the obtaining from different locations of coal. Despite this, silica and alumina are the main components of FA (Satapathy, 2000; Matsunaga et al., 2002)

2.1.4. Physical Properties of Fly Ash

Fly ash is very fine grained material. Colors of FA change from light gray to dark gray. The darkness and lightness of color depends on the obtained coal and burning property. Unburned carbon in the FA gives the black color due to the absence of complete combustion of coal. FA, obtained as a result of better combustion, is much lighter than another. Ashes, contain a large amount of carbon, is in dark gray color, while ashes, containing more iron, is in the light gray color.

Fly ash particles can be found different shapes such as spherical glassy particles, in solid or hollow, structures containing set of small spheres in a large sphere, structures containing irregular scattered and amorphous gaps on the surface, structures having liquid droplets on the surface, structures covered with crystal, deformed structures and structures having amorphous deposits on the surface (Yazıcı, 2004).

2.1.5. Utilization Areas of Fly Ash

In the world, manufactured FA amount is around 600 million tons per year. Less than 25% of the total produced FA is recycled in the world. The assessment rate according to the countries exhibit differences. More than 95% of the total produced FA is utilized in the Netherlands, Germany and Belgium, while about 50% of FA is used in the United Kingdom. Utilization percent is 32 and 40 in the United States and China, in where the large amount of FA is produced, respectively. In our country, the sufficient data on FA utilization is not found. In various publications, however, it is emphasized that the utilization of FA, in cement and concrete production, is approximately 5% and it is being used in place of aggregate or as a mineral admixture (Kutahya Cement, 2012). The remedies for the utilizations of FA wastes based on the properties of fly ash are presented in Figure 2.3 for the producers of thermal electricity (Wang and Wu, 2006).
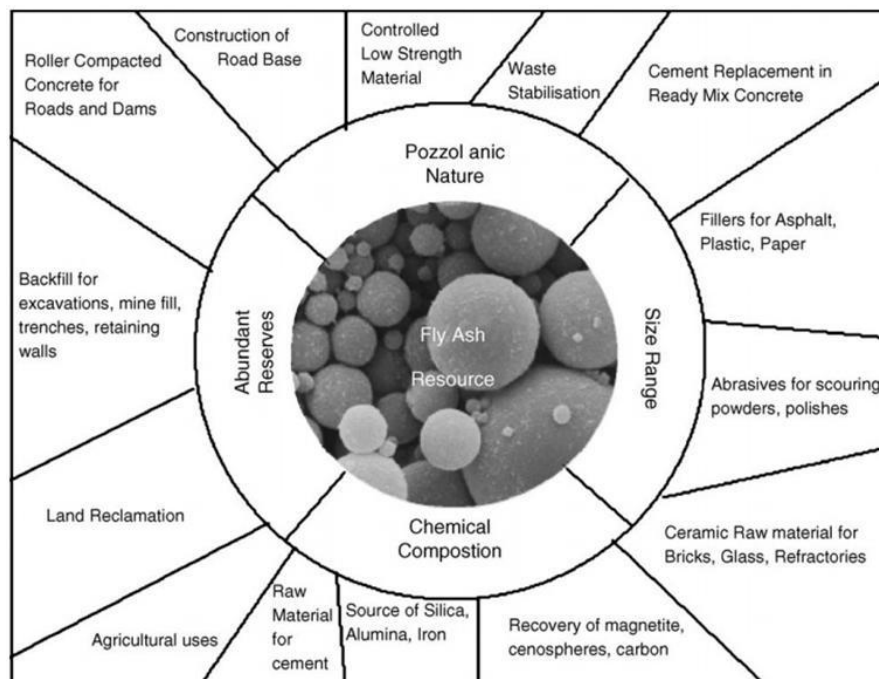
Figure 2.3 Possible fly ash utilization areas (reproduced from Wang and Wu, 2006)

The concrete and grout productions form the greatest part of the utilization area in both the United States and Europe. Figure 2.4 demonstrate the utilization areas in the United States for 2011 year, and in Europe for 2006 year.
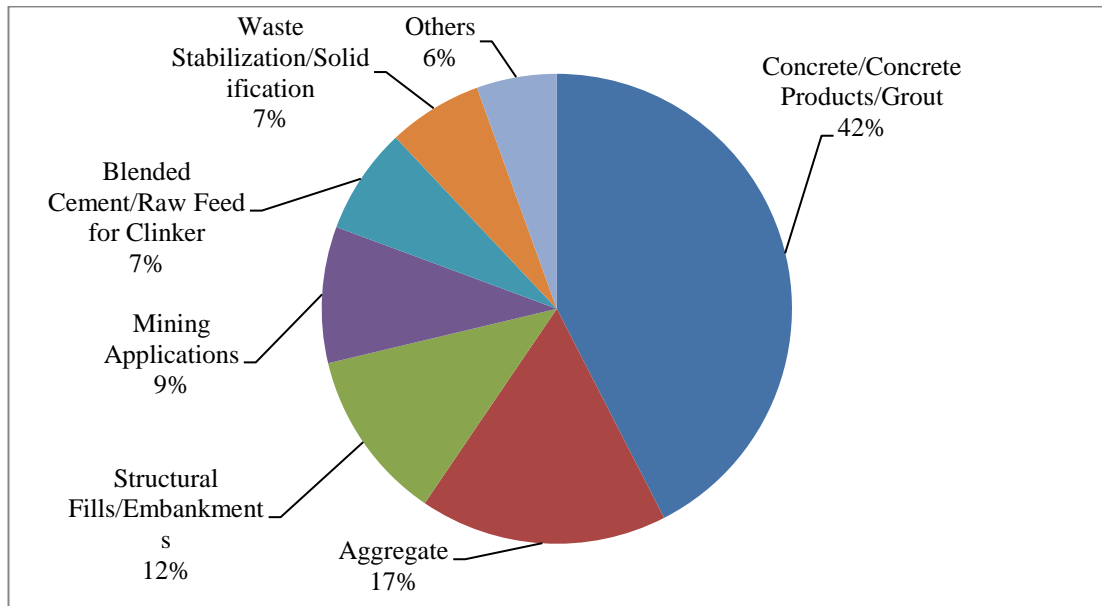
a)
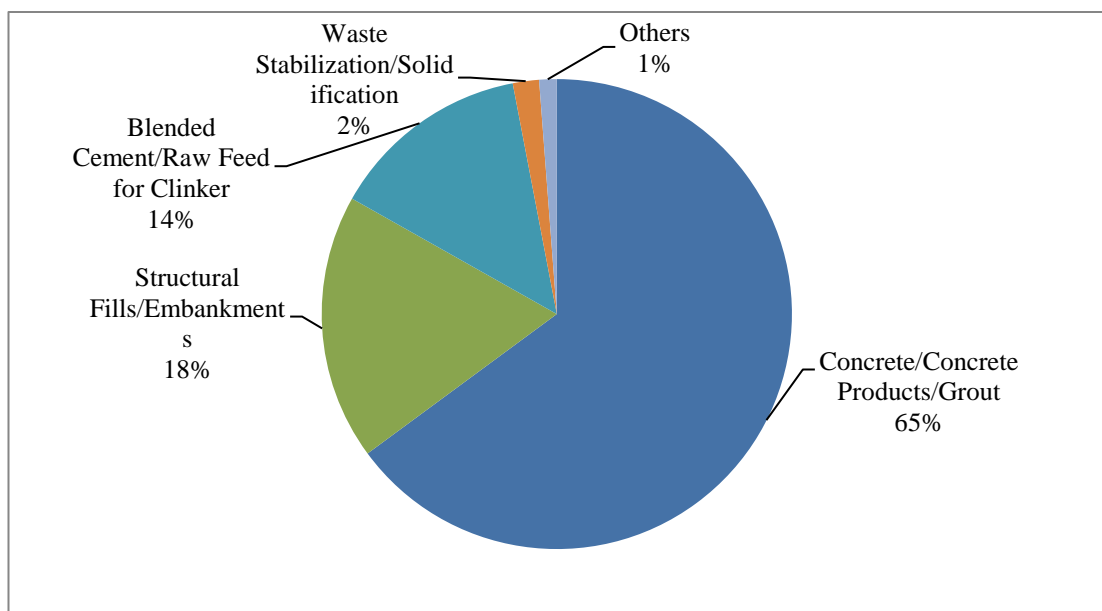
b)

Figure 2.4 Utilization areas of fly ash: a) in the United States (ACAA, 2011) and b) in Europe (ACAA, 2006)

2.2. Lightweight Aggregate

Lightweight aggregate is a granular material that has bulk density less than 1200 kg/m^3 or a particle density less than 2000 kg/m^3 (Gonzalez-Corrochano et al., 2009). Lightweight aggregates are generally classified with respect to production process and method. Lightweight aggregates can be manufactured from natural materials or artificial. Natural lightweight aggregates can be extracted from different types of geological materials, such as igneous rocks like pumice and tuffs (Riley, 1951; De'Gennaro et al., 2004) or sedimentary and metamorphic rocks, such as claystone, slate and shale (Conley et al., 1948; Dahab, 1980; Decleer and Viaene, 1993). Artificial lightweight aggregates are manufactured from wastes and industrial by-products such as glass, fly ash, and slag (Baykal and Döven, 2000; Videla and Matinez, 2002; Kim et al., 2005; Mahmood, 2012). Lightweight aggregates, both natural and artificial, should meet the requirements of ASTM C330.

2.2.1. Lightweight Aggregate Production with Fly Ash

Thermal coal-fired power plants generate large amounts of FA and only a very small proportion of FA is utilized in the worldwide for a various purposes. Large quantities of fly ash remain unutilized and unutilized FA leads to environmental damage by causing air and water pollution on a large scale (Babbitt and Linder, 2005; Soco and Kalembkiewicz, 2007; Koçkal and Özturan, 2010). Convenient way for recycling of FA is the lightweight aggregate production. In recent years, many attempts have been made for the utilization of FA for manufacturing the FA pellets and three methods, sintering, autoclaving and cold bonding, have been applied on the fresh pellets to harden them.

2.2.1.1. Sintering Method

Sintering is the one of the methods which has been used for producing lightweight FA aggregates since the early 1950s (Popovics, 1992). This method consists of many stages to get hardened lightweight fly ash aggregates. In first stage, fresh fly ash pellets are obtained by the mixing fly ash with water. This is followed by firing on a traveling grate or on a sintering strand to about 1260 °C. One advantage of using pulverized coal fly ash can be seen in this stage, the carbon in FA aids bring pellets to the sintering temperature and supplements the heat needed to evaporate the

moisture in them (Ramachandran, 1981; Koçkal and Özturan, 2010). After strand, the sintered pellets are separated. Aggregates, passing from 2.5 mm sieve, are pulled off and the others, remaining on 2.5 mm sieve, are used for the production of lightweight concretes (Ramadan, 1995; Gesoğlu, 2004).

2.2.1.2. Autoclaving (Hydrothermal Treating) Method

Fly ash pellets are hardened by using pressurized saturated steam curing and this application is known autoclaving (or hydrothermal treating). In the autoclaving method, 45% quartz sand, 47% fly ash, 4.5% lime, 2.0% additives and 1.5% water by weight are used to fly ash aggregates manufacturing. All of the mixture is pelletized and then heated in a high humidity environment and then heated for 6.5 hours at 200 °C to produce lightweight aggregate that finds its primary use in masonry units (Bremner and Thomas, 2004; Koçkal, 2008).

2.2.1.3. Cold Bonding Method

Cold bonding is a type of bonding which accounts for the capacity of fly ash to react with calcium hydroxide at ambient temperature to obtain a material having water resistivity bonding that accounts for the pozzolanic reactivity of fly ash. FA, Portland cement and water are used to produce pelletized or extruded aggregates, and they are cured for several days to produce an aggregate (Döven, 1996; Gesoğlu, 2004; Koçkal, 2008; Booya, 2012).

2.2.2. Pelletization Theory

Pelletization process is a well known technique for the production of artificial aggregates in the world. Although this technique was enhanced in 1940's, it has not been widely used in the construction sector. Properties of the pelletized material, the amount of moisture in the medium, and the mechanical process parameters such as the angle of rotating disc to the normal and the revolution speed are the functions that affect the performance of pelletization process (Baykal and Döven, 2000).

When a fine-grained material is humidified, a slim moist film is formed on the surface of particles. Structures like bridges are shaped a meniscus or crescent among fragments by this film (Figure 2.5 a). By the revolving the particles in a balling disc,

the sphere shaped structures are formed with the enhanced bonding forces between particles owing to centrifugal and gravitated forces (Figure 2.5 b and c) (Baykal and Döven, 2000). During the pelletization, the airs among the grains are being expelled by the developed force on the pellets, and the free spaces are being filled with water as well as grains. When the particles and water fill the airs between grains, the pellet become denser. A denser pellet means closer packed particles that enhance the structural coherence and create intensive and strengthened fresh pellets for handling and storing (Pietsch, 1991).
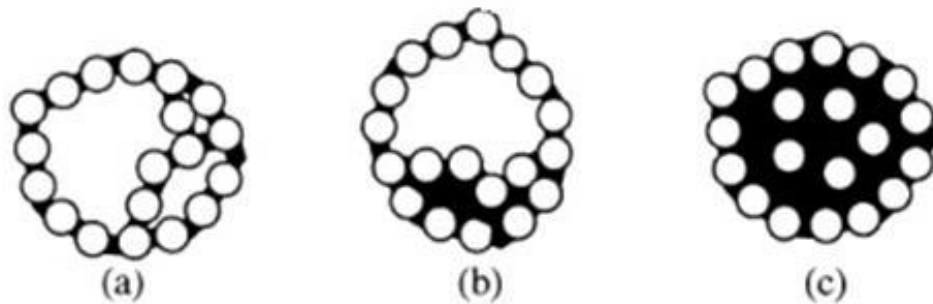
Figure 2.5 Mechanism of pellets formation (Baykal and Döven, 2000)

The amount of the cohesive forces applied on the grains during production and interlocking are the two factors determining the strength of the fresh pellets. The previous experimental studies are concluded that the maximum strength of the pellets can be achieved only if the all capillaries are filled with water in the production. The capillary forces and mechanical forces applied on the pellets are proportional with the coherence of the structure.

The filling of intergranular spaces with water is affected three stages in pelletization process (Döven, 1996; Gesoğlu, 2004);

- The pendular state, only the contact point of the particles has water,
- The funicular state, in addition to situations occurred in previous stage, the water fills some of pores completely, and
- The capillary state, the water fills all intergranular spaces completely and water film on the pellets surfaces does not exist.

The granulometric distribution of pelletized material is as well as excessive significance. During the pelletization, the granulometric distribution of pellets can be

arranged by controlling the water content and the feeding amount of binders. The optimum water content for fly ash is between 20% and 25% by weight. Figure 2.6 and 2.7 demonstrate mechanism of pellet formation at below optimum state and above optimum state. Below optimum state occurs when the moisture content is below optimum water content and above optimum state occurs when the moisture content is above optimum water content (Jaroslav and Rurickova, 1987).
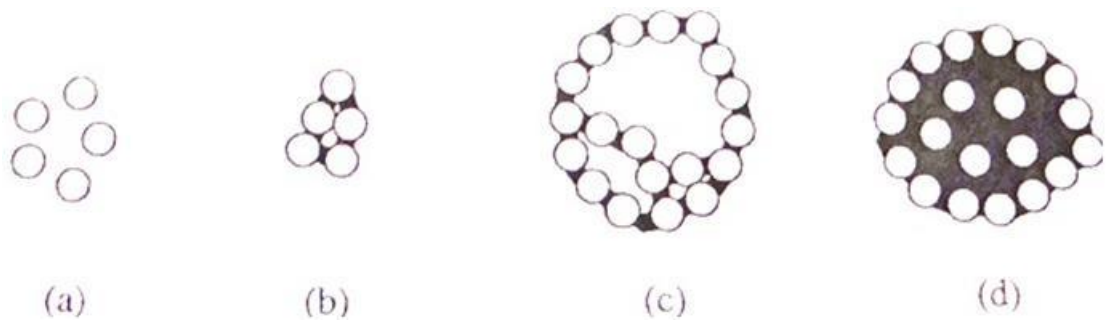
Figure 2.6 Mechanism of ball nuclei formation (water content below optimum state)
(Jaroslav and Rurickova, 1987)
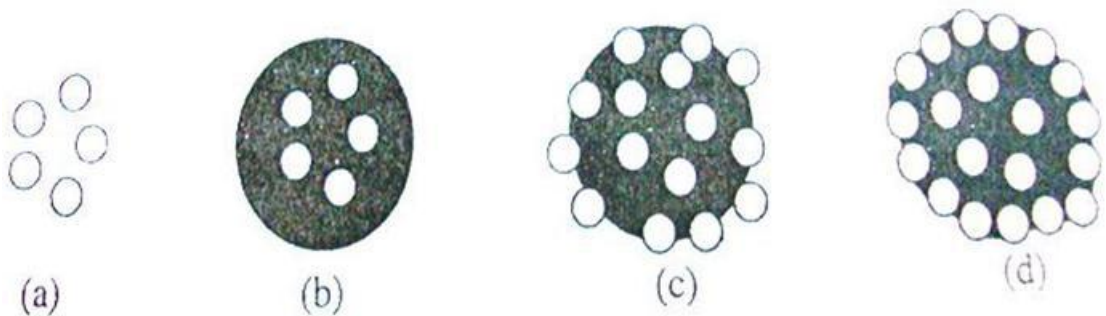
Figure 2.7 Mechanism of ball nuclei formation (water content above optimum state)
(Jaroslav and Rurickova, 1987)

2.3.   Steel Fiber

As a result of the rapid progress in concrete technology, high strength concretes can be easily produced (Balaguru et al., 1992). The ductility of concrete decreases when its strength increases and this is the main apprehension of high strength concretes. The higher the strength of concrete, the higher is its brittleness. This serious problem, inverse relation between strength and ductility, can be solved by adding short fibers (Wafa and Ashour, 1992).

Although steel fiber was first tried to utilize in concrete in 1910 by Porter (Naaman, 1985), the fiber reinforced concrete (FRC) was first investigated scientifically in 1963 in United States (Nanni, 1998). FRC is composite material comprised of conventional hydraulic cement, aggregates (fine and coarse), water and a dispersion of discontinuous small fibers. Superplasticizers can also be used to improve workability. The fibers, used to produce FRC, may be manufactured from steel, plastic, glass and other natural materials and the shape, raw material, length, diameter and type of cross-section are the engineering specifications of fiber. Steel fibers are defined as the steel having an aspect ratio (ratio of length to diameter) between 20 and 100 with short, discrete lengths and any of the several cross sections, and that are sufficiently small to be easily and randomly dispersed in fresh concrete mixture using conventional mixing procedures (ACI 544.1R, 1996). The steel fibers may be manufactured in different geometries (Figure 2.8) and these geometries are shaped during manufacturing (Figure 2.9).
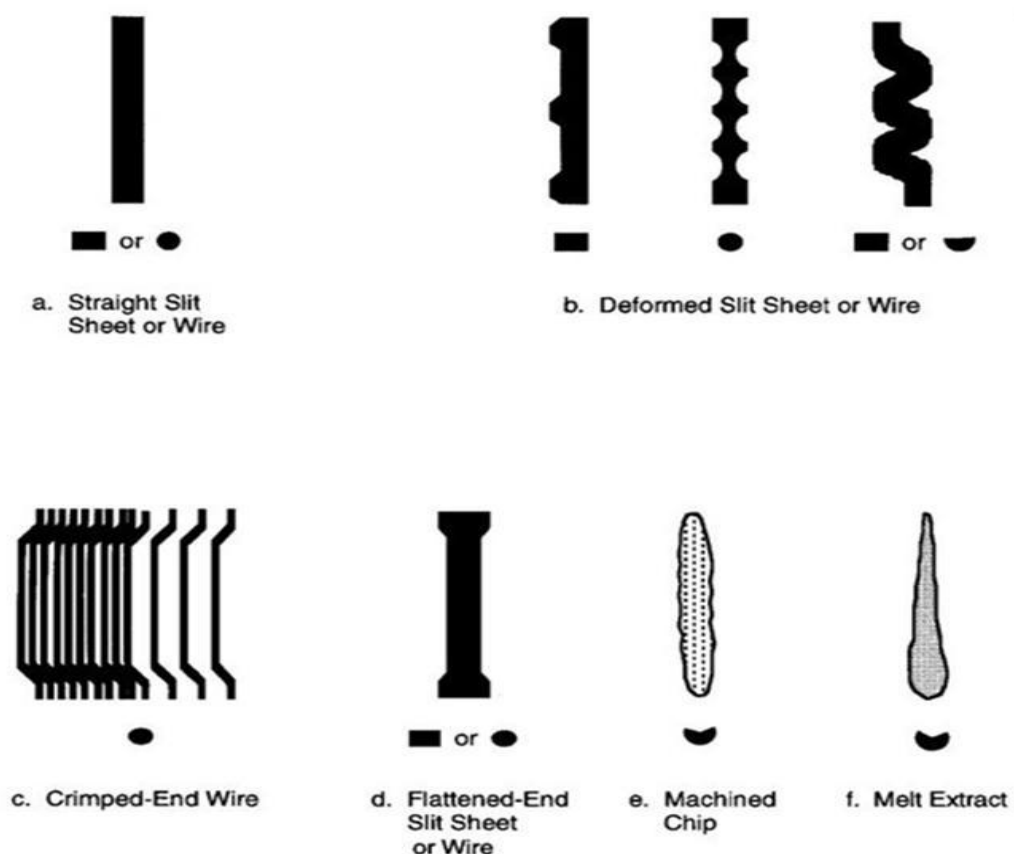
Figure 2.8 Different steel fiber geometries (ACI 544.1R, 1996)

Figure 2.9 Different types of steel fiber (Weiler and Grosse, 2010)

When steel fibers added to the concrete, they enhance many mechanical properties of concrete such as toughness, ductility, shear and tensile strength, and modify the micro and macro cracking. The improvement degree depends on steel fiber type, shape, length, cross-section, bond characteristic of fiber, fiber content (Shah and Naaman, 1976; Wafa and Ashour, 1992; ACI 544.1R, 1996; Nanni, 1998; Altoubat and Lange, 2001; Bayramov et al., 2004; Cucchiara et al., 2004; Akçay and Taşdemir, 2012; Behbahani et al. 2012; Hassanpour et al., 2012). Due to the crack block effect of the fibers, tensile strength of concrete significantly increases by adding steel fiber (Nanni, 1998). Many researchers considered that the utilization of steel fibers in concrete improve the flexural strength of concrete because of having high strain value (Shah and Naaman, 1976). Addition of steel fiber in concrete significantly improves the splitting tensile strength and provides an increase in the energy required for fracture by resultant crack arresting process, and aspect ratio and volume fraction has an important effect on the splitting tensile strength and fracture energy (Bayramov et al., 2004).

2.3.1. Type of Steel Fibers

ASTM A820 classifies the steel fibers based upon the product used in their manufacture. Cold-drawn wire fibers, cut sheet fibers, melt-extracted fibers, and other fibers are the four different classes of steel fibers according to ASTM A820.

- Type I (Cold wire fibers): This type is the most commercially available steel fiber, and it is manufactured from drawn steel wire.
- Type II (Cut sheet fibers): As the name implies, this type of steel fibers are manufactured by laterally shearing off steel sheets.

- Type III (Melt-extracted fibers): This type of steel fiber is manufactured with a relatively complicated technique. Liquid metal is lifted from a molten metal surface by using a wheel. After that the lifted molten metal is rapidly frozen into fibers and thrown off the wheel by centrifugal force. Crescent-shaped cross section fibers are obtained.
- Type IV (Other fibers): these fibers are manufactured for tolerances to length, diameter, aspect ratio, minimum tensile strength and bending requirement (ASTM, 2011).

2.3.2. Utilization of Steel Fiber in Concrete

The volume range for utilization of steel fiber in concrete is between 0.25% and 2%. Utilization more than 2% generally reduces the workability and fiber dispersion, and also special mix design and concrete placement techniques are need when steel fiber is used more than 2% (UM, 2012).

Bekaert, one of the biggest manufacturers of steel fiber, recommends that steel fibers must never be added as first component in the mixer and they can be introduced together with sand and aggregates, or can be added in freshly mixed concrete (Bosfa, 2012). Due to the fact that using steel fiber, particularly at higher concentrations, decreases the workability, using superplasticizer is recommended to prevent workability loss (MWM, 2012).

2.3.3. Application of Steel Fiber Reinforced Concrete

The usage of SFRC has been so varied and so widespread in recent years, that makes the categorization of SFRC application difficult. Pavements, tunnel, linings, slabs, shotcrete, airport pavements and slabs, bridge deck slab repairs, etc. are the most common applications of SFRC.

1. Shotcrete application: Shotcrete is a type of concrete (highly fluid) that can be applied onto almost any surface by spraying. Applications of use shocrete are generally projected onto irregular or vertical surfaces. Before spraying of shotcrete on the application surface, steel mesh can be installed to provide a adhesive substrate for the shotcrete. Steel fibers are generally used to reinforce the shotcrete and provide cohesion which eliminates the using of

steel mesh (eHow, 2012). A thin plain shotcrete applied monolithically on the fiber shotcrete for covering it, and this may prevent surface staining due to rusting. Rock slope stabilization, tunnel lining and bridge repair are the general application areas of steel fiber shotcrete (Gambhir, 1995).

2. Hydraulic structures application: Because of having SFRC good resistance against cavitations or erosion damage produced by water flow with high velocity, it can be utilized in the hydraulic structures (Gambhir, 1995).

3. Tunnel application: Precast concrete elements, cast-in elements, shotcrete or their combination are used to construct tunnel linings. Tunnels need high resistance against soil or water which causes constant load on it. Because of providing SFRC additional flexural strength, reducing shrinkage cracking and permeability, it is commonly used in tunnel construction (eHow, 2012).

4. Precast application: Precast concrete elements are manufactured before transportation and installation on site. They are used in apartment buildings, offices, bridges, substructures and tunnels. Using SFRC in precast industry provides additional flexural and impact strengths (Gambhir, 1995; eHow, 2012).

5. Industrial ground slabs: In the industrial ground slabs, SFRCs, having high durability and flexural strength, are used against repeated loading and impact load. Repeated loads are caused from forklifts in warehouses, cranes in factories, and traffic loads in airport runways. SFRC also leads to minimize the thickness of slabs. SFRC has a greater tensile strain capacity than plain concrete, and that results in lower maximum crack widths (Gambhir, 1995; eHow, 2012).

2.4.   Bond of the Steel Reinforcement in Concrete

Whereas loads are always applied to the concrete, they are not directly applied to the steel in reinforced concrete structures. The concrete have tendency to crack due to the being weakness in tension region. At the cracked places, the loads are transferred to the steel and in this situation some of the tension forces returns to the concrete. The basis of the reinforced concrete theory is based on this simple stress transfer mechanism. The bond stresses between concrete and steel are caused by the stress transfer. The importance of bond between these two structural materials has been

concerned by engineers and researchers since 1877 (ACI Committee 408, 2003). The structural behavior of reinforced concrete is controlled and working of steel and concrete with together is obtained by the stress transfer between two structural materials.

Bond design equations are based on adequate bond strength which can be defined as amount of transferred load between concrete and steel bar (ACI committee 408, 2003; Rteil, 2007). Because transferring enough force by adequate bond strength will yield the steel and that will provide ductility for a reinforced concrete member (Rteil, 2007). Bar geometries and size, concrete qualities and properties, surface condition of the bar, and confinement on the bar influence the bond strength. Compressive and shear stresses of the concrete contact surfaces balance the forces occurred on the bar surface. They are converted to the tensile stresses, and leads to parallel and perpendicular tensile stress to the reinforcement. They cause cracking of planes as illustrated Figure 2.10a and 2.10b. Formation of conical failure surface for bars projected from concrete can be caused the cracks shown in Figure 2.10a which is also known as Goto (1971) cracks. When the concrete cover or the distance between the bars is small, the cracks shown in Figure 2.10b occurs and resulting in splitting cracks as shown in Figure 2.10c. A pullout failure, as shown in Figure 2.10d is resulted by failing of system due to shearing along a surface at the top of the ribs around the bars. This situation occurs only if a splitting failure is prevented or delayed by the sufficient concrete cover, bar spacing or transverse reinforcement (ACI committee 408, 2003).
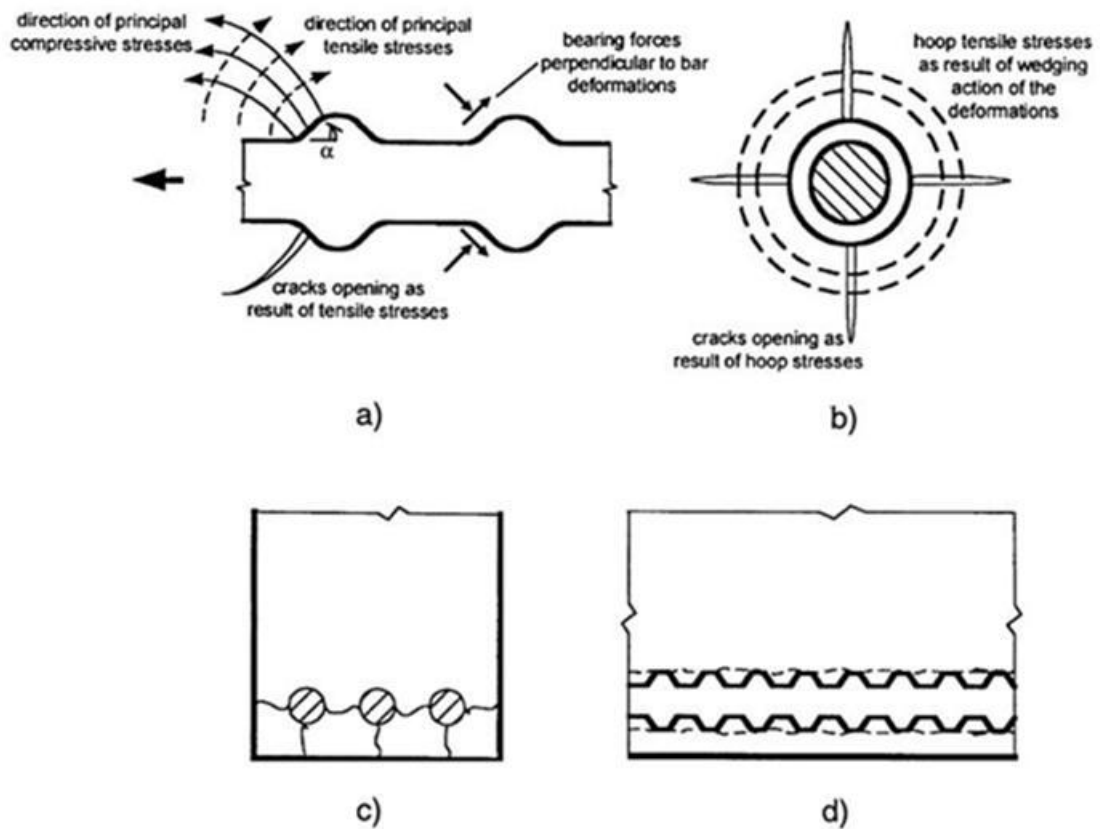
Figure 2.10 Cracking and damage mechanisms in bond: a) side view of a deformed bar with deformation face angle α showing formation of cracks, b) end view showing formation of splitting cracks parallel to the bar, c) end view of a member showing splitting cracks between bars and through the concrete cover, and d) side view of member showing shear crack and/or local concrete crushing due to bar pullout (ACI committee 408, 2003)

2.4.1. Load Transfer

Transfer of axial forces from steel bars to the surrounding concrete is known as bond strength, and by transferring the forces cause the development of tangential stress components along the contact surface area (Pillai and Kirk, 1983). When the steel bar is bonded to the surrounding concrete properly, the reinforced concrete will work as composite material. Little or no slip of the steel in the concrete can be achieved only if a good bond is formed between the steel and the concrete and carrying out this situation means that the stress is transferred across the steel-concrete (Warner et al., 1998). The transfer of forces from deformed steel bars through the concrete is shown in Figure 2.11 and it occurs by the following situations:

- Chemical adhesion between the bar and the concrete;

- Friction and slip between the steel bar and the surrounding concrete;

- Mechanical anchorre or bearing of the ribs against the concrete surface (ACI committee 408, 2003).
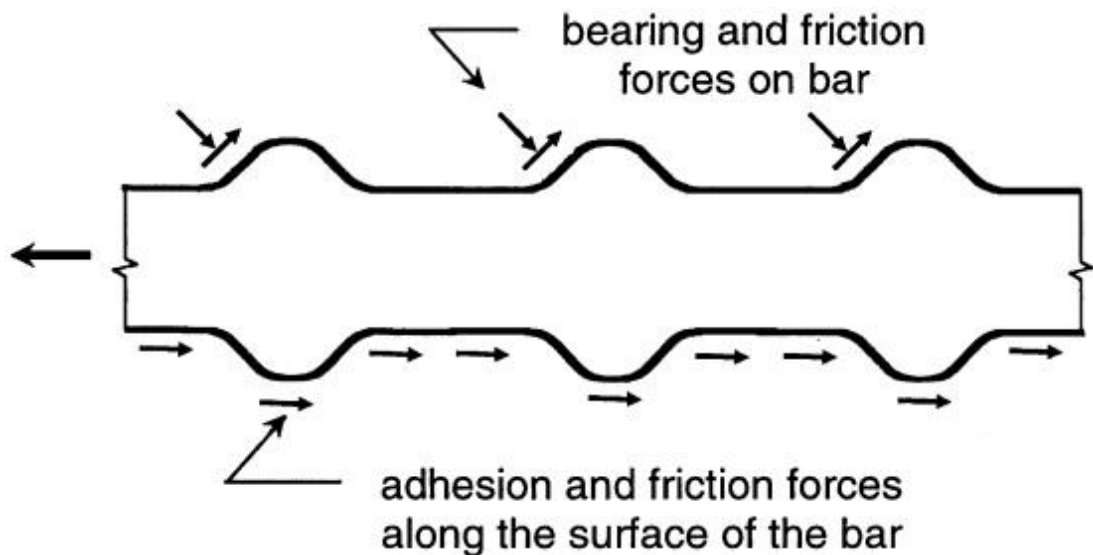
Figure 2.11 Bond force transfer mechanism (ACI committee 408, 2003)

The adhesion between the steel bar and the concrete is responsible for carrying the initial loads, and the adhesion prevents the slipping of the steel bar from the surrounding concrete. When the load on the steel bar excesses the adhesion resistance, the surface adhesion is lost. After the failing of the adhesion resistance, slip begins and the most of the force is transferred by bearing forces on the ribs as well as friction forces between the concrete and bar ribs plays an important role in force transfer. The principal mechanism of force transfer is due to bearing forces and friction forces which are acted on the ribs. Slip increases as a result of increasing of load, and this cause reduction in friction forces occurred on the surface area of the reinforcement (ACI committee 408, 2003). The relationship (Figure 2.12) between the bond stress and slip is given by Eligehausen et al. (1983).
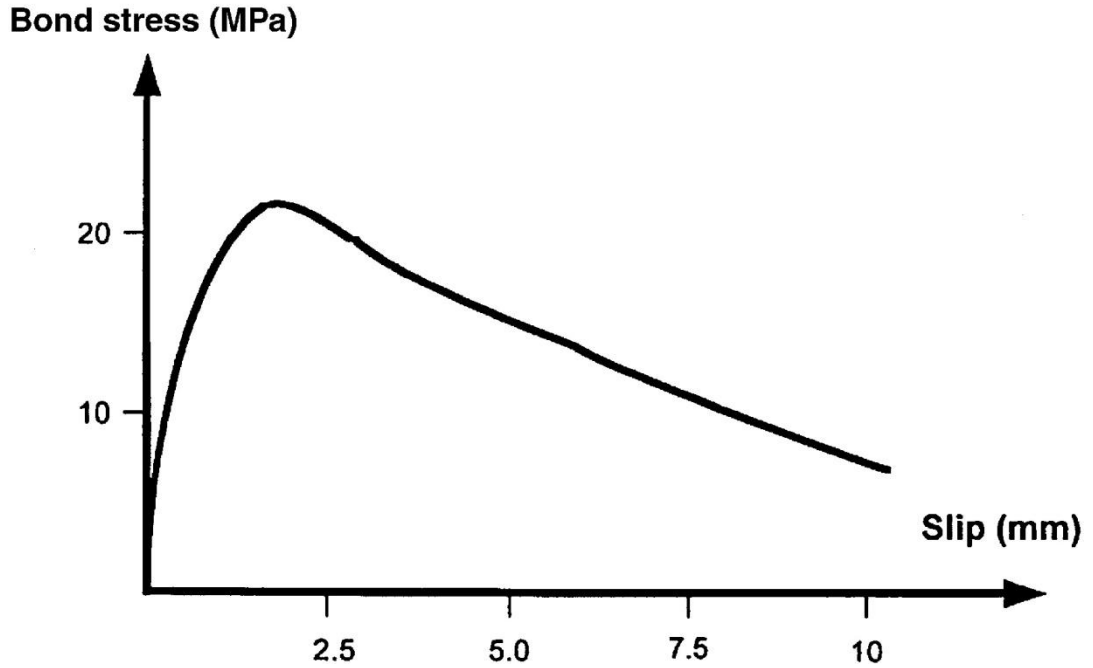
Figure 2.12 Bond stress-slip curve for bar loaded monotonically and failing by pullout (Eligehausen et.al., 1983)

2.4.2. Test Specimens

There are so many test specimen configurations for the determination of bond between reinforcing bars and concrete. The configurations, shown in Figure 2.13, are the four most common types. The details of the specimen affect both the measured bond strength and the nature of the bond response (ACI committee 408, 2003).
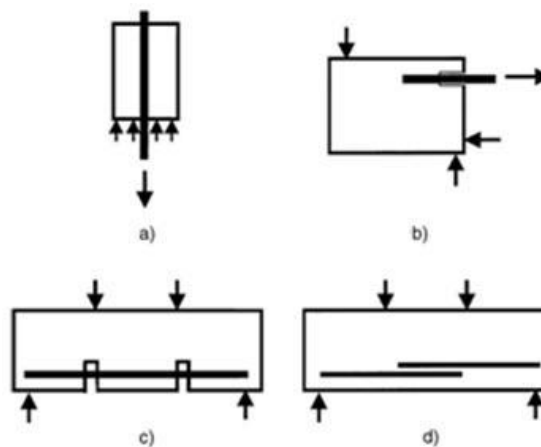
Figure 2.13 Schematic of: a) pullout specimen; b) beam-end specimen; c) beam anchorage specimen; and d) splice specimen (ACI committee 408, 2003)

Because of the matching the stress fields within the specimen with few cases in actual life, the most realistic of the four test specimens, shown in Figure 2.13, is pullout specimen and it is widely used type of bond strength determination test setup due to its easy fabrication and being simple test. In the pullout test specimen, the bar is placed in tension while the concrete is placed in compression. Moreover, the bar surface is placed in compression by the forming the compressive struts between the support points for the concrete and the surface of the reinforcing bar (ACI committee 408, 2003).

2.4.3. Factor Affecting the Bond Strength

There are many factors that affect the bond strength of reinforcement in concrete such as:

- Development length
- Bar casting position
- Bar size
- Bar geometry
- Bar surface condition
- Compressive and tensile strength of concrete
- Confinement

2.5. Fracture Mechanics of Concrete

Fracture mechanics is a science which investigates the strain replacement and stress around the cracks. The properties and mechanical behavior of materials used in structures significantly affect the mechanical behavior of the structure. The designing of concrete in application is based on the compressive strength theory, and the brittleness of concrete is ignored in this theory. Therefore, the definition of the fracture parameters of concrete with its brittleness has to be done (Akçay, 2007). The fracture mechanics investigate the places, formation and circumstances of failure and the effects that prior to propagation of present cracks. Linear Elastic Fracture Mechanics (LEFM) and Nonlinear Fracture Mechanics (NFM) were developed for this reason. LEFM can be applied to brittle and homogenous materials such as glass and NFM is the modified state of LEFM due to being inefficient of LEFM for quasi-brittle and heterogeneous materials like concrete (Taşdemir et al., 1996). LEFM and

NFM will be explained and their application on LWAC will be given in a detailed manner in this section.

2.5.1. Linear Elastic Fracture Mechanics

The stress concentration occurs at the tip of space in the material, which contain a space and is under the load, due to discontinuity. Being obliged of the stress flow, taking place due to loading, to move around the cracks causes the stress concentration at the tip of crack and the stress relaxation at the upper and lower faces of crack. According to Linear Elastic Fracture Mechanics (LEFM), the stress, occurs the tip of crack, goes infinity as the crack becomes sharper. Griffith was introduced LEFM for brittle and homogeneous materials and this introducing was landmark for the theory of fracture mechanics (Akçay, 2007). The fundamental contributions to develop this theory were done by Orowan and Irwin for non-brittle materials (Irwin, 1957). Concrete is a quasi-brittle material and the fracture mechanics theory was first accomplished to concrete by Kaplan (1961). He also emphasized that the LEFM could not be used for the extracting of fracture parameters of concrete because of including of concrete the fracture process zone (FPZ) which defined as the inelastic zone around the crack tip (Mindess and Diamond, 1982; Taşdemir and Karihaloo, 2001).

The existing of small cracks and other crack-like defects in hard brittle materials causes a large distinctness between the real and theoretical tensile strengths of these materials (Griffith, 1920). Glass sheet, shown in Figure 2.14, illustrates this theory. When the constant remotely stress was applied to a sheet of brittle material with existing of a sharp crack, the stresses near the crack tip goes to infinity (Karihaloo, 1995). Thereby, the load capacity of the sheet became crucial at the stress state in the surroundings of the sheet (Akçay, 2007).
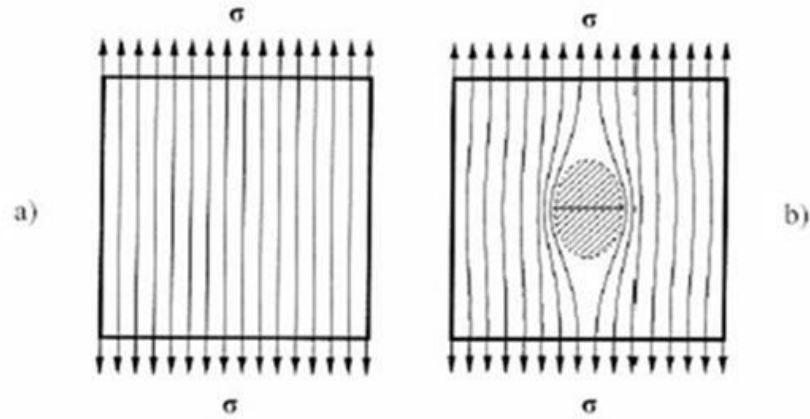
Figure 2.14 Stress flow lines in thin sheet subjected to axial tensile loading: a) without void and b) including void (Karihaloo, 1995)

Strain energy determined by Griffith (1920) as follows

$$\sigma = \sqrt{\frac{2E\gamma}{\pi a}} \tag{2.1}$$

where E is the modulus of elasticity, γ is the surface energy density.

The Griffith Theory was modified to ductile materials by Irwin (1957). He added the new strain energy using for plastic deformation (γ_p) to the Griffith (1920) strain energy as follows

$$\sigma = \sqrt{\frac{2E(\gamma + \gamma_p)}{\pi a}} \tag{2.2}$$

The modes of crack surface displacement, as shown in Figure 2.15 which occurs at a crack tip affect the deviation of the stresses near a sharp crack tip. It is called as r-singularity, where r is the distance from the crack tip and this singularity is also independent of the boundary conditions, geometry and loading.
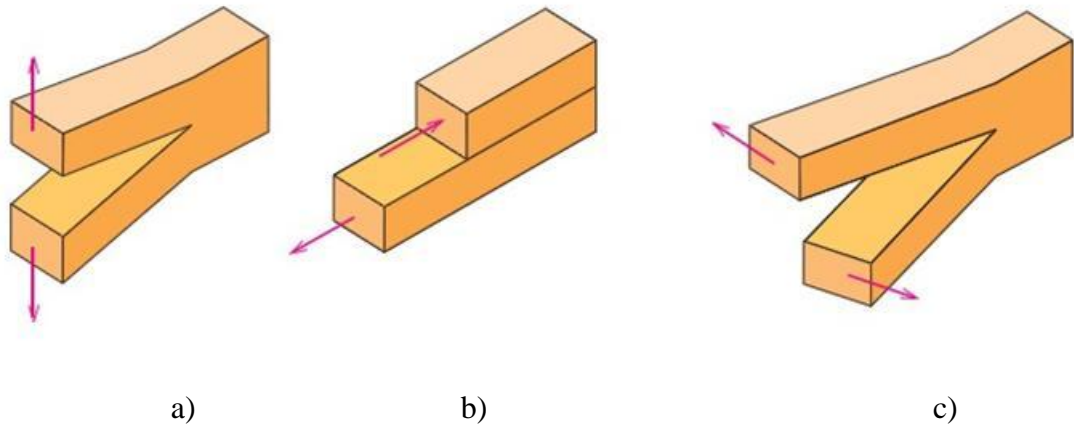
Figure 2.15 The three modes of crack surface displacement: a) mode I, opening or tensile mode, b) mode II, sliding mode, and c) mode III, tearing mode (Karihaloo, 1995)

Assumption for approaching the stresses near the crack tips to infinity causes an inconsistency between the linear elastic models and real situation where the tensile load is applied to materials. This is a problem for the Griffith and Irwin theories of brittle fracture. Primary assumptions for elasticity considering small strains are as well neglected in these theories (Akçay, 2007). Cohesive crack model first raised alternative to LEFM to eliminate the stress singularity (Barenblatt, 1959; Dugdale, 1960). Hillerborg generalized the concept of process zone, removing the small nonlinear zone requirement, and more recently, the researchers have indicated that this generalization may be regarded as a particular case of continuum mechanics nonlocal formulation (Hillerborg et al., 1976).

2.5.2. Non-linear Fracture Mechanics

There are so many researches which have been carried out to make LEFM applicable to concrete and to establish the theories of nonlinear fracture mechanics (Akçay, 2007). Figure 2.16 briefly indicates the differences between concepts.
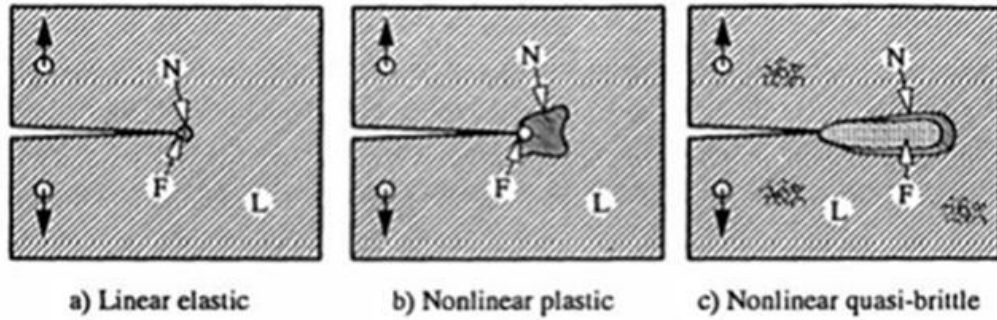
Figure 2.16 Main differences between materials modeling with: a) linear elastic fracture mechanics, b) non-linear plastic fracture mechanics (Dugdale, 1959), and c) non-linear quasi-brittle fracture mechanics. Linear elastic material is denoted with an L, non-linear material behavior with an N, while fracture behavior is denoted by F (Karihaloo, 1995)

There are six approaches which is based on the predominant fracture mechanics; the fictitious crack model (Hillerborg et al., 1976), the crack band model (Bažant and Oh, 1983), the size effect law (Bažant, 1984), the two parameter fracture model (Jenq and Shah, 1985), the effective crack model (Nallathambi and Karihaloo, 1990), and the recently proposed concepts of boundary effect and local fracture energy distribution (Hu and Wittmann, 2000; Duan et al., 2003). These approaches have been recommended for the determination of the fracture parameters of concrete, and the fictitious crack model, the size effect law, and the two parameter models are among the RILEM recommendations (1985).

Fictitious crack model (FCM), which is proposed by Hillerborg et al. (1976), is the first non-linear theory of fracture mechanics. There are similarities between cohesive crack models and fictitious crack model. But, the closing stresses are not constant and they increase allied with tensile strength of material, which occurs at the tip of the fictitious crack (Figure 2.17).
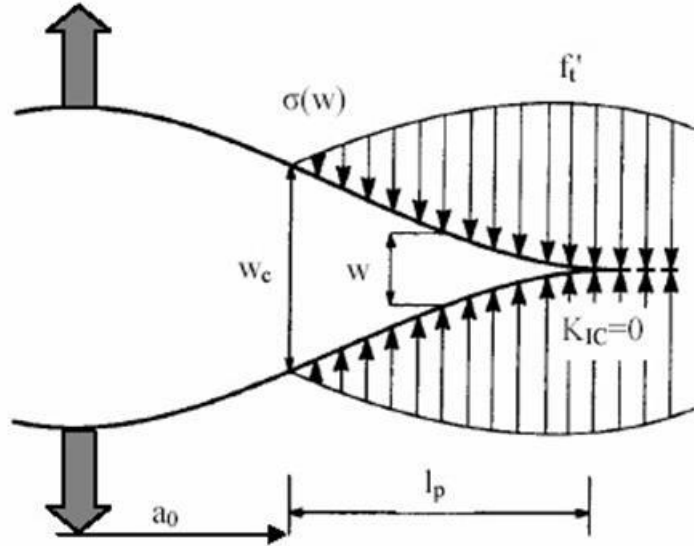
Figure 2.17 Fictitious crack behind the real traction-free crack (Karihaloo, 1995).

The area under the load versus displacement at mid-span curve is used to determine fracture energy in this model.

$$G_F = \int_0^{w_c} \sigma(w)dw \qquad (2.3)$$

where, w_c is the critical crack opening at which the closing stress is equal to zero. Another fracture parameter is characteristic length, which is used to evaluate the ductility properties of cementitious composites. It is determined in terms of modulus of elasticity (E), fracture energy (G_F) and direct tensile strength (f_t').

$$l_{ch} = \frac{EG_F}{(f_t')} \qquad (2.4)$$

The model of Hillerborg et al. (1976) is modified by Bažant and Oh (1983). They modeled the fracture process zone with using the fixed width of uniformly and continuously distributed microcracks instead of occurring discretely as in FCM. They used the following equation for evaluating the fracture energy (G_F) using the width of the crack band, h_b (Figure 2.18), and the area under the stress-strain curve.

$$G_F = h_b\ (1+\frac{E}{E_t})\frac{f_t^2}{2E} \qquad (2.5)$$

where E is the modulus of elasticity, E_t is the strain-softening modulus and f_t is the tensile strength of the material.

a)   b)
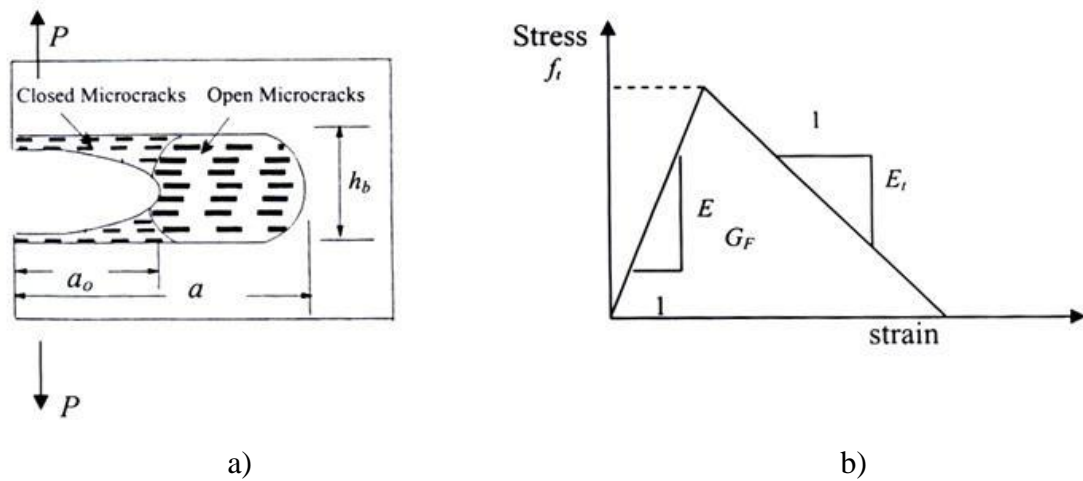
Figure 2.18 Crack band model for fracture of concrete: a) a microcrack band fracture
and b) stress-strain curve for the microcrack band proposed by Bažant and Oh, 1983
(Shah et al., 1995)

Two fracture parameters, the critical energy release rate and the critical effective
crack length, are needed to extrapolate the laboratory size specimens to the
laboratory size specimens to real-size engineering structures. In the Bažant's size
effect law (1984), the critical energy release rate is the unit fracture energy required
for the crack initiation in an infinite specimen and the critical effective crack length
can be defined as the length of the FPZ between the notch tip and the crack tip of
peak load of an infinitely large specimen.

Two fracture parameters, the critical stress intensity factor (K_{IC}^{s}) and the critical crack
tip opening displacement (CTODc), are determined using the only one size three-
point bending specimens which is loaded up to maximum stress, and then exposed to
an unloading and reloading cycle (Shah et al., 1985). This is known as the two
parameter fracture model (TPM), proposed by Jeng and Shah (1985).

Nallathambi and Karihaloo (1990) proposed the effective crack model (ECM) in
which the basic concept of effective crack is similar to the TPM. The effective crack
model is based on the effective-elastic crack approach as in the TPM. While the
elastic part of unloading compliance is used to determine the effective-elastic crack
length in the TPM, the secant compliance at the maximum load is used in the ECM.
The secant compliance at the maximum load comprises the effects of both elastic and
inelastic deformation and the elastic part of unloading compliance comprises the only

elastic deformation. Therefore, the critical effective crack length achieved in this model is usually greater than that obtained from the TPM (Shah et al., 1995).

2.6. Mechanical and fracture properties of steel fiber reinforced lightweight aggregate concretes

2.6.1. Compressive strength

Since the artificial fly ash aggregates are weaker than the matrix, the decreasing effect of the lightweight aggregates on the compressive strength of concrete was reported by many authors. The increasing the amount of lightweight cold bonded fly ash aggregate resulted in gradually decreasing of compressive strength was reported by Gesoğlu et al. (2004) as shown in Figure 2.19.
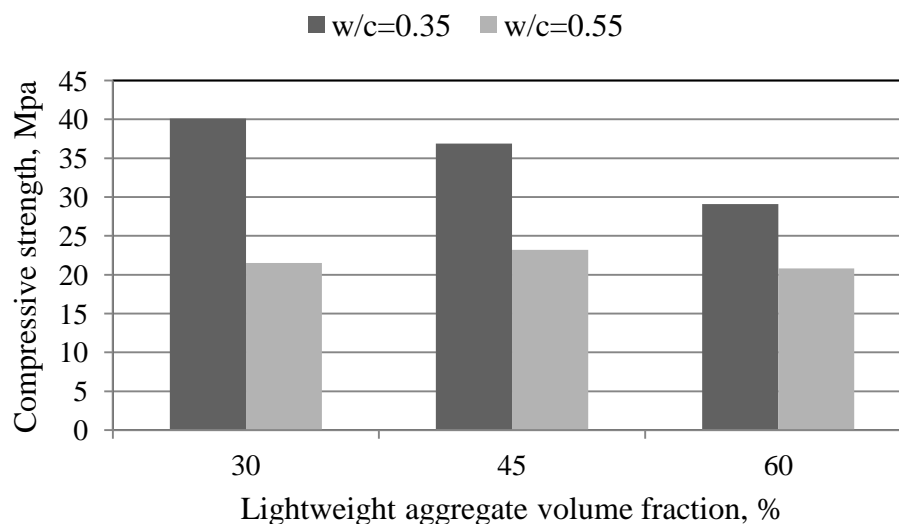
Figure 2.19 Variation in compressive strength for different lightweight aggregate volume fraction (Gesoğlu et al., 2004)

Güneyisi et al. (2012) was also utilized the cold bonded fly ash lightweight aggregate to produce LWAC. They achieved the compressive strength of more than 40 MPa with using LWA as coarse aggregate and also reported the decreasing effect LWA.

While Gesoğlu et al. (2004) and Güneyisi et al. (2012) used the artificial lightweight aggregate for the production of the concrete, Düzgün et al. (2005) substituted 25%, 50%, 75% and 100% of normal coarse aggregate by the pumice lightweight aggregate and they also resulted that the compressive strength of the concrete

produced with lightweight aggregate decreases with the increasing lightweight aggregate content.

Libre et al. (2011) reported the highest increase in compressive strength for steel fiber sanded LWAC. They added 0.5% and 1.0% volume of steel fiber (L=35 mm and D=0.55 mm) to natural pumice LWAC and the compressive strength increased by up to 60% and 50%, respectively. The detailed results of compressive strength produced with different pumice lightweight aggregate and steel fiber volume fractions in study of Düzgün et al. (2005) are shown in Figure 2.20. Using higher volume fraction of steel fiber may decrease the compressive strength due to the difficulty in dispersing the fiber and inadequate compaction of concrete (Gao et al., 1997). In addition to that, increasing of compressive strength up to 30% (Campione et al., 2001), 22% (Gao et al., 1997), 21% (Düzgün et al., 2005), 20% (Kang et al., 2011) and 14% (Shafigh et al., 2011) have also been reported in steel fiber LWAC with good workability (Hassanpour et al., 2012). However it is reported by some researchers that the compressive strength of high strength lightweight aggregate concrete is not affected by utilization of steel fiber (Balendran et al., 2002; Altun, 2006).
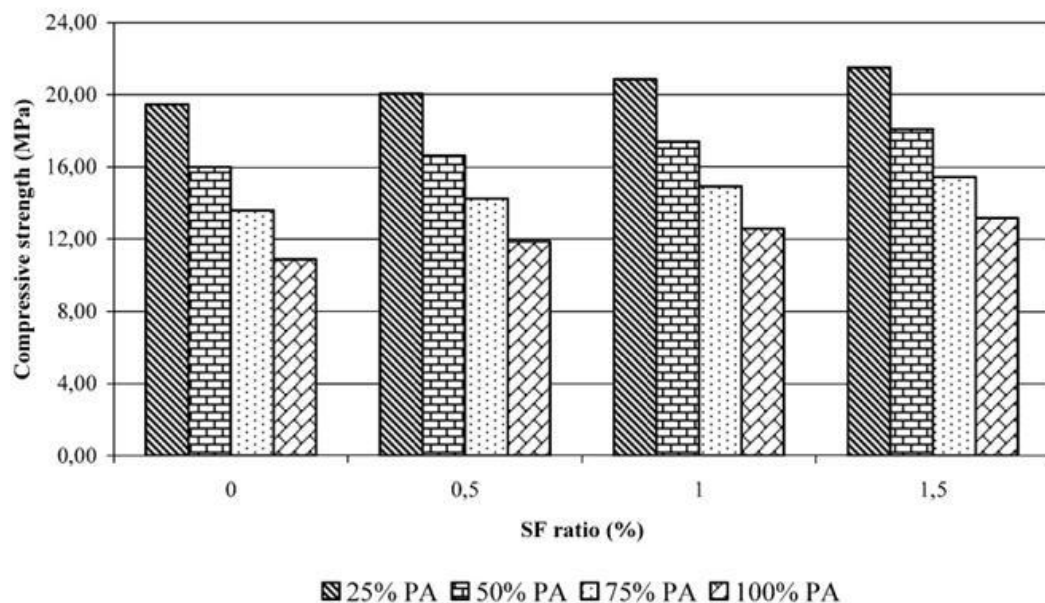
Figure 2.20 Effect of steel fiber and pumice aggregate content on the compressive strength (Düzgün et al., 2005)

The effectiveness of steel fiber on the compressive strength of LWAC significantly depend on the aggregate type has been revealed by Campione et al. (2001). They reported that the addition of steel fibers into the matrix of expanded clay LWAC indicated an increase in the compressive strength of up to 30%, while in the case of pumice stone LWAC the variation in the strength was negligible.

2.6.2. Splitting tensile strength

While the increasing the amount of normal coarse aggregate increases the splitting tensile of concrete, increasing the lightweight coarse aggregate content decreases the splitting tensile strength (Gesoğlu et al., 2004). The utilization of steel fiber and increasing the steel fiber content increase the splitting tensile strength of both normal weight and lightweight concretes at all ages of curing relative to control concrete. The plain concrete compared to fiber reinforced concrete, the fiber reinforced concrete has superior tensile properties (Wang et al., 1990). Previous studies (Gao et al. 1997; Campione et al., 2001; Balendran et al., 2002; Kayali et al., 2003; Chen et al., 2004; Campione et al., 2005; Chen and Liu, 2005; Düzgün et al., 2005; Domagala, 2011; Libre et al., 2011; Shafigh et al., 2011) have shown that the addition of steel fiber to LWAC less than 0.5% (very low volume fraction) increases the splitting tensile strength, when compared to concrete without fiber, in the range of 16-61%, addition of steel fiber between 0.5 and 1.0% (low ratio) increases splitting tensile strength of about 19-116% and utilization of steel fiber between 1.0 and 2.0% (higher volume fraction) resulted in an increase between 61-118% have been reported. Bayramov et al. (2004) used the steel fibers with aspect ratio (L/d) of 55, 65 and 80 in NWC with volume fraction of 0.24%, 0.46% and 0.64% and they reported significantly improvement as shown in Figure 2.21.

2.6.3. Modulus of elasticity

The utilization of lightweight coarse aggregate instead of normal weight coarse aggregate has significant effect on the modulus of elasticity. Utilization of LWA significantly decreases the modulus of elasticity of concrete when it compared with the concrete produced with normal weight aggregate. Some researchers concluded that increasing the lightweight aggregate content in LWAC causes a lower modulus of elasticity (Gesoğlu et al., 2004; Düzgün et al., 2005; Kurugol et al., 2008).

Bayramov et al. (2004) concluded that utilization of steel fiber in concrete does not have any remarkable effect on the modulus of elasticity. Whereas the increasing the modulus of elasticity by using steel fiber was reported in some studies (Campione et al., 2001; Kayali et al., 2003; Bilodeau et al., 2004; Domagala, 2011; Shafigh et al., 2011), the decreasing effect of steel fiber depending on type of LWA and steel fiber volume fraction was also reported (Campione et al., 2001; Kayali et al., 2003; Bayramov et al., 2004).
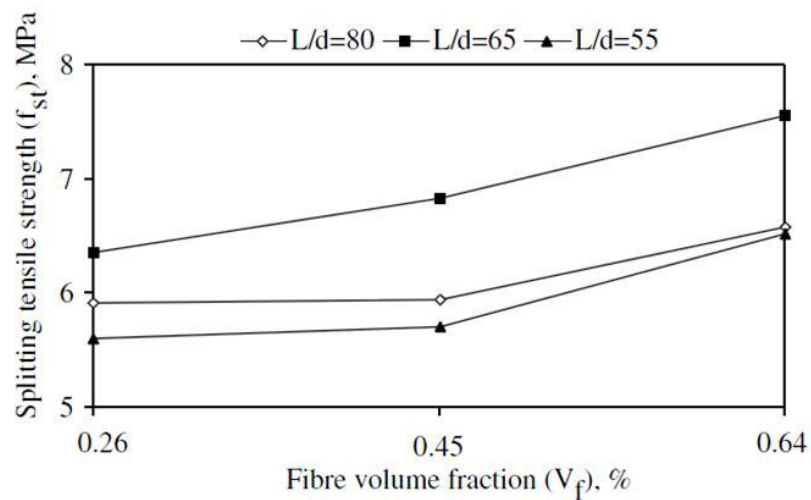
Figure 2.21 Splitting tensile strength versus fiber volume fraction with different aspect ratio (L/d) where the splitting tensile strength of plain concrete is 5.3 MPa (Bayramov et al., 2004)

2.6.4. Flexural strength

Domagala (2011) reported that the flexural strength of plain LWAC is lower than NWC of the same compressive strength. Utilization of steel fiber in LWAC also increases its flexural strength. Gao et al. (1997) explained the reason as the fibers carry the load that concrete is subjected after the matrix cracks. Therefore, resistance against cracks propagation occurs by utilization of steel fiber and it does not fail suddenly, this situation results in increasing of the load carrying capacity (Hassanpour et al., 2012). Balendran et al. (2002) reported that the increase in the flexural strength due to addition of steel fiber in LWAC is higher than in NWC.

Bayramov et al. (2004) used the steel fibers with aspect ratio (L/d) of 55, 65 and 80 in NWC with volume fraction of 0.24%, 0.46%, and 0.64% and they reported significantly improvement as shown in Figure 2.22.
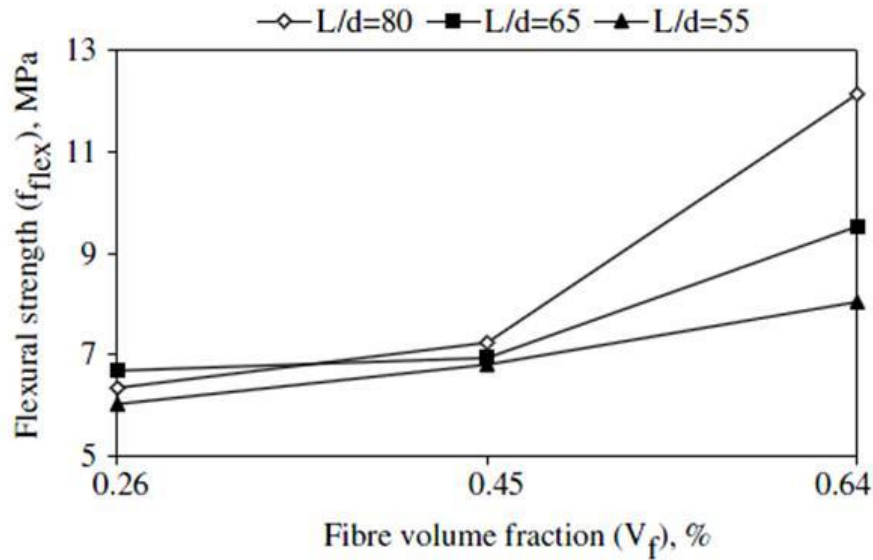
Figure 2.22 Variation in flexural strength at different volume fraction with different aspect ratios (the flexural strength of plain concrete is 6.1 MPa) (Bayramov et al., 2004)

2.6.5. Fracture energy

Akçay and Taşdemir (2009) used the crushed natural pumice as LWA, was also concluded that the utilization and increasing content of lightweight aggregate in concrete causes decreasing of fracture energy. The steel fiber is mostly used to enhance the fracture properties of concrete (Mehta and Monteiro, 2006). They indicated that the increase in toughness was as much as 20 times which clearly shows that the improvement in the toughness is much higher than the improvement in other properties. Libre et al. (2011) resulted that the effectiveness of fiber for improving the toughness of LWAC is much higher than NWC. This may be because of the brittleness of LWAC being higher than NWC. For the fracture energy, steel fiber using significantly enhance it. Because fracture energy calculated according to RILEM 50-FMC (1985) consists of two parts; energy supplied by the actuator and by the own weight of the beam. The area under the load versus displacement curve was used in the calculation of fracture energy as the energy supplied by the actuator, and

33

the weight of the beam was used in the calculation as the energy supplied by own weight of the beam. Since the steel fiber addition into concrete and increasing the amount of steel fiber in concrete significantly increases the area under the load versus displacement curve and the final displacement of concrete subjected to three point bending test, the fracture energy also increases. The increasing the area under the load-displacement curve by steel fiber addition can be seen in Figure 2.23 (Akçay and Taşdemir, 2012). Bayramov et al. (2004) used the steel fibers with aspect ratio of 55, 65 and 80 in NWC with volume fraction of 0.24%, 0.46% and 0.64% and they reported increasing the volume fraction from 0 (plain) to 0.64% were 37, 41, and 48 times, respectively as indicated in Figure 2.24.
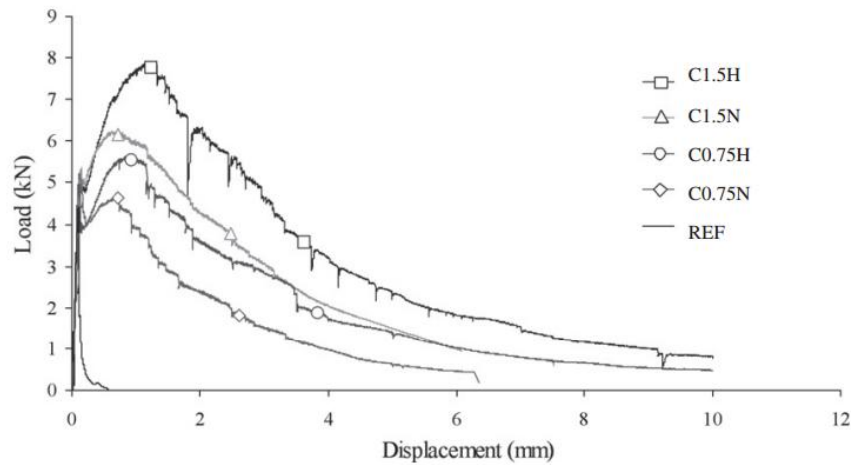
Figure 2.23 Typical load versus displacement curves of concretes with and without steel fiber under bending (Akçay and Taşdemir, 2012)
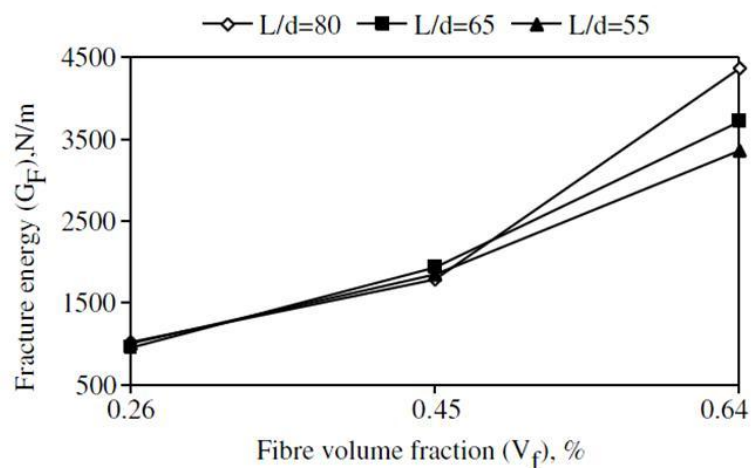
Figure 2.24 Fracture energy versus fiber volume fraction with different aspect ratio where the fracture energy of plain concrete is 91 N/m (Bayramov et al., 2004)

2.6.6. Characteristic length

Characteristic length, which is the measure of brittleness, is also affected by type and amount of aggregate. Akçay and Taşdemir (2012) used the crushed natural pumice as lightweight aggregate in their study with two different sizes of 2-4 mm and 4-8 mm. They reported that utilization of lightweight aggregate and increasing the content significantly affect the characteristic length as well as the fracture energy. Figure 2.25 shows the relationship between fracture energy and characteristic length versus lightweight aggregate content and size.
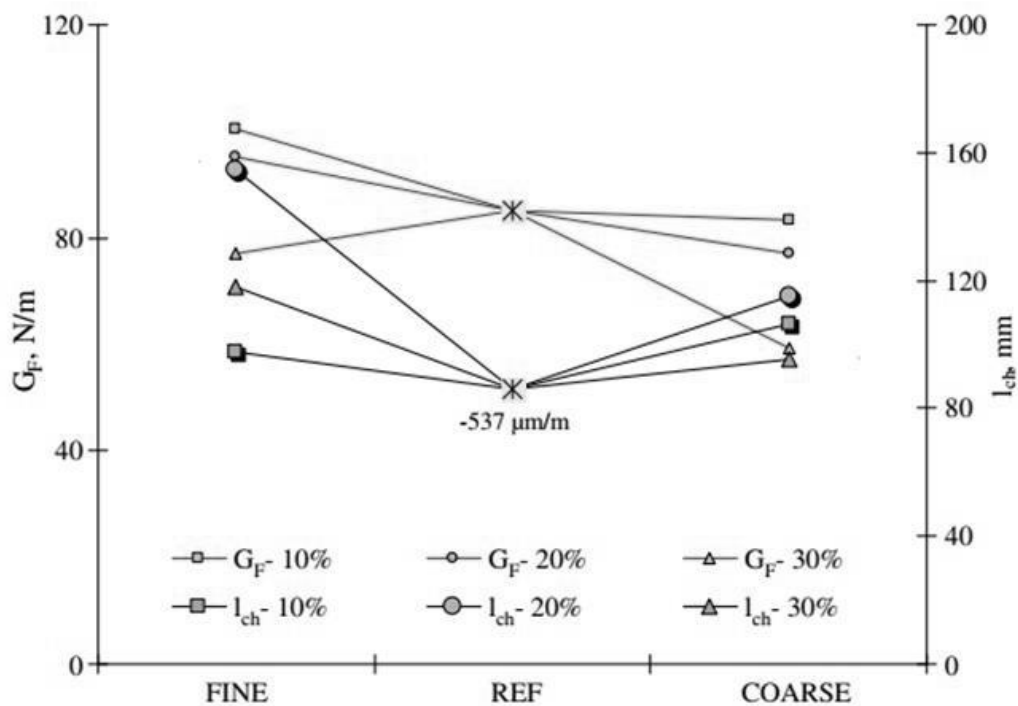
Figure 2.25 Effect of size of LWA on both fracture energy and characteristic length
(Akçay and Taşdemir, 2009)

2.6.7. Bond strength

Adding the steel fiber into concrete enhance the adherence between reinforcement steel bar and concrete. Yu-Cheng et al. (2003) reported the steel fiber utilization increases the bond strength when compared to without steel fiber. Gesoğlu et al. (2013) concluded that addition of steel fiber and increasing the steel fiber volume fraction are increasing the bond strength significantly as well as ductility of pull-out failure. They used two different types of steel fiber with aspect ratio 40 and 80 with

two different volume fraction and they accomplished 70% enhancement in bonding strength capacity by combined incorporation of SF and steel fibers. Harajli and Salloukh (1997) reported that the utilization of steel fiber up to 2% by volume increases the bonding strength by up to 55% for the beam specimens. Krstulovic-Opara et al. (1994) also concluded that 10-20% increase in the pull-out strength is achieved by addition of 1% steel fiber as the volume of concrete.

CHAPTER 3

3. EXPERIMENTAL STUDY

3.1. Materials

3.1.1. Cement

Ordinary Portland cement (CEM I 42.5R) with specific gravity of 3.15 g/cm^3 and Blaine fineness of 326 m^2/kg was utilized in this study conforming to the TS EN 197-1 (Turkish Standard TS EN 197-1, 2002) (which mainly based on the European EN 197-1). It was used in the production of both artificial lightweight aggregates and concretes. Physical properties and chemical compositions of the cement are given in Table 3.1.

Table 3.1 Chemical compositions and physical properties
of Portland cement and fly ash

Chemical analysis (%)	Portland cement	Fly ash
CaO	63.84	2.24
SiO_2	19.79	57.2
Al_2O_3	3.85	24.4
Fe_2O_3	4.15	7.1
MgO	3.22	2.4
SO_3	2.75	0.29
K_2O	-	3.37
Na_2O	-	0.38
Loss on ignition	0.87	1.52
Specific gravity	3.15	2.04
Fineness (m^2/kg)	326*	379*

* Blaine specific surface area

3.1.2. Fly Ash

Class F FA according to ASTM C 618 (ASTM C618-08, 2000) with a specific gravity of 2.04 g/cm^3 and Blaine fineness of 379 m^2/kg was utilized in the manufacturing of cold bonded fly ash lightweight aggregates was supplied from Zonguldak Çatalağzı Thermal Power Plant. Physical properties and chemical compositions of the fly ash are given in Table 3.1.

3.1.3. Superplasticizer

Sulphonated naphthalene formaldehyde-based superplasticizer used to obtain target workability and reducing the balling effect of fiber (Tsai et al., 2009; Kumar et.al., 2005). It had a specific gravity of 1.22 g/cm^3. The properties of superplasticizer are given in Table 3.2.

Table 3.2 Properties of the superplasticizer

Specific Gravity, kg/lt	State	Freezing Point	Color	Chloride Content	Nitrate Content	Main Component
1.22	Liquid	-4 °C	Dark Brown	None	None	Sulphonated naphthalene

3.1.4. Aggregates

3.1.4.1. Lightweight aggregates (LWAs)

Artificial lightweight fly ash aggregates utilized in the concrete production were produced through the cold bonding agglomeration process of fly ash (FA) and Portland cement (PC) in a tilted pan at an ambient temperature. For that reason, a dry powder form of 10% Portland cement and 90% class F fly ash were mixed in the pelletizer as shown in Figure 3.1. A pelletizer with a pan diameter of 800 mm and a depth of 350 mm (Figure 3.1) was used for producing the fly ash pellets. The total pelletization time of a typical production was determined as 20 min. During the first

10 min of the manufacturing, the water was sprayed onto the dry powder mixture of fly ash-cement to act as coagulant.

The amount of sprayed water was determined 22% of the material by weight. The pelletizer disc was continued to rotate in the second half of the agglomeration to obtain compacted and stiff spherical fresh pellets (Figure 3.2). Afterwards, fresh pellets were maintained in plastic bags and stored for 28 days in a curing room in which the temperature and the relative humidity were 20 °C and 70%, (Ke et al., 2009) respectively (Figure 3.3). At the end of the curing period, hardened aggregates were sieved.

The coarse aggregates used in the concrete production were obtained from passing a 12-mm sieve and retained on 4-mm sieve. Specific gravity test of the saturated surface dry aggregates and the water absorption test were carried out according to ASTM C127 (ASTM C127, 2007). Specific gravity of the SSD aggregates was 1.71 gr/cm^3, and water absorption at 24 h was 22.2% by weight. Sieve analysis and physical properties of lightweight coarse aggregate are presented in Table 3.3.

Moreover, crushing strength test of coarse aggregates was performed according to BS 812, part 110 (BS812 part 110, 1990). The result of the crushing strength tests is shown in Figure 3.5. The crushing force was measured by a dial gage and it was transformed to the load (Figure 3.4) and the crushing strength was calculated by following equation:

$$\sigma = \frac{2.8*P}{\pi*X^2} \qquad\qquad (3.1)$$

where X is the distance between loading points and P is the fracture load (Yashima et al., 1987; Li et al., 2000; Mangialardi, 2001; Cheeseman et al., 2005;).
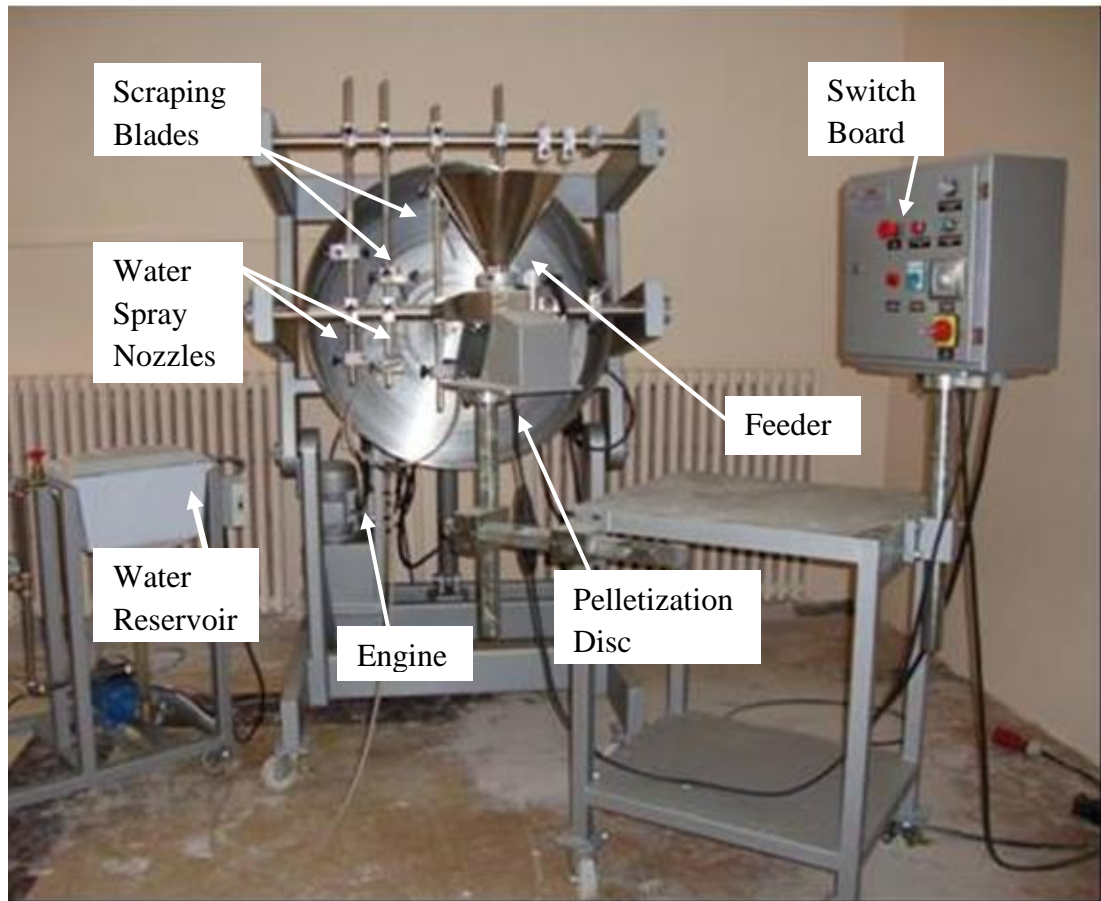
Figure 3.1 The general view of the pelletization disc

Figure 3.2 Fresh artificial lightweight aggregates

Figure 3.3 Keeping the aggregate in sealed plastic bags
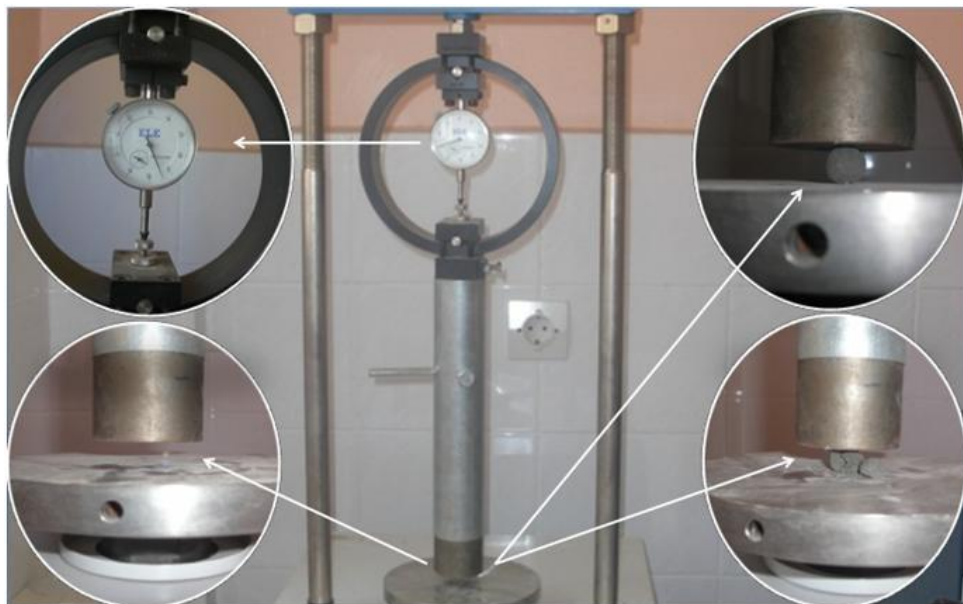
Figure 3.4 Crushing strength test set up
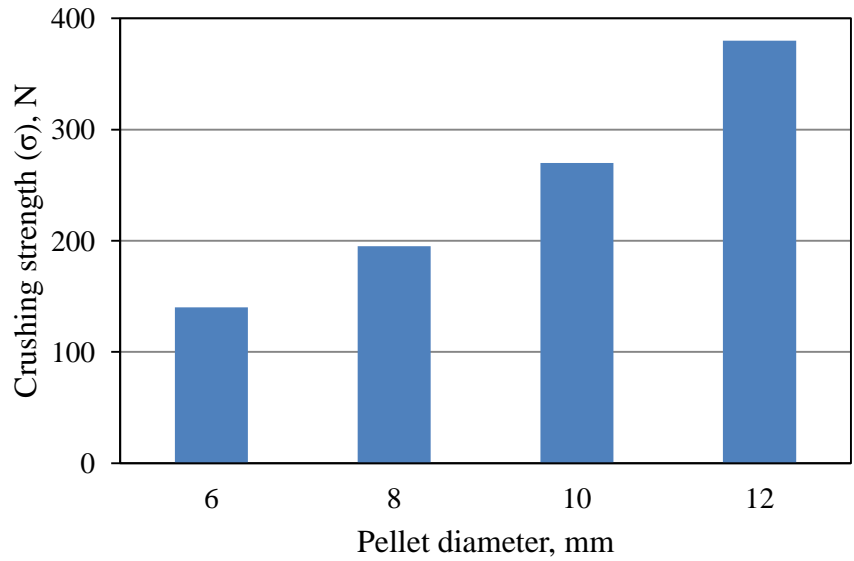
Figure 3.5 Crushing strength of lightweight aggregate

3.1.4.2. Normal weight aggregates

Crushed limestone sand with specific gravity of 2.42 g/cm^3 was used to produce concrete containing cold-bonded lightweight aggregate and steel fiber. Sieve analysis and physical properties of crushed limestone aggregate (CLA) are shown in Table 3.3. Grades of the aggregates are illustrated in Figure 3.6.
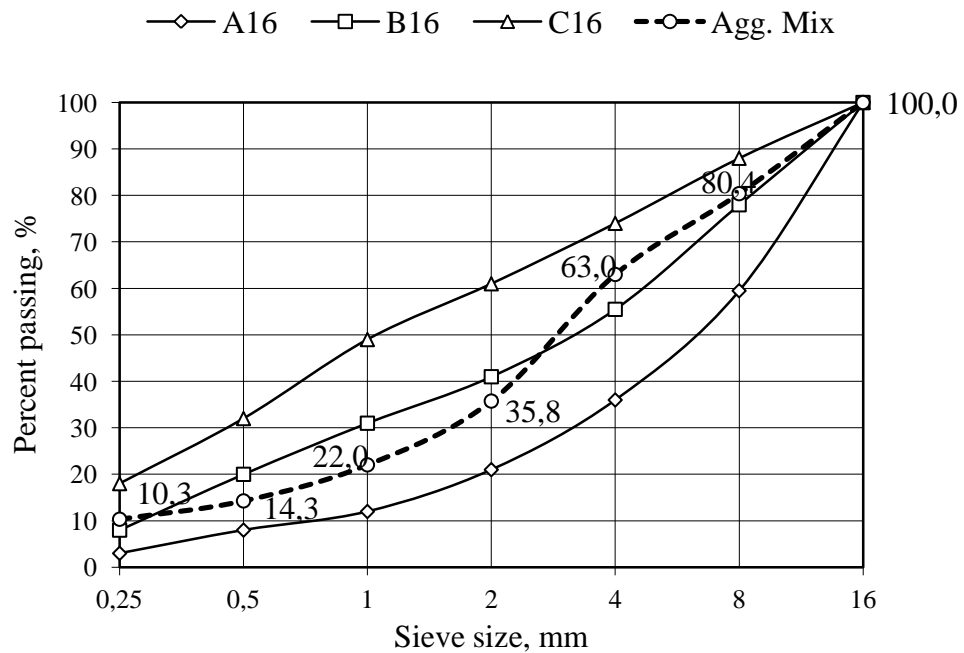
a)
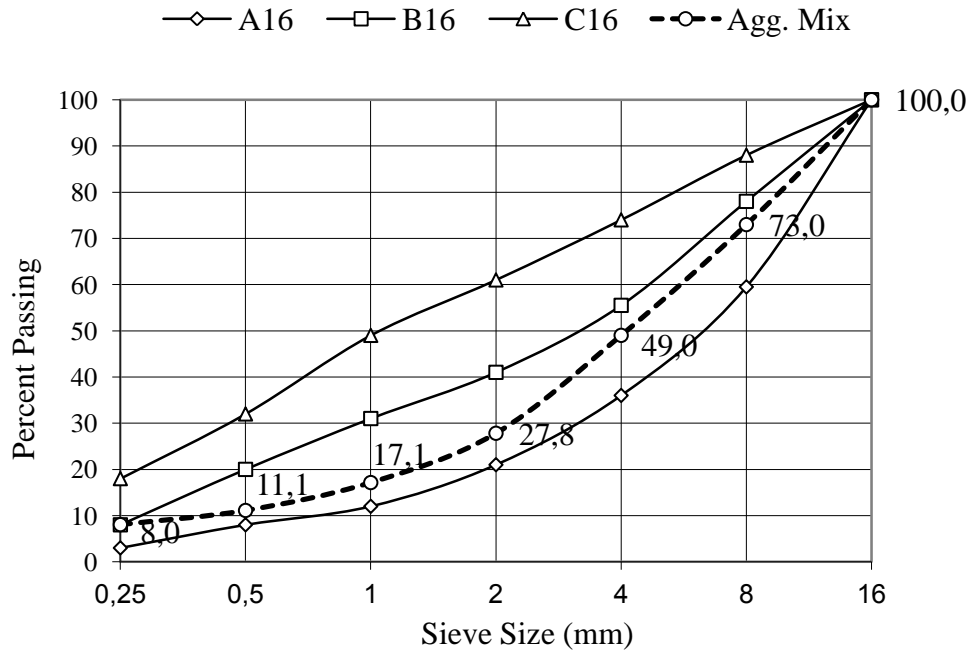
b)

Figure 3.6 Grading of: a) 55% CLA with 45% LWA and b) 40% CLA with 60%

LWA

Table 3.3 Sieve analysis and physical properties of normal weight and lightweight

aggregates

Sieve size (mm)	Natural fine aggregate (%)	Lightweight coarse aggregate (%)
16.0	100	100
8.0	100	47.3
4.0	100	0
2.0	56.8	0
1.0	35.0	0
0.50	22.7	0
0.25	16.4	0
Specific gravity (gr/cm^3)	2.42	1.71

3.1.5. Steel Fiber

Hooked-end bundled steel fibers were used with three different aspect ratios (l/d: length over diameter ratios) of 55, 65, and 80 (Figure 3.7). The physical and mechanical properties of steel fibers are given in Table 3.4.

Table 3.4 Physical and mechanical properties of steel fibers

Length (L), mm	Diameter (d), mm	Aspect ratio (L/d)	Density, g/m^3	Tensile Strength, N/mm^2
60	0.75	80	7.85	1050
60	0.92	65	7.85	1160
30	0.55	55	7.85	1345
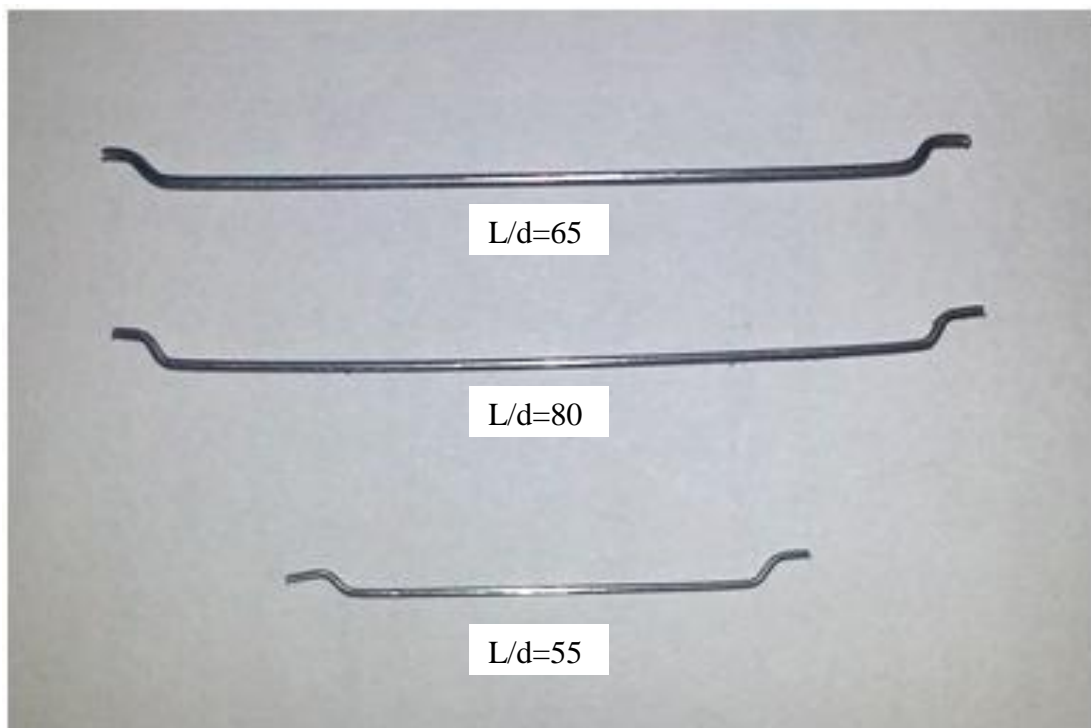
Figure 3.7 Hooked-end steel fibers

3.1.6. Steel Bar

Reinforcing ribbed steel bars having 16 mm diameter and minimum yield strength of 420 MPa were utilized for preparing the reinforced concrete specimens to be used for testing the bonding strength.

3.2. Concrete Mixture Details

To investigate the effect of cold bonded lightweight fly ash aggregates volume fraction and steel fibers on mechanical and fracture properties of concrete, 26 concrete mixes, plain and reinforced by steel, were designed with constant water-to-cement ratio (w/c) of 0.40. Concrete containing two different cold bonded fly ash lightweight aggregate volume fractions of 45% and 60% was produced. Besides, to improve the mechanical and fracture properties of lightweight concrete, the steel fiber was added during casting. For that purpose, the steel fibers with three different aspect (length/diameter) ratios of 55, 65 and 80 and four different volume fractions of 0.35%, 0.70%, 1.0%, and 1.5% as the total volume of concrete was used.

The slump test was carried out in accordance with BS EN 12350-2 (BS EN 12350-2, 2009) and the test results were in the range of 15±2 cm and 8±2 cm for steel fiber volume fraction of low (<1%) and moderate (>1%), respectively.

Mix proportions for 1-m^3 concrete are given in Table 3.5. In mix ID, volume fraction of lightweight aggregate is represented by L while the volume fraction and aspect ratio of steel fiber are denoted by F and A, respectively. For example, L45F35A55 indicates that the concrete mixture is designed with LWA content of 45%, steel fiber content of 0.35%, and steel fiber aspect ratio of 55.

Table 3.5 Mix proportions for 1 m³ concrete (in kg/m³)

Mix ID	Cement	Water	SP* (%)	SP*	Crushed limestone sand	Volume fraction of LWA* (%)	LWA*	Volume fraction of SF* (%)	SF*
L45F0A0	400	160	3	12	935.5	0.45	540.8	0	0
L45F35A55	400	160	3	12	935.5		540.8	0.35	27.475
L45F35A65	400	160	3	12	935.5		540.8	0.35	27.475
L45F35A80	400	160	3	12	935.5		540.8	0.35	27.475
L45F70A55	400	160	3	12	935.5		540.8	0.70	54.95
L45F70A65	400	160	3	12	935.5		540.8	0.70	54.95
L45F70A80	400	160	3	12	935.5		540.8	0.70	54.95
L45F100A55	400	160	3	12	935.5		540.8	1.00	78.5
L45F100A65	400	160	3	12	935.5		540.8	1.00	78.5
L45F100A80	400	160	3	12	935.5		540.8	1.00	78.5
L45F150A55	400	160	3	12	935.5		540.8	1.50	117.75
L45F150A65	400	160	3	12	935.5		540.8	1.50	117.75
L45F150A80	400	160	3	12	935.5		540.8	1.50	117.75

Table 3.5 (Continue) Mix proportions for 1 m^3 concrete (in kg/m^3)

Mix ID	Cement	Water	SP* (%)	SP*	Crushed limestone sand	Volume fraction of LWA* (%)	LWA*	Volume fraction of SF* (%)	SF*
L60F0A0	400	160	2	8	683.6	0.60	724.6	0	0
L60F35A55	400	160	2	8	683.6		724.6	0.35	27.475
L60F35A65	400	160	2	8	683.6		724.6	0.35	27.475
L60F35A80	400	160	2	8	683.6		724.6	0.35	27.475
L60F70A55	400	160	2	8	683.6		724.6	0.70	54.95
L60F70A65	400	160	2	8	683.6		724.6	0.70	54.95
L60F70A80	400	160	2	8	683.6		724.6	0.70	54.95
L60F100A55	400	160	2	8	683.6		724.6	1.00	78.5
L60F100A65	400	160	2	8	683.6		724.6	1.00	78.5
L60F100A80	400	160	2	8	683.6		724.6	1.00	78.5
L60F150A55	400	160	2	8	683.6		724.6	1.50	117.75
L60F150A65	400	160	2	8	683.6		724.6	1.50	117.75
L60F150A80	400	160	2	8	683.6		724.6	1.50	117.75

*SP: Superplasticizer, LWA: Lightweight aggregate, SF: Steel fiber

3.3.   Specimen Preparation and Curing

Power-driven revolving pan mixer with capacity of 30 liter was used to mix all concrete with following the special procedure for batching and mixing. Cold bonded artificial lightweight fly ash aggregates were used as coarse aggregates for all of the concrete mixtures. Before each mixing, sufficient LWA were immersed in water for 30 min for saturation. Then the LWA was taken out of water and put on mesh for the outflow of excessive surface water for about 30 s. The extra water on the surface of the pellets was rubbed out manually by a dry towel (Figure 3.8). This is an effective way to obtain SSD condition for the artificial lightweight aggregates (Gesoğlu, 2004; Joseph and Ramamurthy, 2009; Gesoğlu et.al., 2012).

The saturated surface dry aggregate and cement were poured and mixed in the mixer. Then, crushed limestone sand was added on aggregate-cement mixture. Water and superplasticizer were mixed before pouring into the mixer. After adding of water, the mixture was mixed for 5 min. Finally, steel fibers, which waited in the water for about 10 min to solve the glue between fibers and prevent the workability loss of fresh concrete (Figure 3.7), were added on the fresh concrete and allowed to be mixed until good dispersion of steel fiber was observed.

Since the capacity of the mixer is not enough for the needed volume of the mixture, two identical batches were produced with same procedure and materials. As an end, concrete was poured into the steel moulds in two and three layers for plain and steel fiber concrete, respectively, with vibration for a couple of seconds. Following the concrete casting, all moulded specimens were wrapped with plastic sheet and left in the casting room for 24 h at 20±2 °C and then they were demoulded and cured in water for 28 days.

Specimens were cast from each mixture consisted of three 150x150x150-mm cubes for compressive strength testing, three 150x150x150-mm cubes for bonding strength testing, three Φ150x300-mm cylinders for splitting tensile strength determination, three Φ150x300-mm cylinders determination of modulus of elasticity, three 100x100x500 prisms for determination of fracture energy and flexural strength, were utilized. Transverse notches having 5 mm width and 40 mm height were open in the middle of the beam specimens one day before the testing.
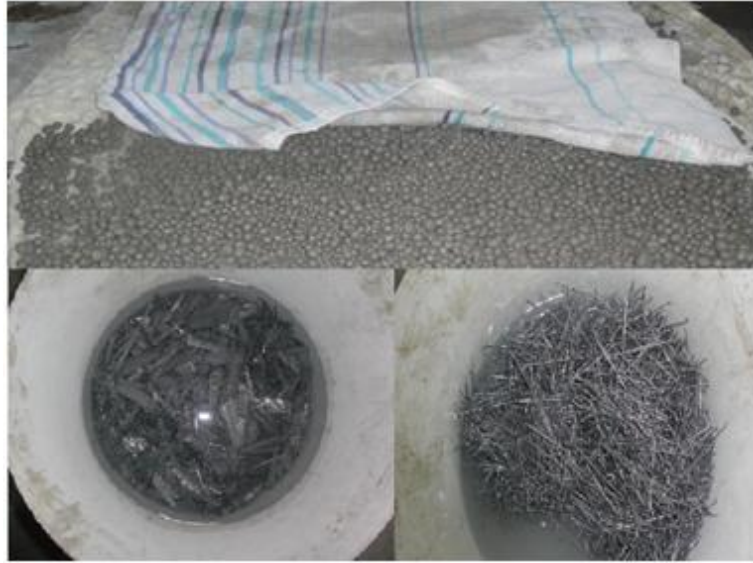
Figure 3.8 Saturation of LWA and waiting the steel fibers in water

3.4. Test Methods

The mechanical and fracture tests were all carried out at the age of 28 days.

3.4.1. Compressive Strength

The compression test was conducted on cube specimens (150x150x150 mm) by a 2000 kN capacity testing machine with respect to ASTM C39 (ASTM C496, 2011) as shown in Figure 3.9. Average of three specimens was reported for each parameter.

Figure 3.9 Compressive strength test machine with 2000 kN capacity

3.4.2. Splitting Tensile Strength

Splitting tensile strength was performed on the specimens having $\Phi 150\text{x}300$ mm size according to the specification per ASTM C496 (ASTM C496, 2011). Three test specimens were utilized for each parameter. Splitting tensile strength of a cylinder specimen is obtained using the following equation:

$$f_{\text{st}} = \frac{2P}{\pi h \Phi} \tag{3.2}$$

where P, h, and Φ are the maximum load, length and diameter of the cylinder specimen, respectively.

3.4.3. Modulus of Elasticity

Static modulus of elasticity was determined by the testing of cylinders with a dimension of $\Phi 150\text{x}300$ mm according to ASTM C469 (ASTM C469/C469M-10, 2010). Each of the specimens was fitted with a compressometer containing a dial gage capable of measuring deformation to 0.002 mm (Figure 3.10) and then loaded three times to 40% of the ultimate load. The ultimate load was determined based on the compressive strength test results for each mix. The first set of readings of each cylinder was discarded and the modulus was reported as the average of the second two sets of readings. For each parameter, three specimens were used.

Figure 3.10 Measuring of modulus of elasticity

3.4.4. Fracture Energy

The test for the determination of the fracture energy (G_f) was conducted with respect to the recommendation of RILEM 50-FMC Technical Committee (RILEM 50-FMC, 1985). The displacement was measured simultaneously by using a linear variable displacement transducer (LVDT) at mid-span. A closed-loop testing machine (Instron 5590R) with a maximum capacity of 250 kN was used to apply the load. The details of the testing machine and specimen as well as placing linear variable displacement transducer (LVDT) were shown in Figure 3.12.

Figure 3.11 Universal testing devices and three point flexural testing fixture
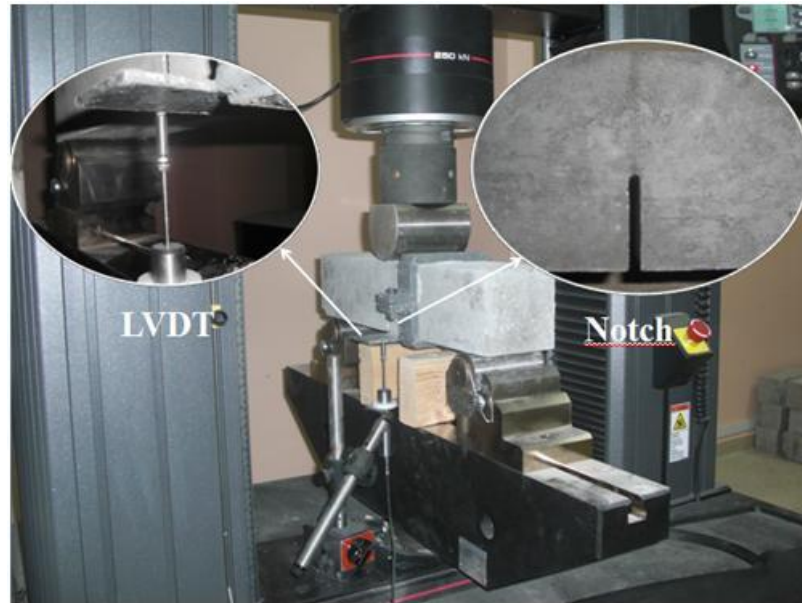
a)
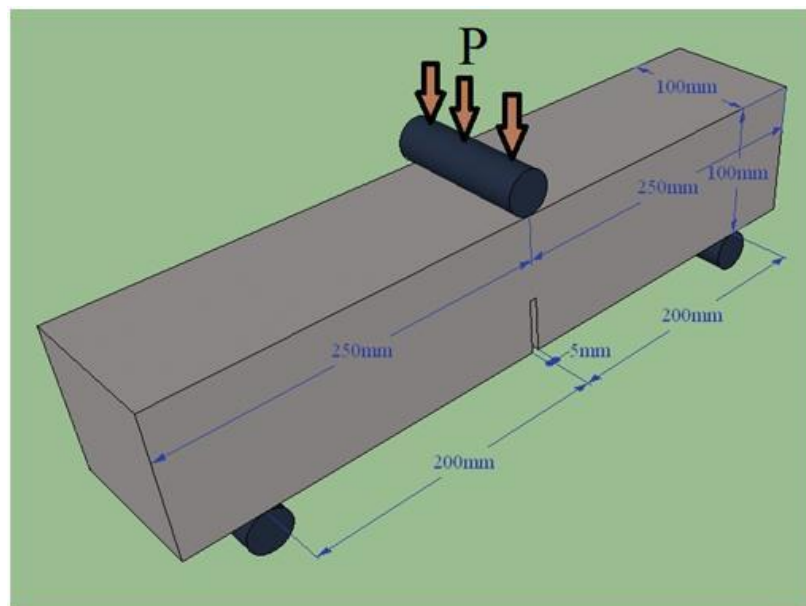
b)

Figure 3.12 a) Photographic view of notched beam specimen b) Dimensions of the notched beam specimen

The beams with 500 mm in length and 100x100 mm in cross-section were prepared for the fracture energy test. The notch to depth ratio (a/D) of specimens was 0.4 and the notch opening was achieved through reducing the effective cross section to 60x100 mm by sawing in order to accommodate large aggregates in more abundance, and the distance between supports was 400 mm. Load versus deflection at the mid-

span (δ) curve was obtained for each specimen and area under the load versus displacement at mid-span (W_o) was used in the determination of the fracture energy. The fracture energy was calculated by using the formula given by RILEM 50-FMC Technical Committee (RILEM 50-FMC, 1985).

$$G_F = \frac{W_o + mg\frac{S}{U}\delta_s}{B(W-a)} \tag{3.3}$$

where B, W, a, S, U, m, δ_s, and g are the width, depth, notch depth, span, length, mass, specified deflection of the beam (for fiber reinforced concrete $\delta_s = 10$ mm) and gravitational acceleration, respectively. At least three specimens for each concrete mixture were tested at 28-day age. For the plain concrete, calculation of fracture energy is based on the area under the complete load versus displacement at mid span curve. For the concrete with steel fiber, however, fracture energy was calculated with respect to the area under the load versus displacement curve up to a specified displacement. 10-mm displacement was chosen as cut-off point. The plain beams were loaded at a constant rate of 0.02 mm/min, while beams with steel fiber were loaded with a rate of 0.3 mm/min till 2-mm displacement and with a rate of 1.5 mm/min till 10-mm displacement.

The notched beams were used to calculate the net flexural strength using the following equation on the assumption that there is no notch sensitivity, where P_{max} is the ultimate load.

$$f_{\text{flex}} = \frac{3P_{max}S}{2B(W-a)^2} \tag{3.4}$$

By the following expression, the brittleness of materials can be determined in terms of characteristic length (Hillerborg, 1985):

$$l_{\text{ch}} = \frac{EG_F}{f_{st}^2} \tag{3.5}$$

where f_{st}, E, and G_F are the splitting tensile strength, static modulus of elasticity, and fracture energy, respectively. In this study, splitting tensile strength was used instead of direct tensile strength.

In order to emphasize the increase in ductility of concrete by using steel fibers is calculated by the following formula.

$$\text{ductility ratio} = \frac{G_F[\text{concrete with fibers}]}{G_F[\text{plain concrete}]} \qquad (3.6)$$

3.4.5. Bonding Strength

Bonding strength of the concrete was determined with respect to RILEM RC6 (RILEM RC6, 1996). Bonding strength, τ, is calculated by the following equation:

$$\tau = \frac{F}{\pi \; x \; d \; x \; L} \qquad (3.7)$$

where F is the tensile load at failure (N), d and L are the diameter (mm) and embedment length (mm) of the reinforcing steel bar, respectively. Due to using 16-mm steel bar and 150-mm cubic specimen in this study, d and L are taken as 16 mm and 150 mm. Details of the bonding strength test specimen is demonstrated in Figure 3.13. Universal testing machine with the capacity of 600 kN was used for the loading by installation of specially modified test apparatus to it (Figure 3.14).
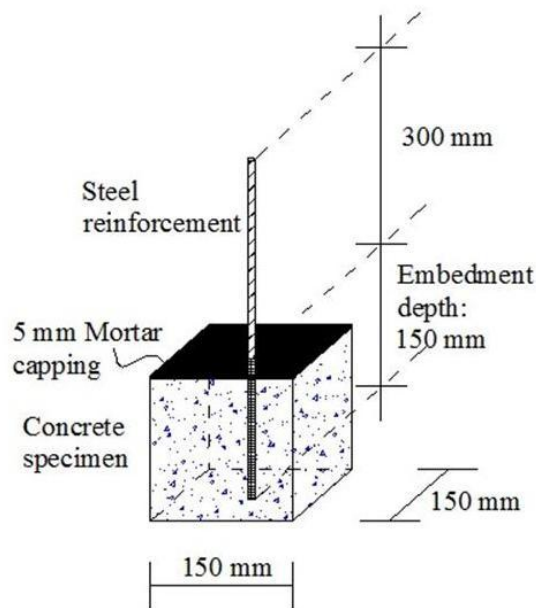
Figure 3.13 Details of the bond strength test specimen

Figure 3.14 Photographic view of the pullout test set up during testing the specimen

CHAPTER 4

4. TEST RESULTS AND DISCUSSIONS

The mechanical and fracture properties of lightweight cold bonded fly ash aggregate concrete reinforced with steel fiber are investigated in this thesis. The summary of test results regarding the compressive, splitting tensile, flexural and bond strength, modulus of elasticity, fracture energy, characteristic length and ductility ratio of concretes produced with two artificial lightweight aggregate volume fractions, three different steel fiber aspect ratios and four steel fiber volume fractions are given in Tables 1-7. The data presented in these tables were used for graphical presentation of the test results for evaluation and discussion.

4.1. Compressive Strength

Compressive strength test results obtained from cubic specimens are given in Table 4.1 and plotted in Figure 4.1. The variation in compressive strength of concrete with 45% LWA and 60% LWA versus steel fiber volume fraction with different aspect ratio are shown in Figure 4.1a and 4.1b, separately. The compressive strength values of plain concretes of 45% and 60% LWA are 43.1 and 39.1 MPa, respectively. It was observed that the compressive strength value of almost 40 MPa can be achieved in LWAC. The compressive strengths ranging from 39.1 to 46.8 MPa for all mixtures satisfied the lower limit (17.2 MPa) to be used for structural purposes (ACI committee 213, 1987). The higher compressive strength value can be obtained by the decreasing the LWA content due to being the artificial fly ash aggregates weaker than the matrix. In the study of Gesoğlu et al. (2004), the similar findings was reported such that the increasing the amount of lightweight aggregate resulted in gradually decreasing of compressive strength. The plain concrete with 45% LWA has

almost 10% more strength than with 60% LWA. This difference between 45% LWA and 60% LWA concretes decreases to below 5% by addition steel fiber. The steel fiber with aspect ratio of 65 has more significant effect on the compressive strength than aspect ratio of 55 and 80. Although steel fiber utilization results in increasing of concrete, the increase is not significant. While increasing the steel fiber volume fraction (V_f) from 0.35% to 1.0% has resulted in an increase of compressive strength for all type of aspect ratio, increasing from 1.0% to 1.5% resulted in the reduction in compressive strength of both 45% LWA and 60% LWA, but the compressive strength of concretes with 1.5% steel fiber is not below the plain concrete.

Using higher volume fraction of steel fiber may decrease the compressive strength due to the difficulty in dispersing the fiber and inadequate compaction of concrete (Gao et al., 1997). In addition to that, increasing of compressive strength up to 30% (Campione et al., 2001), 22% (Gao et al., 1997), 21% (Düzgün et al., 2005), 20% (Kang et al., 2011) and 14% (Shafigh et al., 2011) have also been reported in steel fiber LWAC with good workability (Hassanpour et al., 2012). However, it is reported by some researchers that the compressive strength of high strength lightweight aggregate concrete is not affected by utilization of steel fiber (Altun, 2006; Balendran et al., 2002).

As a result, it can be concluded that the effect of the volume fraction of steel fiber on compressive strength is not consistent and steel fiber utilization may result in increasing the ductility in the compressive failure rather than increasing of compressive strength.

Table 4.1 Compressive strength of concretes

LWA volume fraction (V_a), %	Steel fiber aspect ratio (L/d)	Steel fiber volume fraction (V_f), %	Compressive strength (f_c), MPa	LWA volume fraction (V_a), %	Steel fiber aspect ratio (L/d)	Steel fiber volume fraction (V_f), %	Compressive strength (f_c), MPa
45	**-**	**-**	**43.1**	**60**	**-**	**-**	**39.1**
	55	0.35	43.8		55	0.35	42.1
	55	0.70	44.0		55	0.70	43.0
	55	1.00	45.0		55	1.00	43.6
	55	1.50	43.8		55	1.50	42.4
	65	0.35	44.0		65	0.35	42.9
	65	0.70	44.7		65	0.70	43.5
	65	1.00	46.8		65	1.00	44.4
	65	1.50	46.0		65	1.50	43.8
	80	0.35	43.9		80	0.35	42.8
	80	0.70	44.0		80	0.70	43.1
	80	1.00	45.5		80	1.00	44.1
	80	1.50	44.5		80	1.50	43.7
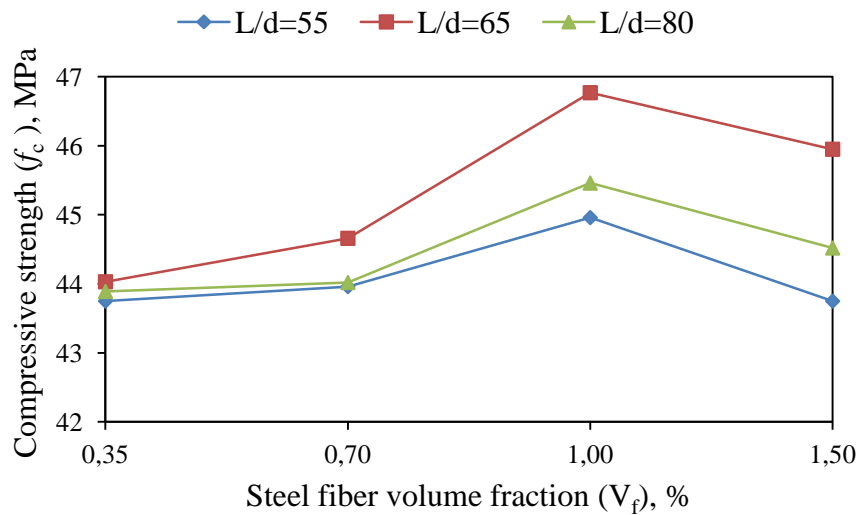
a)
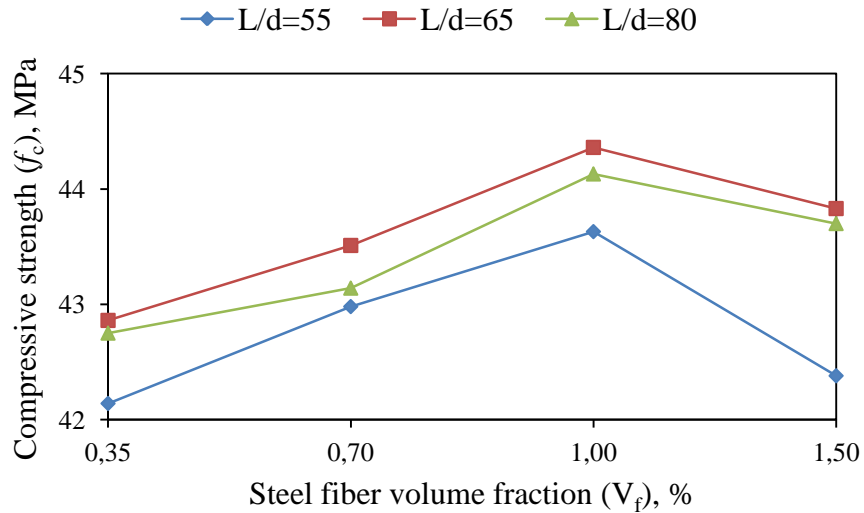
b)

Figure 4.1 Compressive strength versus steel fiber volume fraction with different aspect ratio: a) 45% LWA (In plain concrete, f_c = 43.1 MPa) and b) 60% LWA (In plain concrete, f_c = 39.1 MPa)

4.2. Splitting Tensile Strength

Splitting tensile strength values, evaluated from cylindrical specimens with the Equation 3.2, are presented in Table 4.2. The variation in splitting tensile strength of LWAC with 45% and 60% cold bonded fly ash lightweight aggregate versus steel fiber volume fraction with different aspect ratio are shown in Figure 4.3a-4.3b and Figure 4.4a-4.4b. The splitting tensile strengths of plain concrete of 45% and 60% LWA are 1.76 and 1.65 MPa, respectively. The decreasing the lightweight aggregate volume fraction increases the splitting tensile strength of concretes. Gesoğlu et al. (2004) reported similar result for cold bonded lightweight fly ash concretes. Due to being the artificial fly ash aggregates weaker than the matrix, this result occurs (Gesoğlu et al., 2004).

As the steel fiber volume fraction increases, the splitting tensile strength also increases. The increase of steel fiber volume fraction from 0 (plain concrete) to 1.5% has resulted in an increase of almost 58% in corresponding splitting tensile strength for the aspect ratio of 65 in both concrete with 45% and 60% LWA. The increasing amount for 55 and 80 of aspect ratio was almost 52% and 56%, respectively. The plain concrete compared to fiber reinforced concrete, the fiber reinforced concrete

has superior tensile properties (Wang et al., 1990). The steel fiber with aspect ratio of 65 has more significant effect on the splitting tensile strength than aspect ratio of 55 and 80. This result may be obtained due to the fact that the steel fiber with aspect ratio of 65 has larger cross-section area than aspect ratio of 55 and 80. The crack propagation in splitting tensile strength test was due to two different behaviors of steel fibers, one was the broken of steel fibers and the other one was pulling-out of fibers from the matrix. The concretes containing fewer cross-sections than aspect ratio of 65 might be failed due to both situations, but the concretes with aspect ratio of 65 might be failed because of just the pulling-out of fibers from the matrix.

Previous studies (Gao et al. 1997; Campione et al., 2001; Balendran et al., 2002; Kayali et al., 2003; Chen et al., 2004; Campione et al., 2005; Chen and Liu, 2005; Düzgün et al., 2005; Domagala, 2011; Libre et al., 2011; Shafigh et al., 2011) have shown that the addition of steel fiber to LWAC less than 0.5% (very low volume fraction) increases the splitting tensile strength, when compared to concrete without fiber, in the range of 16-61%, addition of steel fiber between 0.5 and 1.0% (low ratio) increases splitting tensile strength of about 19-116% and utilization of steel fiber between 1.0 and 2.0% (higher volume fraction) resulted in an increase between 61-118% have been reported.

While after the failure of the cylindrical specimens without steel fiber, the specimen spliced, utilization of steel fiber prevented the splicing of the specimen (Figure 4.2).

a)

b)

Figure 4.2 Photographic views of splitting tensile test specimens: a) plain concrete and b) including steel fiber

Table 4.2 Splitting tensile strength of concretes

LWA volume fraction (V_a), %	Steel fiber aspect ratio (L/d)	Steel fiber volume fraction (V_f), %	Splitting tensile strength, (f_{st}), MPa	LWA volume fraction (V_a), %	Steel fiber aspect ratio (L/d)	Steel fiber volume fraction (V_f), %	Splitting tensile strength, (f_{st}), MPa
45	**-**	**-**	**1.76**	**60**	**-**	**-**	**1.65**
	55	0.35	2.03		55	0.35	1.88
	55	0.70	2.42		55	0.70	2.14
	55	1.00	2.98		55	1.00	2.86
	55	1.50	3.68		55	1.50	3.42
	65	0.35	2.33		65	0.35	2.19
	65	0.70	2.81		65	0.70	2.65
	65	1.00	3.76		65	1.00	3.44
	65	1.50	4.18		65	1.50	3.99
	80	0.35	2.26		80	0.35	2.16
	80	0.70	2.75		80	0.70	2.49
	80	1.00	3.52		80	1.00	3.36
	80	1.50	3.92		80	1.50	3.77
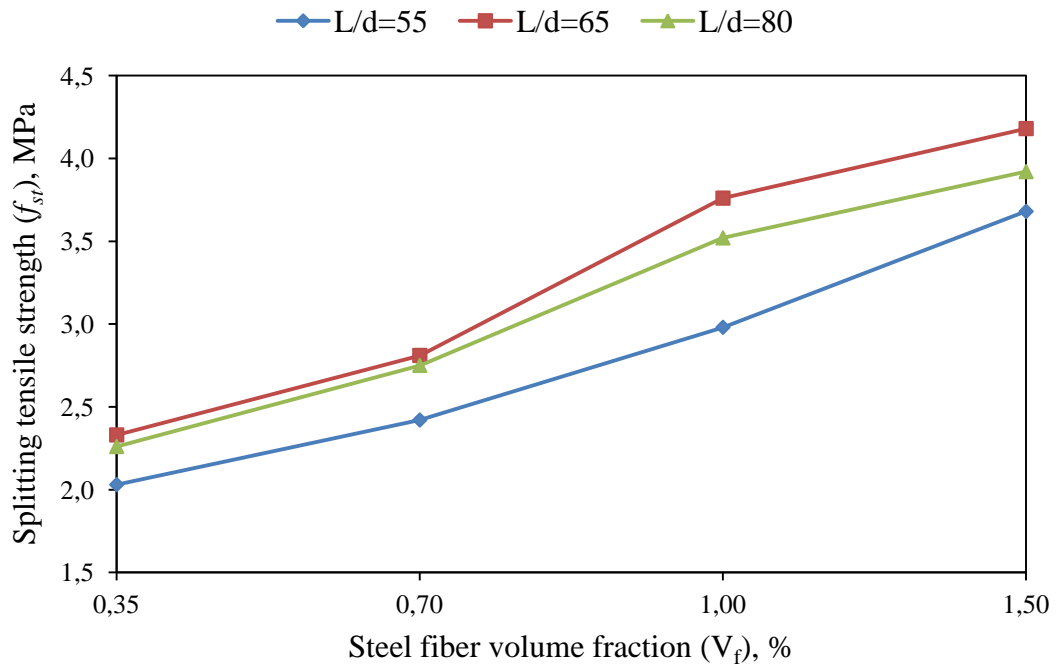
a)
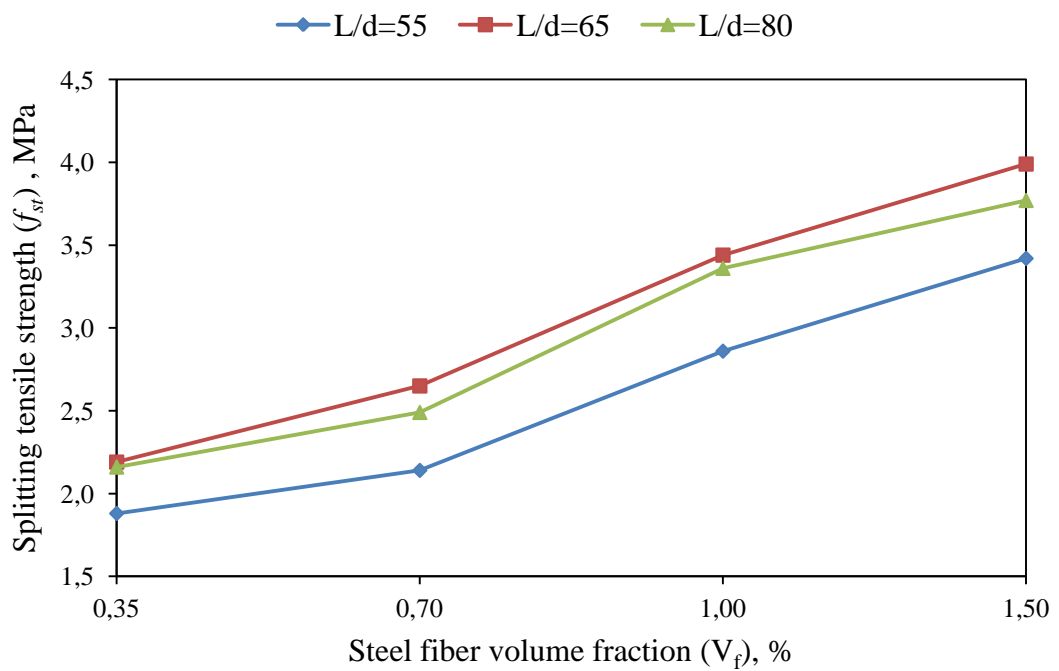
b)

Figure 4.3 Splitting tensile strength versus steel fiber volume fraction with different aspect ratio: a) 45% LWA (In plain concrete, f_{st} = 1.76 MPa) and b) 60% LWA (In plain concrete, f_{st} = 1.65 MPa)
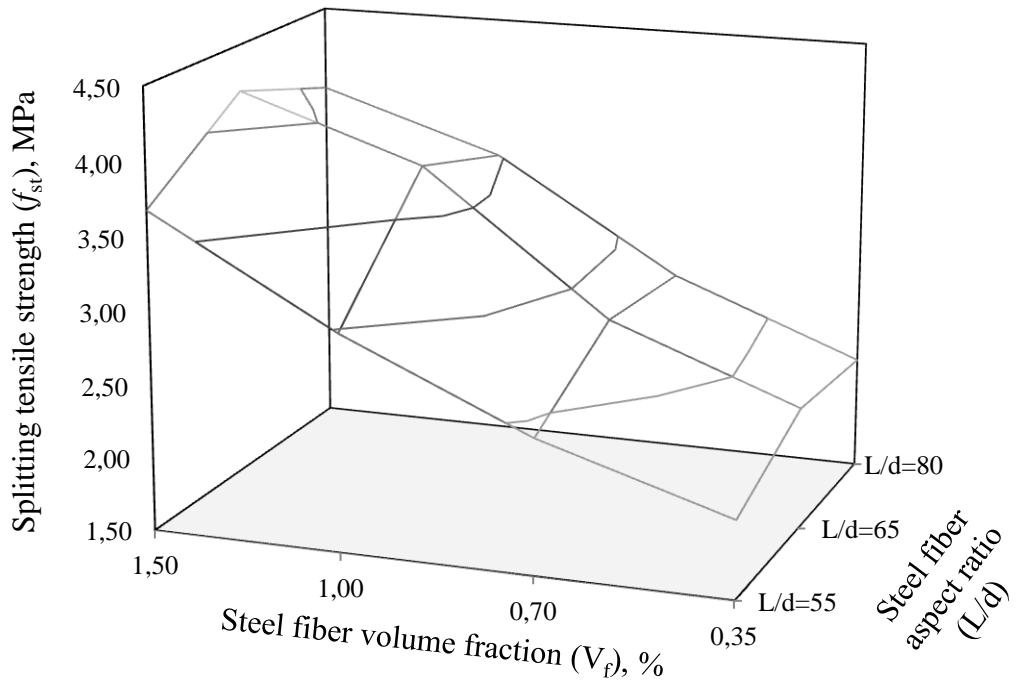
a)
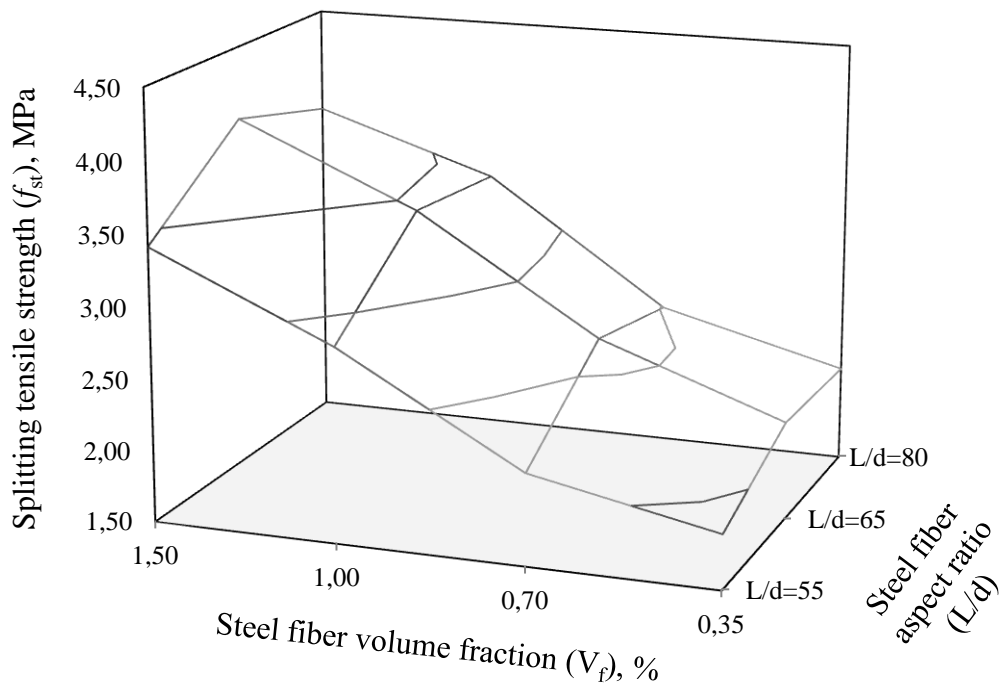
b)

Figure 4.4 Variation of f_{st} with L/d and V_f: a) 45% LWA and b) 60% LWA

4.3.   Modulus of Elasticity

Elasticity moduli values evaluated from cylindrical specimens are given in Table 4.3. The modulus of elasticity of concretes are range 24.8-28.2 GPa and 22.5-24.6 GPa for concrete with 45 and 60% LWA, respectively. The modulus of elasticity for plain concrete of 45 and 60% LWA are 28.2 and 24.6 GPa, respectively. Decreasing the amount of lightweight coarse aggregate content resulted in increase in modulus of elasticity like compressive and splitting tensile strength value. Some researchers also concluded that increasing the lightweight aggregate content in LWAC causes a lower modulus of elasticity (Düzgün et al., 2005; Kurugol et al., 2008). Moreover, as seen in Table 4.3, there was no significant effect of steel fiber and steel fiber volume fraction on modulus of elasticity. However, in the literature, the effect of steel fiber on elastic modulus of elasticity was contradictory. For example, Hassanpour et al. (2012) reported that the using steel fiber in LWAC did not enhance the modulus of elasticity. Whereas the increasing the modulus of elasticity by using steel fiber was observed in some studies (Campione et al., 2001; Kayali et al., 2003; Bilodeau et al., 2004; Domagala, 2011; Shafigh et al., 2011). Furthermore, the decreasing effect of steel fiber depending on type of LWA and steel fiber volume fraction was also reported in the technical literature (Bayramov et al., 2004; Campione et al., 2001; Kayali et al., 2003).

Table 4.3 Modulus of elasticity of concretes

LWA volume fraction (V_a), %	Steel fiber aspect ratio (L/d)	Steel fiber volume fraction (V_f), %	Modulus of elasticity (E), GPa	LWA volume fraction (V_a), %	Steel fiber aspect ratio (L/d)	Steel fiber volume fraction (V_f), %	Modulus of elasticity (E), GPa
45	**-**	**-**	**28.2**	**60**	**-**	**-**	**24.6**
	55	0.35	27.6		55	0.35	23.8
	55	0.70	26.9		55	0.70	23.2
	55	1.00	26.4		55	1.00	23.3
	55	1.50	26.1		55	1.50	22.7
	65	0.35	26.4		65	0.35	23.6
	65	0.70	26.1		65	0.70	23.8
	65	1.00	25.4		65	1.00	23.1
	65	1.50	25.0		65	1.50	23.4
	80	0.35	24.8		80	0.35	22.5
	80	0.70	25.1		80	0.70	22.6
	80	1.00	25.2		80	1.00	22.9
	80	1.50	25.4		80	1.50	23.5

4.4.   Net Flexural Strength

The net flexural strength values, evaluated with the Equation 3.4 from notched prismatic specimens (Figure 4.5a) subjected to three-point bending test (Figure 4.5b), are presented in Table 4.4. The variation in the net flexural strength of LWAC with 45% and 60% lightweight coarse aggregate versus steel fiber volume fraction with different aspect ratio are shown in Figure 4.6a-4.6b and Figure 4.7a-4.7b. The net flexural strength of plain concrete of 45% and 60% LWA are 3.31 and 3.09 MPa, respectively. The similar effect of lightweight aggregate amount was also obtained in the net flexural strength such that the net flexural strength decreases with increasing the lightweight coarse aggregate content. It is also due to being the matrix harder than artificial cold bonded fly ash aggregates.

Increasing the steel fiber fraction from 0 (plain concrete) to 1.5% has resulted in increasing the flexural strength up to 71% for the aspect ratio of 80, while the increasing amount was 65 and 69% for the aspect ratio of 55 and 65, respectively. The best results were obtained with the aspect ratio of 80, but the contribution degree of the steel fiber with aspect ratio of 55 and 65 on the net flexural strength can be ignored. The reason for increasing in the net flexural strength with utilization of steel fiber is that, after cracking of matrix, the steel fibers will carry the load subjected to concrete until the cracking of the interfacial bond between the fibers and the matrix (Gao et al., 1997). Therefore, resistance against cracks propagation occurs by utilization of steel fiber and it does not fail suddenly, this situation results in increasing of the load carrying capacity (Hassanpour et al., 2012). Gao et al. (1997) propounded that using steel fiber with higher aspect ratio seems to be more significant for increasing the flexural strength.

40 mm-Notch
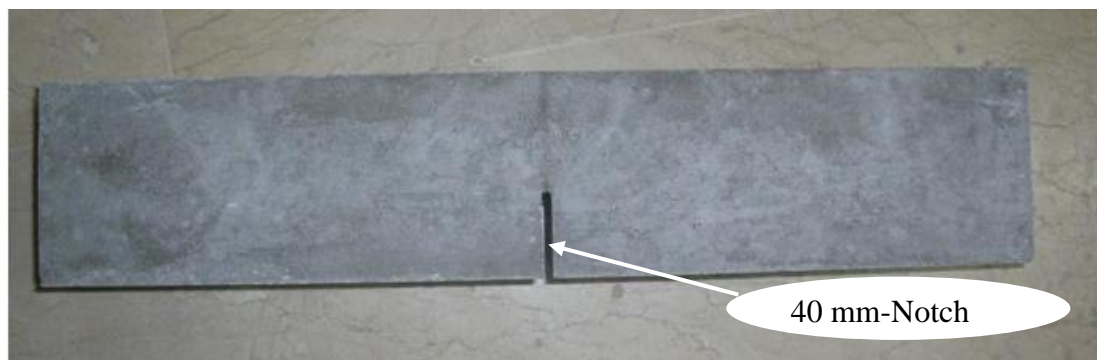
a)

b)

Figure 4.5 Photographic view of: a) notched beam and b) subjected to three-point

bending test

Table 4.4 Ultimate load and flexural strength of concretes

LWA volume fraction (V_a), %	Steel fiber aspect ratio (L/d)	Steel fiber volume fraction (V_f), %	Pmax, kN	Net flexural strength (f_{flex}), MPa	LWA volume fraction (V_a), %	Steel fiber aspect ratio (L/d)	Steel fiber volume fraction (V_f), %	Pmax, kN	Net flexural strength (f_{flex}), MPa
45	**-**	**-**	**1.99**	**3.31**	**60**	**-**	**-**	**1.85**	**3.09**
	55	0.35	2.06	3.43		55	0.35	1.99	3.32
	55	0.70	3.44	5.74		55	0.70	3.19	5.32
	55	1.00	4.37	7.28		55	1.00	3.98	6.63
	55	1.50	5.67	9.45		55	1.50	5.23	8.72
	65	0.35	2.08	3.47		65	0.35	2.05	3.41
	65	0.70	4.18	6.97		65	0.70	3.64	6.06
	65	1.00	5.56	9.44		65	1.00	5.29	8.81
	65	1.50	6.25	10.42		65	1.50	5.94	9.90
	80	0.35	2.23	3.72		80	0.35	2.18	3.64
	80	0.70	4.27	7.12		80	0.70	4.09	6.81
	80	1.00	6.03	10.05		80	1.00	5.50	9.16
	80	1.50	6.80	11.34		80	1.50	6.46	10.77
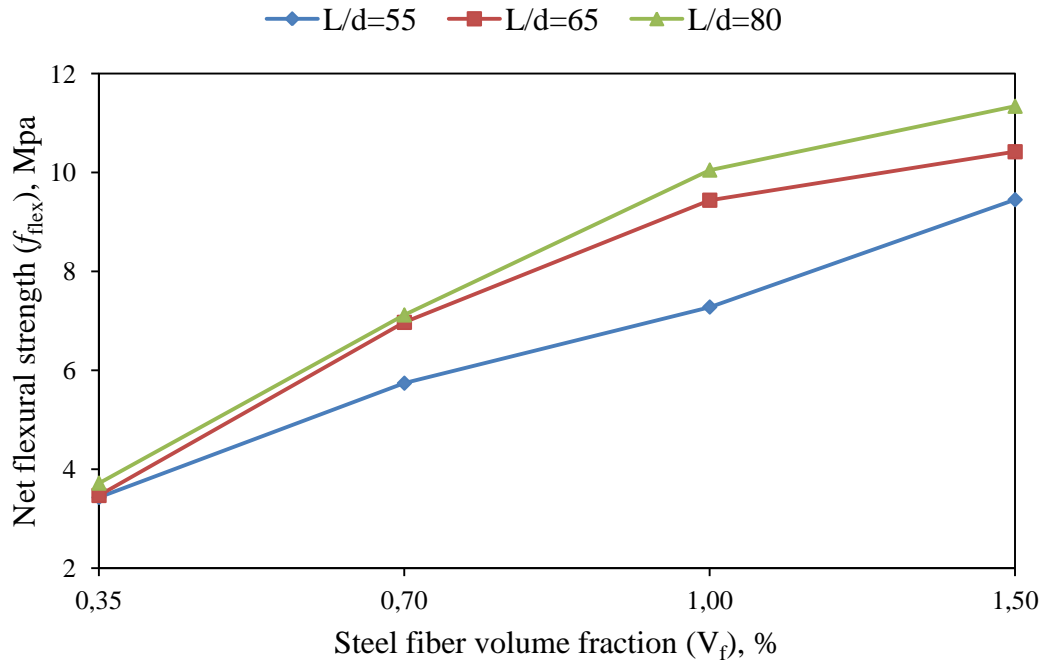
a)
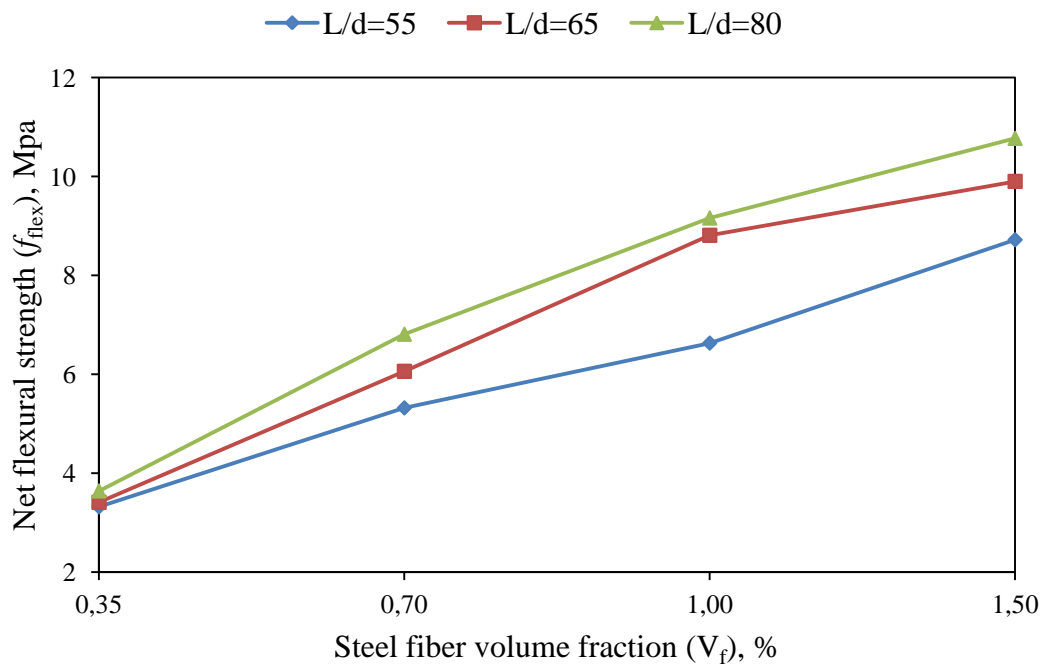
b)

Figure 4.6 Net flexural tensile strength versus steel fiber volume fraction with different aspect ratio: a) 45% LWA (In plain concrete, f_{flex} = 3.31 MPa) and b) 60% LWA (In plain concrete, f_{flex} = 3.09 MPa)
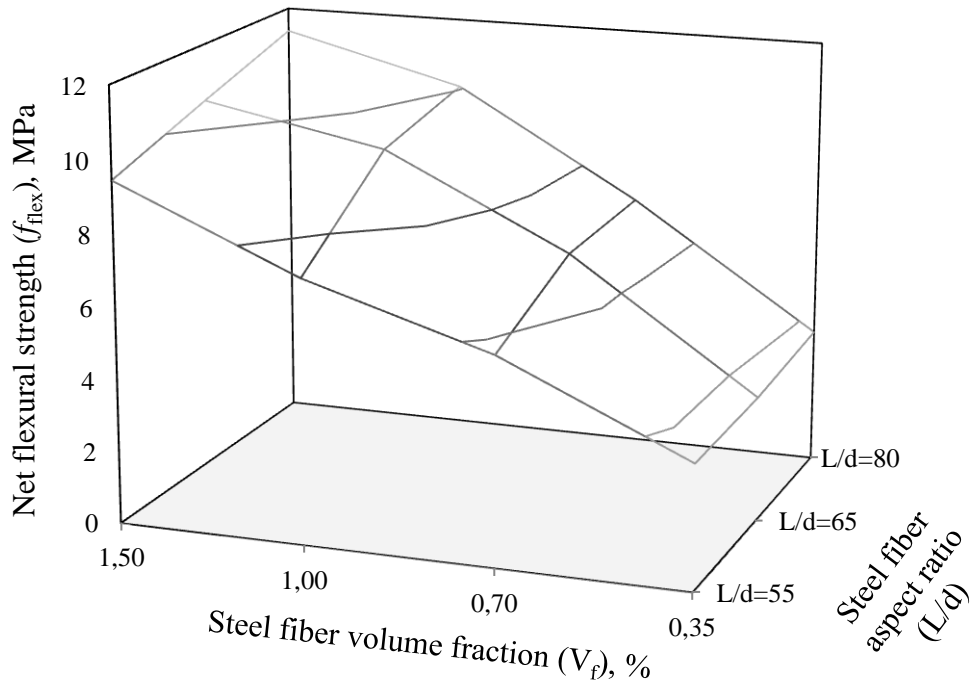
a)
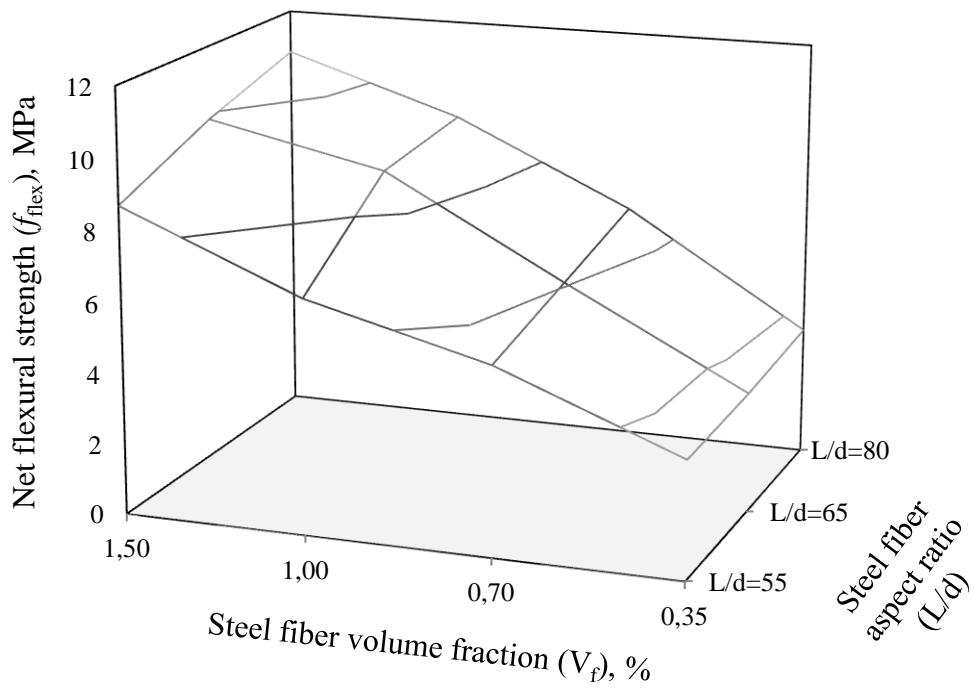
b)

Figure 4.7 Variation of f_{flex} with L/d and V_f: a) 45% LWA and b) 60% LWA

4.5. Fracture Parameters

4.5.1. Fracture Energy (G_F)

Fracture energy (G_F) values, evaluated with Equation 3.3 from notched beams (Figure 4.5a) subjected to three-point bending test (Figure 4.5b), are presented in Table 4.5. The variations in fracture energy of LWACs with 45% and 60% cold bonded fly ash aggregate versus steel fiber volume fraction with different aspect ratio are shown in Figure 4.8a-4.8b and Figure 4.9a-4.9b. The fracture energies of plain concrete of 45% and 60% LWA are 42 and 34.4 N/m, respectively. This lower fracture energy at 60% LWA utilization as compared with 45% LWA utilization is caused due to being artificial fly ash aggregates weaker than the matrix. Akçay and Taşdemir, used the crushed natural pumice as LWA, was also reported same conclusion for the effect of lightweight aggregate on the fracture energy (Akçay and Taşdemir, 2009).

The calculation of fracture energy consists of two parts; energy supplied by the actuator and by the own weight of the beam. The area under the load versus displacement curve was used in the calculation of fracture energy as the energy supplied by the actuator, and the weight of the beam was used in the calculation as the energy supplied by own weight of the beam. While in the plain concretes, the final displacement of the specimens was used in the calculation of energy supplied by own weight, in steel fiber reinforced concretes, the 10 mm displacement was chosen as cut-off point and it is used in the calculation.

As seems in Figure 4.10, the plain concrete with 45% LWA has higher the area under the load versus displacement curve than plain concrete with 60% LWA and also the concrete with 45% LWA is heavier than concrete with 60% LWA due to the using heavier material, crushed limestone sand, instead of 15% LWA. The utilization of steel fiber in concrete significantly increases the area under the load versus displacement curve and increasing the steel fiber volume fraction increases the area under the load versus displacement curve as well as the ultimate load as shown in Figure 4.11, 4.12, and 4.13. However, the increasing rate in the ultimate load is not as much as increasing rate in fracture energy. Increasing the steel fiber volume fraction from 0 (plain) to 1.5% resulted in the increase of the fracture energy more than 200 times, but it resulted in the increase of the ultimate load more than 2.5

69

times. This improving rate may be lower at the normal weight concrete (NWC) (Mehta and Monteiro, 2006). However, Libre et al. (2011) showed that the improving rate of fiber in LWAC is much higher than NWC and they commented this situation as being the brittleness of LWAC much higher than NWC.

As Figures 4.8 and 4.9 show, the best improvement in both ultimate load and fracture energy was obtained from aspect ratio of 80. While the enhancement rate of aspect ratio of 80 with increasing the fiber volume fraction from 0 (plain) to 1.5% was 281 and 256 times for concretes with 45% LWA and 60% LWA, respectively, this rate was 266 and 235 times for aspect ratio of 65 and 209 and 189 times for aspect ratio of 55. Bayramov et al. (2004) used the same steel fibers in NWC with volume fraction of 0.24, 0.46, and 0.64% and they reported similar improvement situation for aspect ratios but their improvement rates of aspect ratio of 55, 65 and 80 with increasing the volume fraction from 0 (plain) to 0.64% were 37, 41, and 48 times, respectively.

Table 4.5 Fracture energy and ductility ratio of concretes

LWA volume fraction (V_a), %	Steel fiber aspect ratio (L/d)	Steel fiber volume fraction (V_f), %	Fracture energy (G_F), N/m	Ductility ratio, %	LWA volume fraction (V_a), %	Steel fiber aspect ratio (L/d)	Steel fiber volume fraction (V_f), %	Fracture energy (G_F), N/m	Ductility ratio, %
45	**-**	**-**	**42**	**1**	**60**	**-**	**-**	**34.4**	**1**
	55	0.35	1628.8	39		55	0.35	1301.8	38
	55	0.70	2968.6	71		55	0.70	2485.4	72
	55	1.00	4905.6	117		55	1.00	4683.9	136
	55	1.50	7894.8	188		55	1.50	7185.1	209
	65	0.35	2184.7	52		65	0.35	1764.6	51
	65	0.70	3854.9	92		65	0.70	3395.8	99
	65	1.00	7652.4	182		65	1.00	6804.2	198
	65	1.50	9678.9	230		65	1.50	9148.9	266
	80	0.35	2654.4	63		80	0.35	2389.7	69
	80	0.70	4582.3	109		80	0.70	4095.8	119
	80	1.00	8338.6	199		80	1.00	7764.6	226
	80	1.50	10754.5	256		80	1.50	9681.1	281
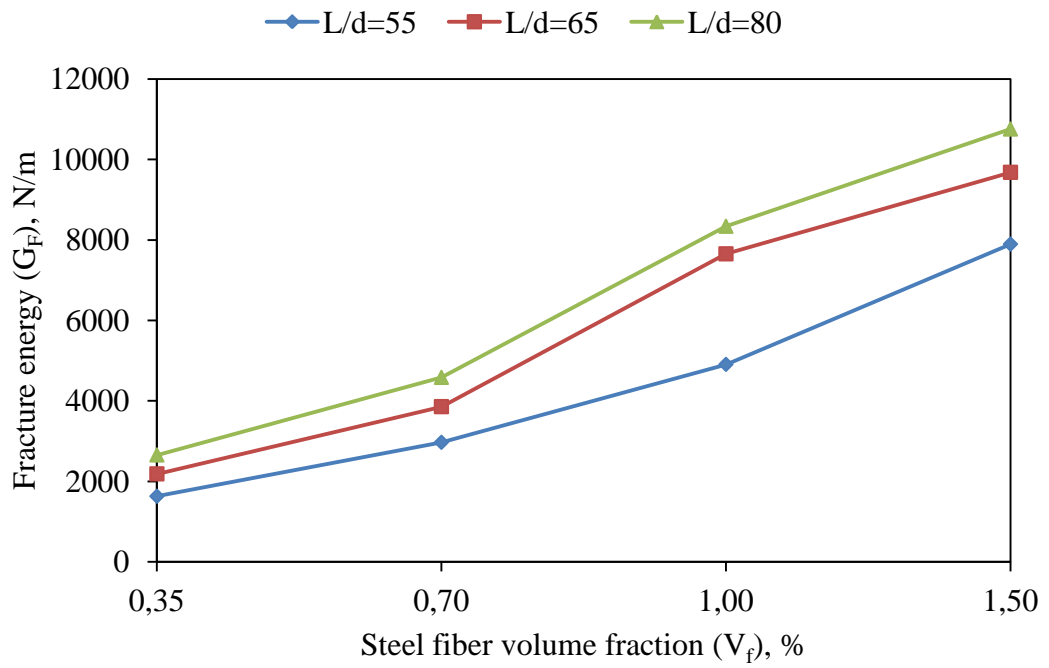
a)
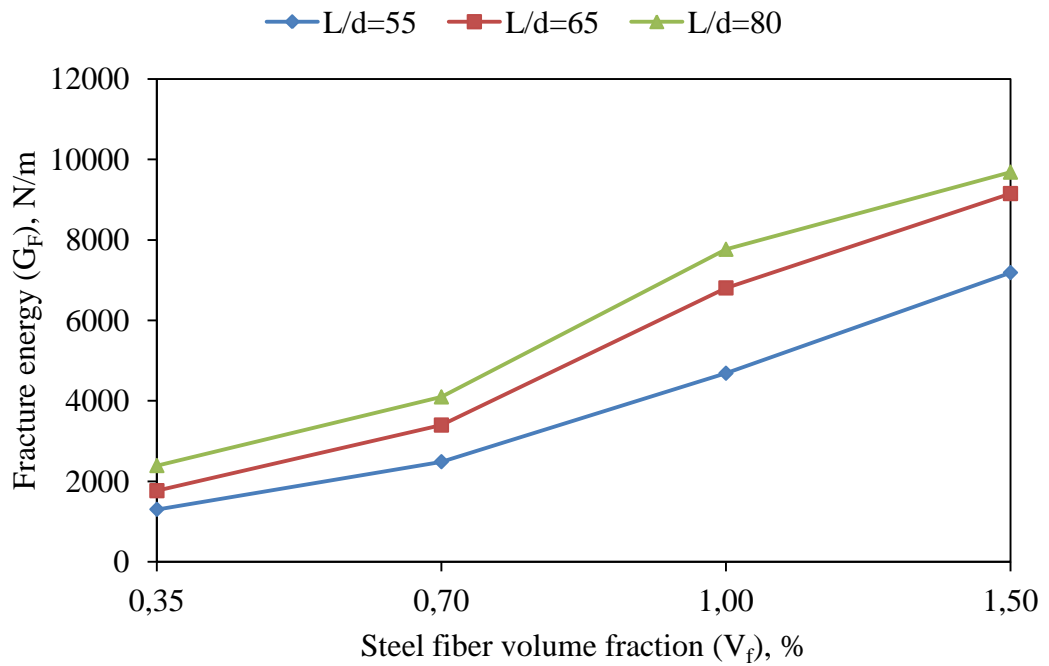
b)

Figure 4.8 Fracture energy versus fiber volume fraction with different aspect ratio: a) 45% LWA (In plain concrete, $G_F = 42.0$ N/m) and b) 60% LWA (In plain concrete, $G_F = 34.4$ N/m)
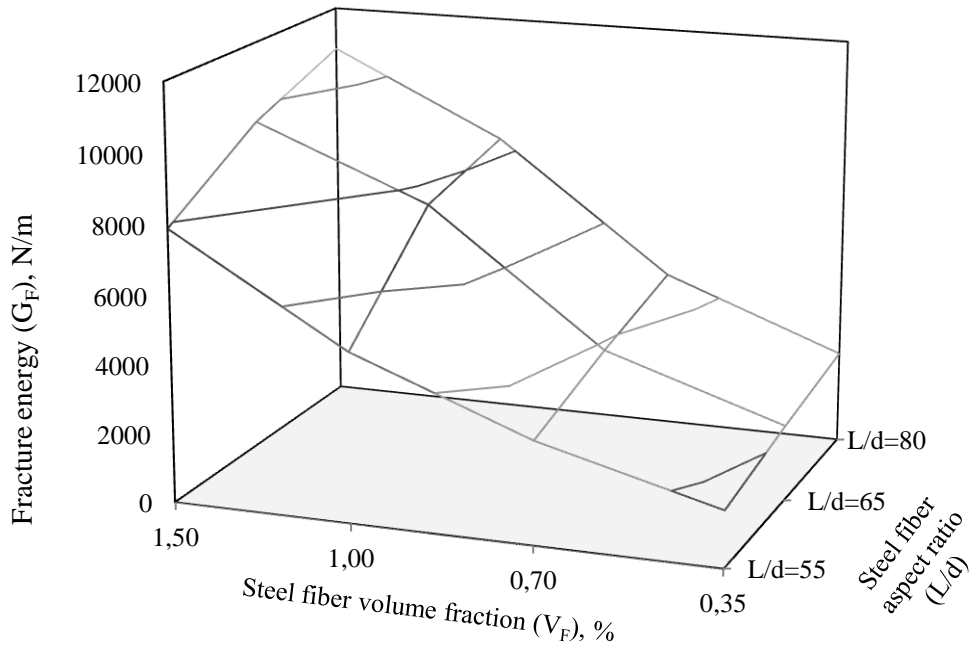
a)
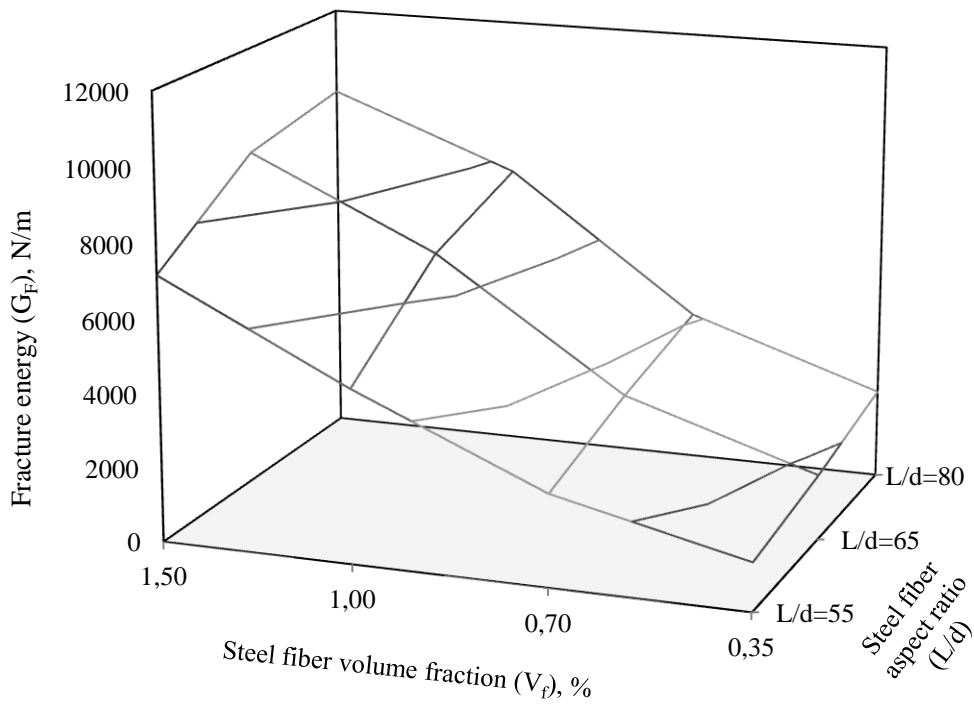
b)

Figure 4.9 Variation of G_F with L/d and V_f: a) 45% LWA and b) 60% LWA
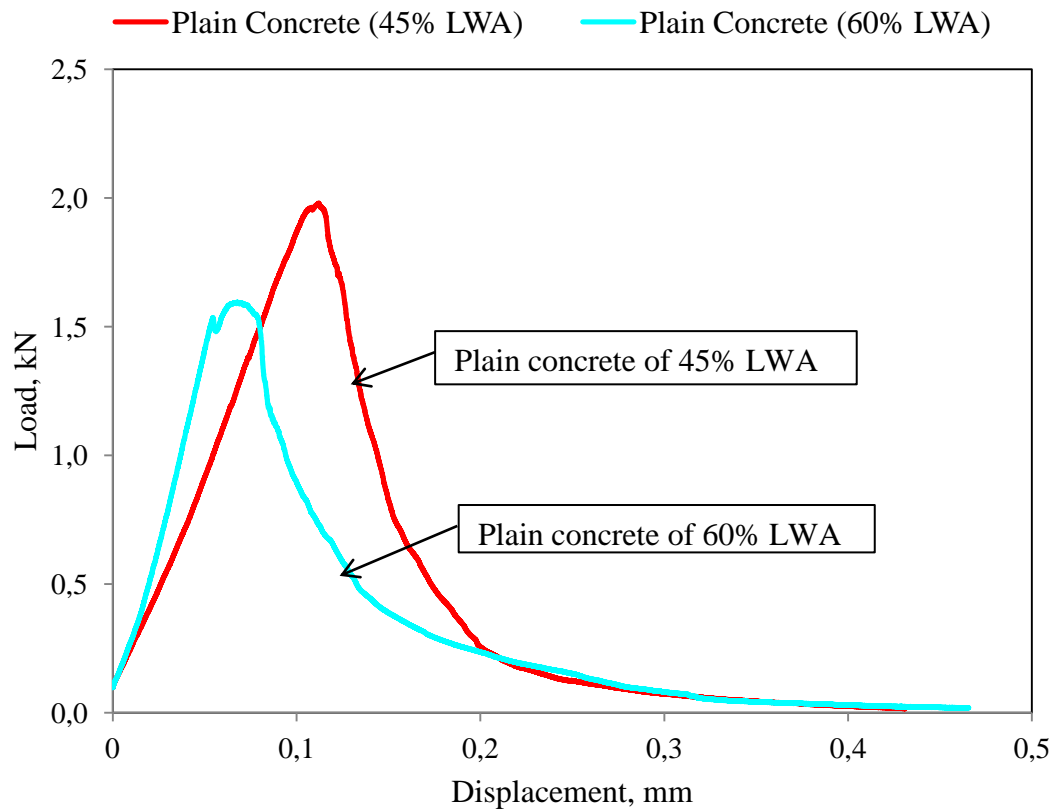
Figure 4.10 Typical load versus displacement curves of plain concretes contained 45% and 60% LWA
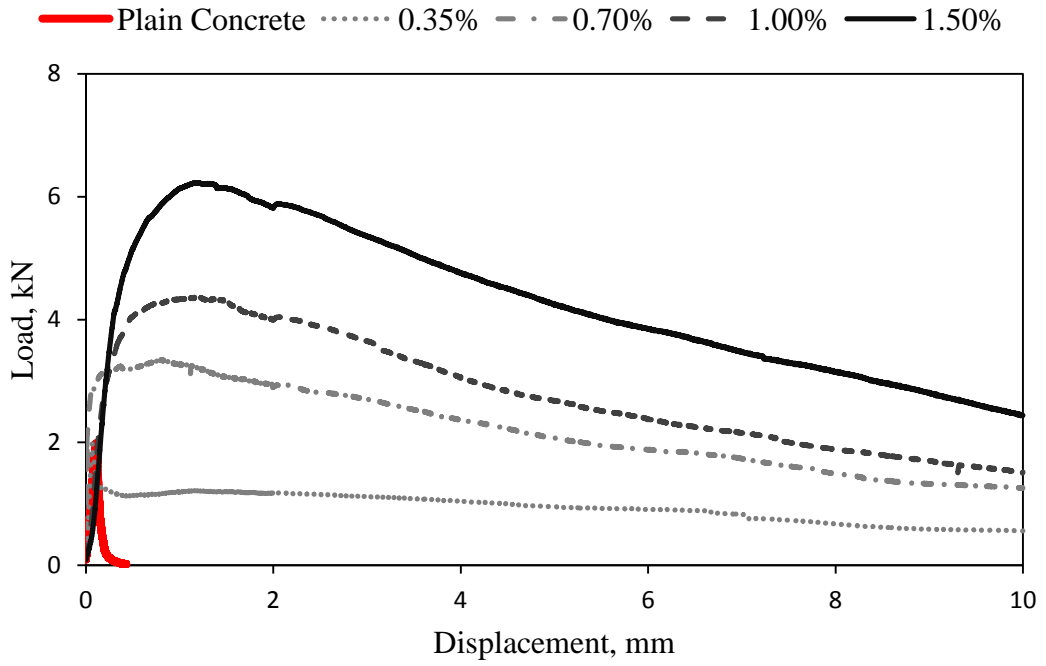
a)
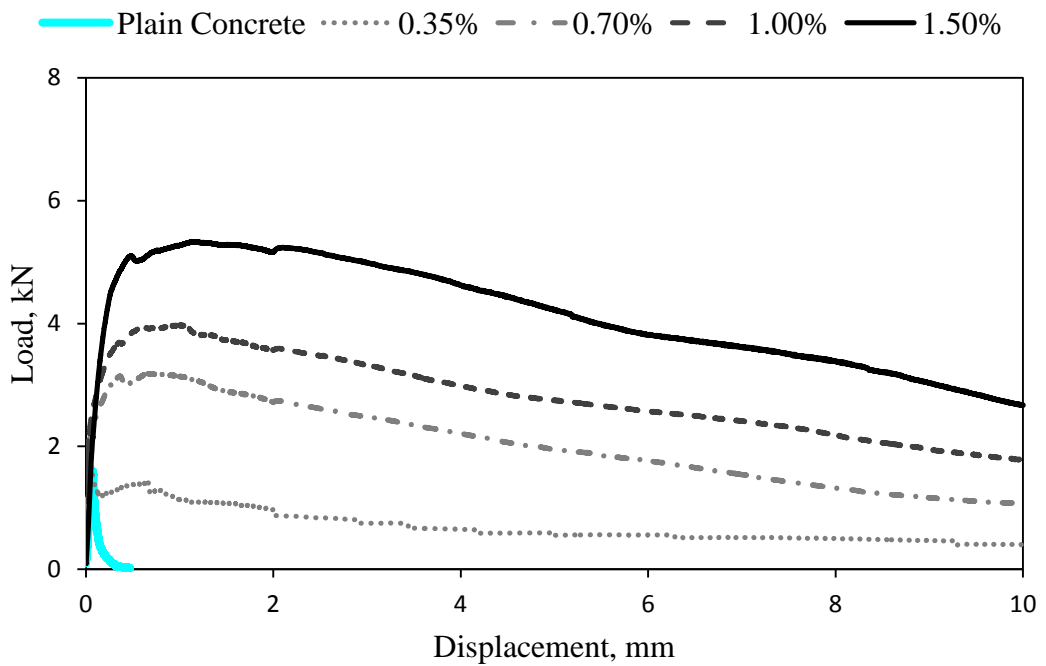
b)

Figure 4.11 Typical load versus displacement curves of L/d=55 with respect to steel fiber volume fraction: a) concretes containing 45% LWA and b) concretes containing 60% LWA
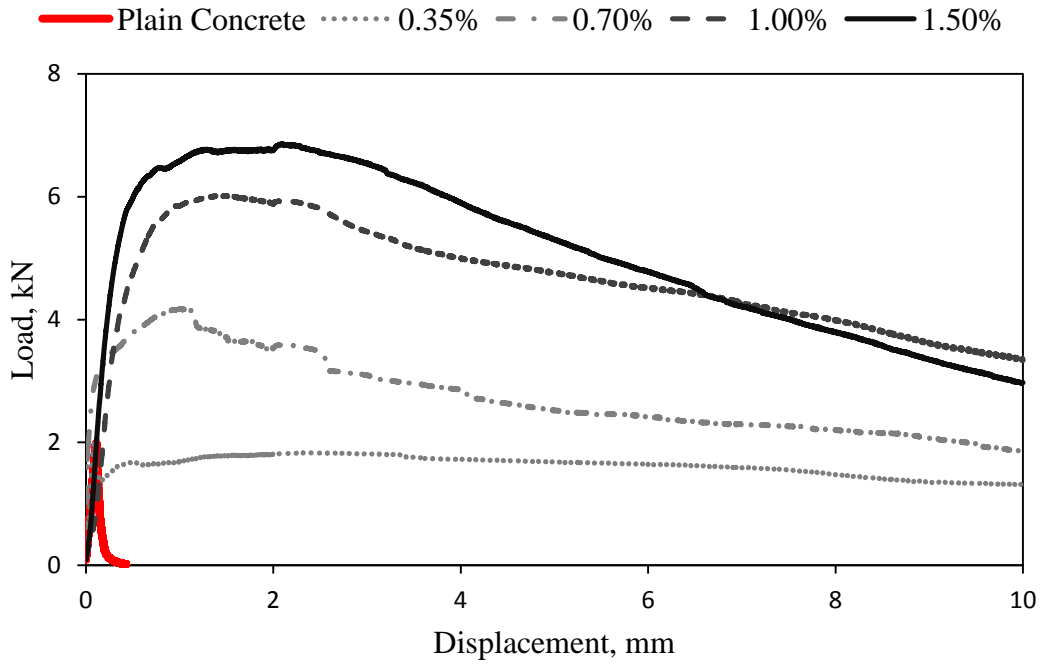
a)
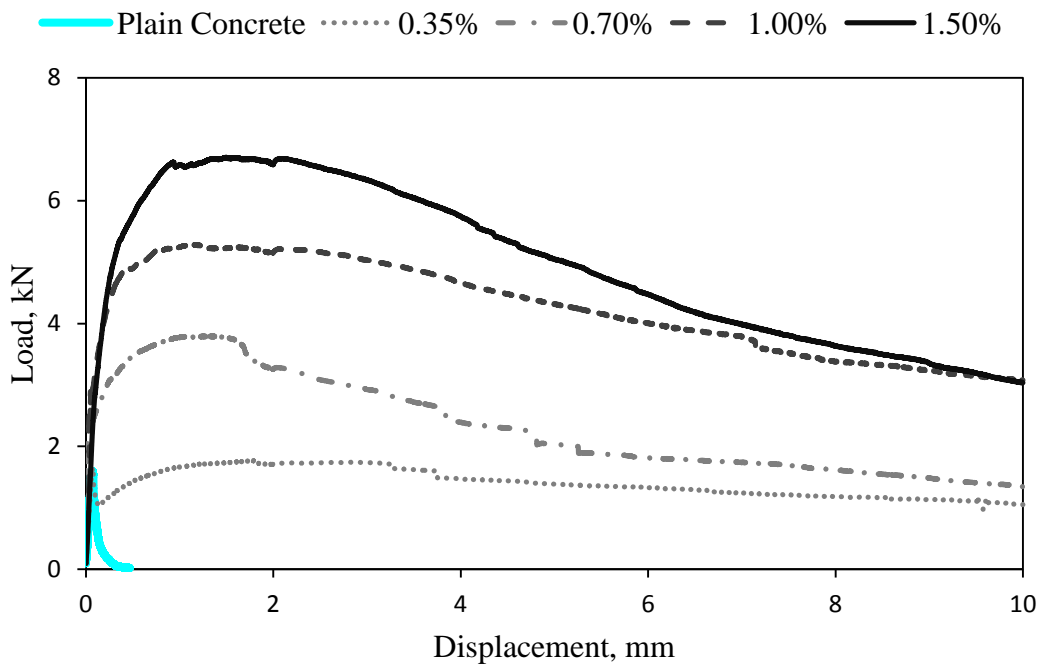
b)

Figure 4.12 Typical load versus displacement curves of L/d=65 with respect to steel fiber volume fraction: a) concretes containing 45% LWA and b) concretes containing 60% LWA
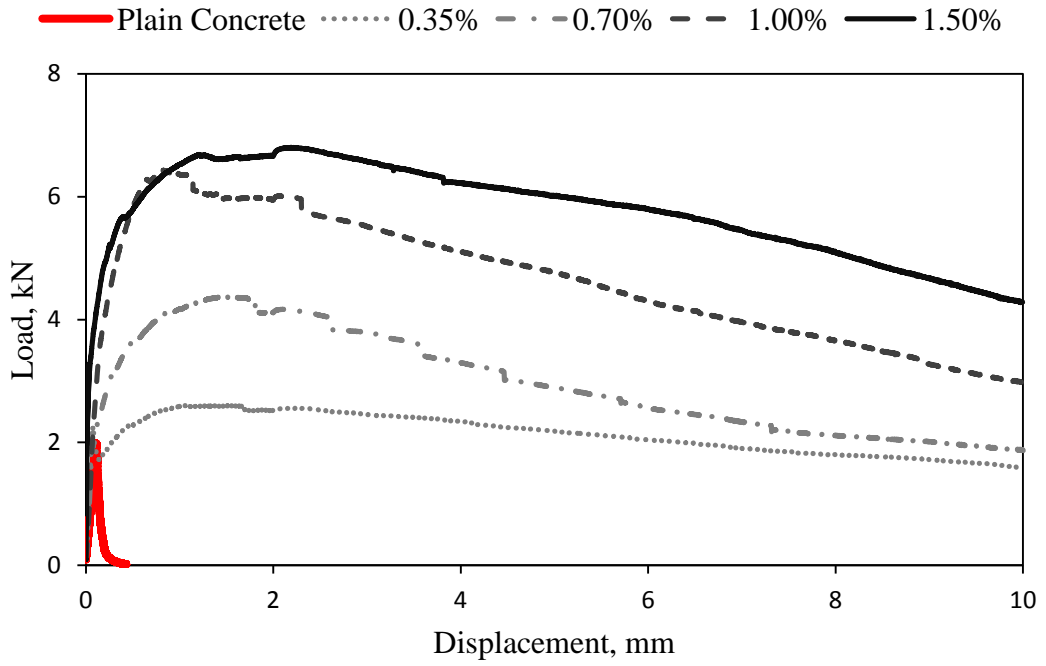
a)
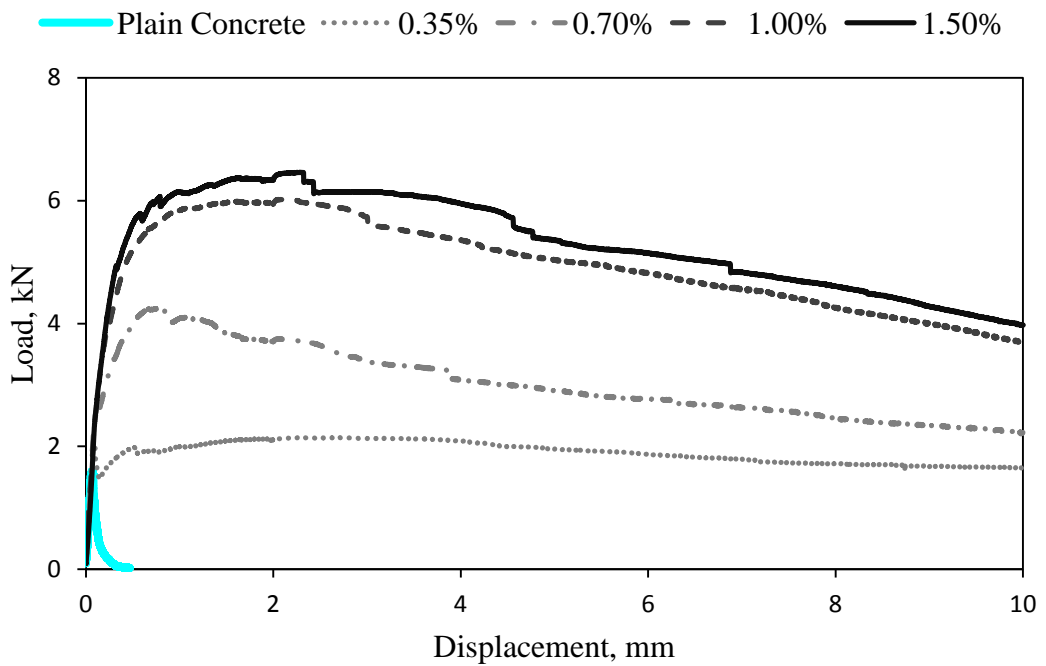
b)

Figure 4.13 Typical load versus displacement curves of L/d=80 with respect to steel
fiber volume fraction: a) concretes containing 45% LWA and b) concretes containing
60% LWA

4.5.2. Characteristic Length (l_{ch})

Characteristic length, which is the measure of brittleness, of concretes was evaluated with Equation 3.5 and they are presented in Table 4.1. The variations in characteristic length of LWACs with 45% and 60% cold bonded fly ash aggregate versus steel fiber volume fraction with different aspect ratio are indicated in Figure 4.14a-4.14b and Figure 4.15a-4.15b. The characteristic lengths of plain concrete of 45% and 60% LWA are 382 and 311 mm, respectively. Concrete with 60% LWA has the lower characteristic length than concrete with 45% LWA, it is due to the having the concrete with 45% LWA higher modulus of elasticity and fracture energy than concrete with 60%. Increasing the amount of normal weight coarse aggregate results in increasing the compressive strength, and this makes the concrete more brittle. Although increasing the amount of lightweight coarse aggregate cause decreasing the compressive strength, it does not make the concrete more ductile because of being the LWCAs weaker than matrix. When the LWAC amount is increased in concrete, the concrete will behave like a high strength concrete and this will cause brittle failing of concrete.

Utilization of steel fiber significantly increases the characteristic length of the concrete. As the steel fiber volume fraction increases, the characteristic length also increases. Increasing the steel fiber volume fraction from 0 (plain) to 1.5% in concrete with 45% LWA resulted in increasing the characteristic length for aspect of 55, 65, and 80 as much as 40, 36, and 46 times, respectively. This increasing rate in concrete with 60% LWA was 45, 43, and 51 times for aspect ratio of 55, 65, and 80, respectively.

As the result show, the enhancement of characteristic length of concrete with 60% LWA is more than improvement in concrete with 45% LWA. It is because of that the concrete including larger amount of artificial fly ash aggregate behave more brittle than the other. As a result, it can be concluded that the addition of steel fiber into quasi-brittle concrete transforms it to ductile material.

Table 4.6 Characteristic length of concretes

LWA volume fraction (V_a), %	Steel fiber aspect ratio (L/d)	Steel fiber volume fraction (V_f), %	Characteristic length (l_{ch}), mm	LWA volume fraction (V_a), %	Steel fiber aspect ratio (L/d)	Steel fiber volume fraction (V_f), %	Characteristic length (l_{ch}), mm
45	**-**	**-**	**382**	**60**	**-**	**-**	**311**
	55	0.35	10909		55	0.35	8766
	55	0.70	13636		55	0.70	12591
	55	1.00	14584		55	1.00	13342
	55	1.50	15215		55	1.50	13945
	65	0.35	10624		65	0.35	8683
	65	0.70	12742		65	0.70	11509
	65	1.00	13749		65	1.00	13282
	65	1.50	13849		65	1.50	13447
	80	0.35	12888		80	0.35	11524
	80	0.70	15209		80	0.70	14930
	80	1.00	16959		80	1.00	15750
	80	1.50	17777		80	1.50	16007
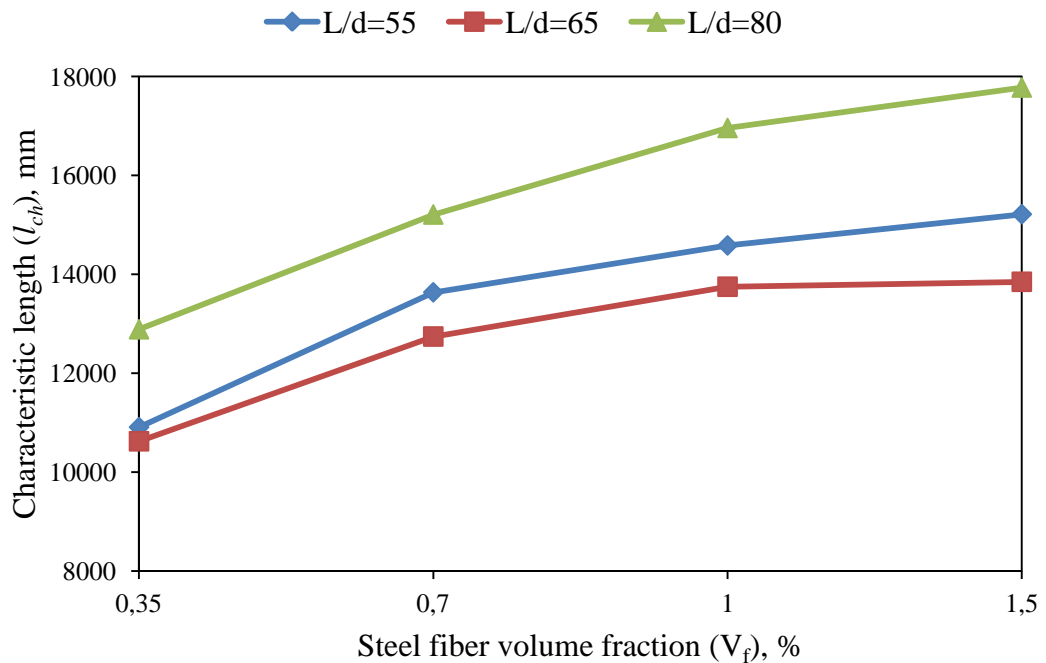
a)
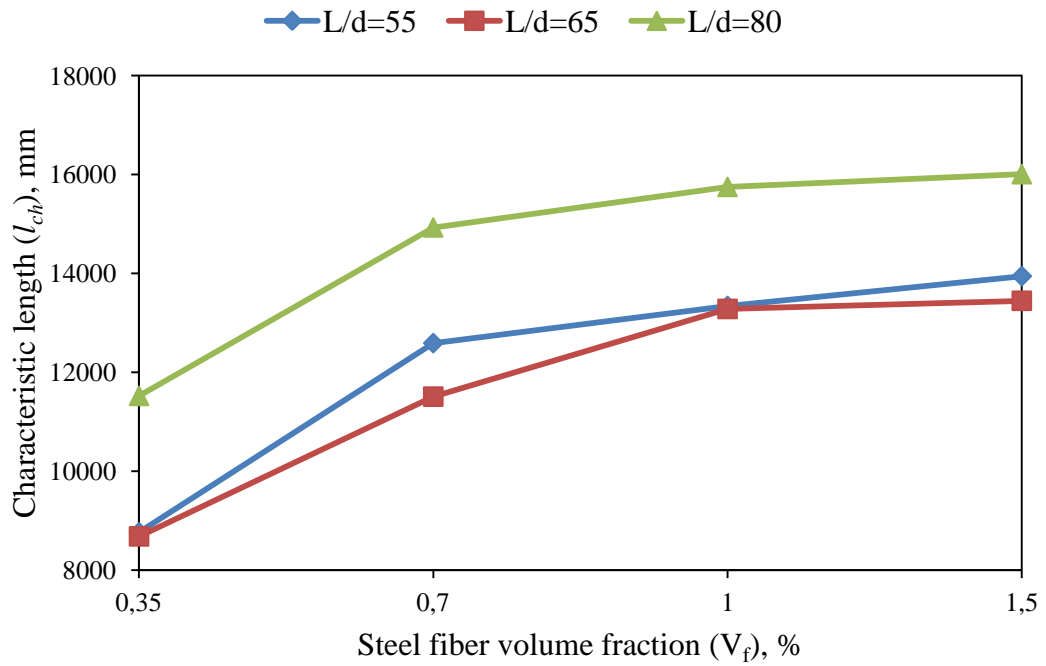
b)

Figure 4.14 Characteristic length versus steel fiber volume fraction with different aspect ratio: a) 45% LWA (In plain concrete, l_{ch}= 382 mm) and b) 60% LWA (In plain concrete, l_{ch}= 311 mm)
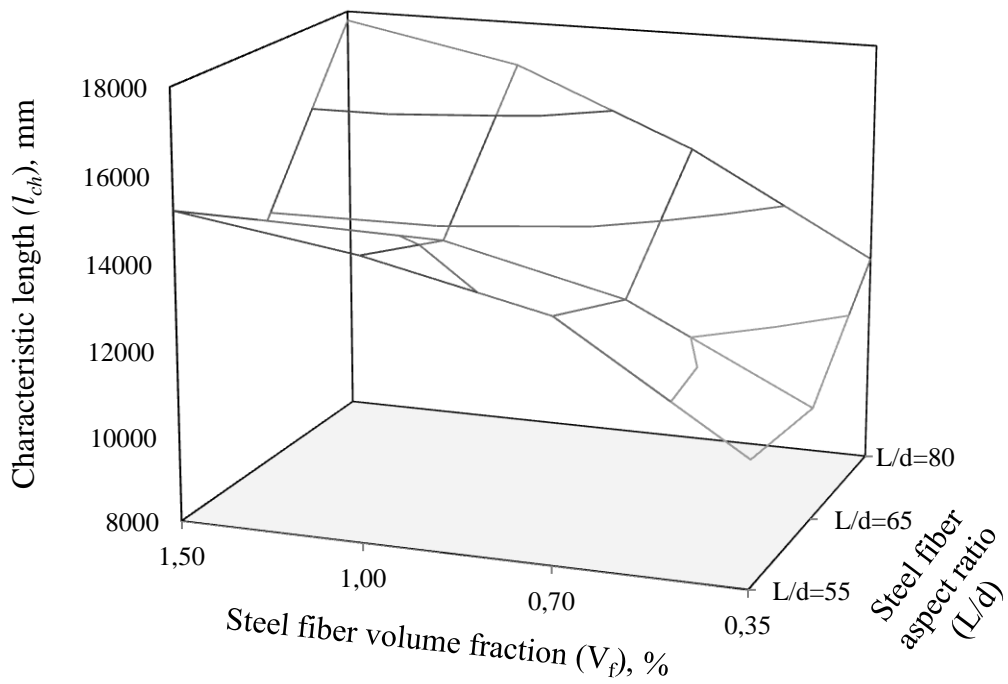
a)
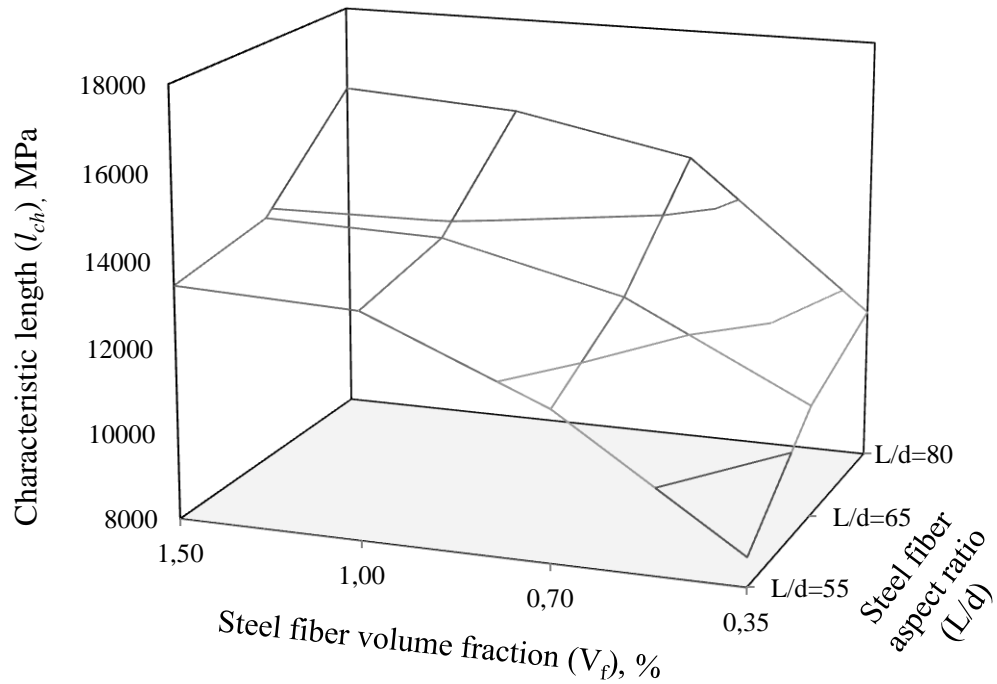
b)

Figure 4.15 Variation of l_{ch} with L/d and V_f: a) 45% LWA and b) 60% LWA

4.5.3. Ductility Ratio

In order to emphasize the increase in ductility by using steel fibers, the ductility ratio was calculated according to Equation 3.6. The variations in ductility ratio of LWACs with 45% and 60% cold bonded fly ash aggregate versus steel fiber volume fraction with different aspect ratio are given in Table 4.5 and indicated in Figure 4.16a-4.16b.

The increasing the steel fiber volume fraction significantly enhance the ductility of the concrete. Increasing the V_f of aspect ratio of 80 from 0 (plain) to 1.5% increased the ductility ratio by up to 256 and 281% for concrete with 45 and 60% LWA, respectively. These increasing rates with increasing the V_f were up to 230 and 266% for aspect ratio of 65, and 188 and 209% for aspect ratio for concrete with 45 and 60% LWA, respectively.
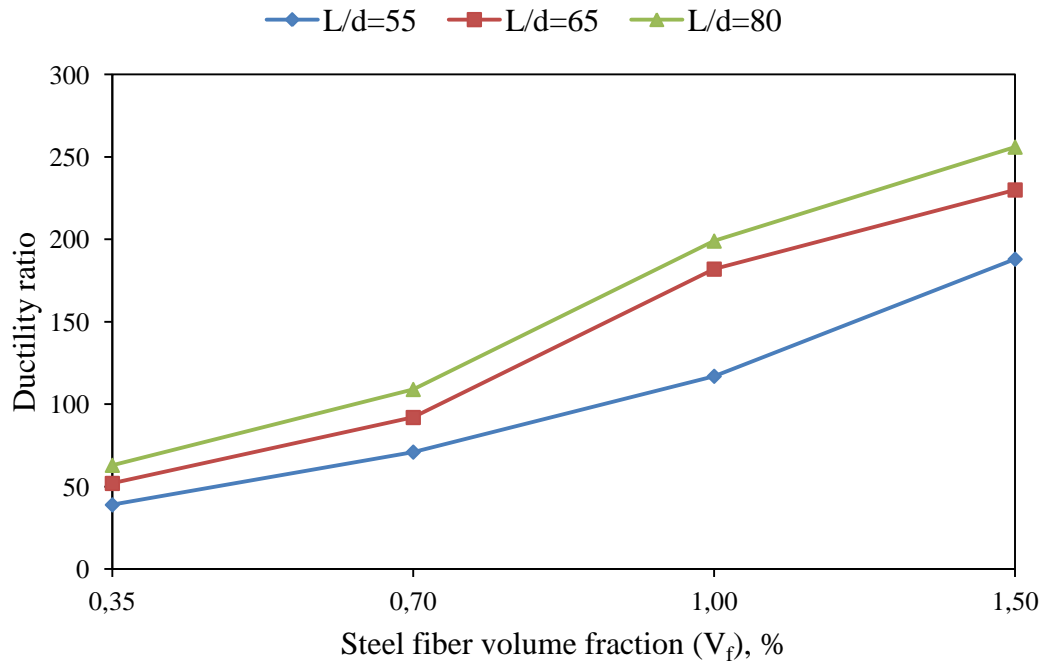
a)
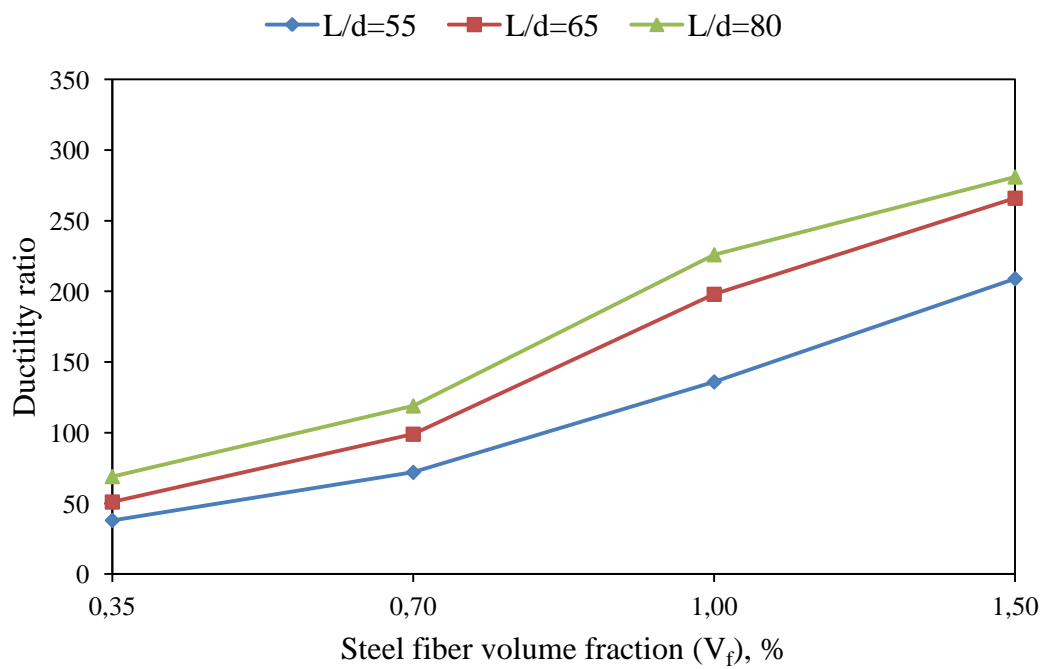
b)

Figure 4.16 Ductility ratio versus steel fiber volume fraction with different aspect ratio: a) 45% LWA and b) 60% LWA

4.6.　Bond Strength (τ)

The bond strength values were evaluated with the Equation 3.7 from cubic specimen including the Φ16-reinforcement bar subjected to tensile load. The variation in the bond strength of LWAC with 45% and 60% lightweight coarse aggregate versus steel fiber volume fraction with different aspect ratio are shown in Figure 4.18. The bond strengths of plain concrete of 45% and 60% LWA are 9.42 and 9.16 MPa, respectively.

There is decreasing of bond strength with increasing the LWA content and significantly increasing in the bond strength by utilization of steel fiber. Increasing the steel fiber volume fraction of aspect ratio of 55, 65, and 80 from 0 (plain) to 1.5% resulted in increasing the bond strength by up to 39, 42 and 43% for concrete with 45% LWA, respectively, while this rates for the same aspect ratios are by up to 40, 42, and 44% for concrete with 60% LWA.

Baran et al. (2012) concluded that steel fibers enhance the pull-out resistance of strands by controlling the crack growth inside concrete blocks. They stated that, by this way, the level of confinement at the strand-concrete interface was increased, which resulted in improvements in both friction and mechanical bond components of the resistance. Their results also indicated that more than 30% increase was achieved in pull-out strength due to fiber reinforcement. Gesoğlu et al. (2013) also concluded that addition of steel fiber and increasing the steel fiber volume fraction are increasing the bond strength significantly.

After the failure, the strand was separated from plain concrete and the concrete specimens were split while this situation does not occur when steel fiber was used in the concrete as shown in Figure 4.17.

Table 4.7 Bond strength of concretes

| LWA volume fraction (V_a), %	Steel fiber aspect ratio (L/d)	Steel fiber volume fraction (V_f), %	Bond strength (τ), MPa	LWA volume fraction (V_a), %	Steel fiber aspect ratio (L/d)	Steel fiber volume fraction (V_f), %	Bond strength (τ), MPa
45	**-**	**-**	**9.42**	**60**	**-**	**-**	**9.16**
	55	0.35	10.64		55	0.35	10.34
	55	0.70	12.92		55	0.70	11.78
	55	1.00	13.74		55	1.00	13.41
	55	1.50	15.48		55	1.50	15.36
	65	0.35	12.46		65	0.35	11.03
	65	0.70	14.33		65	0.70	12.31
	65	1.00	15.40		65	1.00	14.80
	65	1.50	16.13		65	1.50	15.89
	80	0.35	13.39		80	0.35	11.76
	80	0.70	14.92		80	0.70	14.14
	80	1.00	16.07		80	1.00	15.24
	80	1.50	16.52		80	1.50	16.36
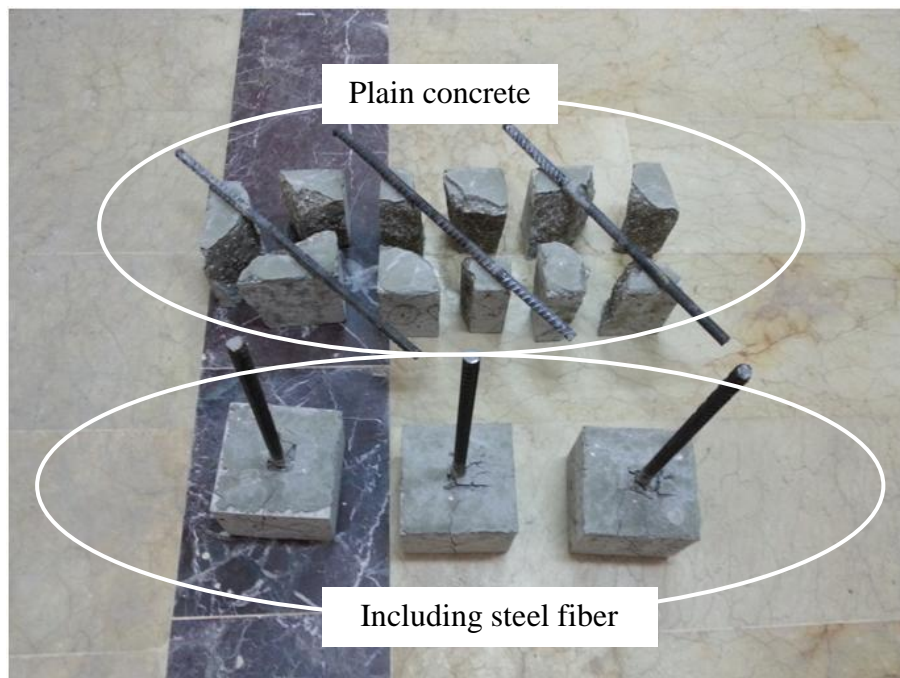
Figure 4.17 Typical failure patterns of concretes
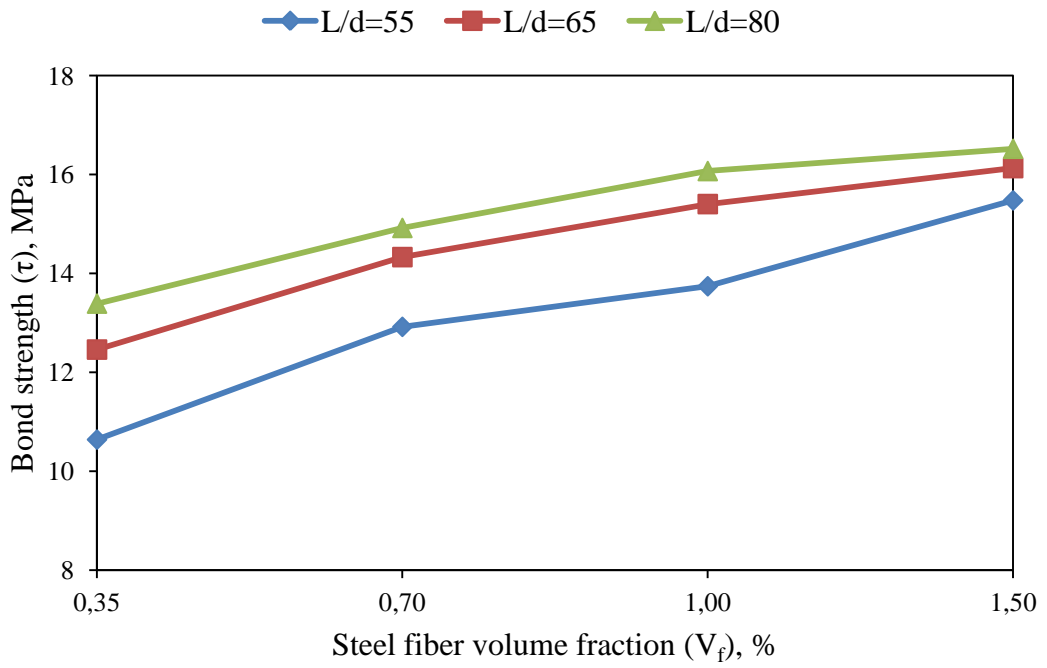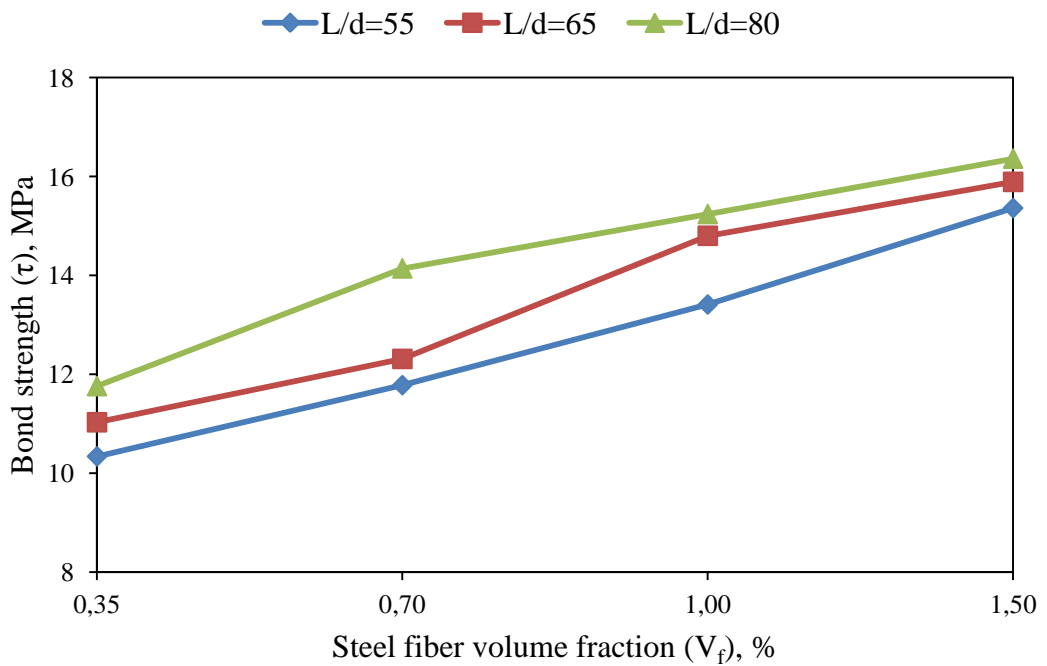
Figure 4.18 Bond strength versus steel fiber volume fraction with different aspect ratio: a) 45% LWA (In plain concrete, τ = 9.42 MPa) and b) 60% LWA (In plain concrete, τ = 9.16 MPa)
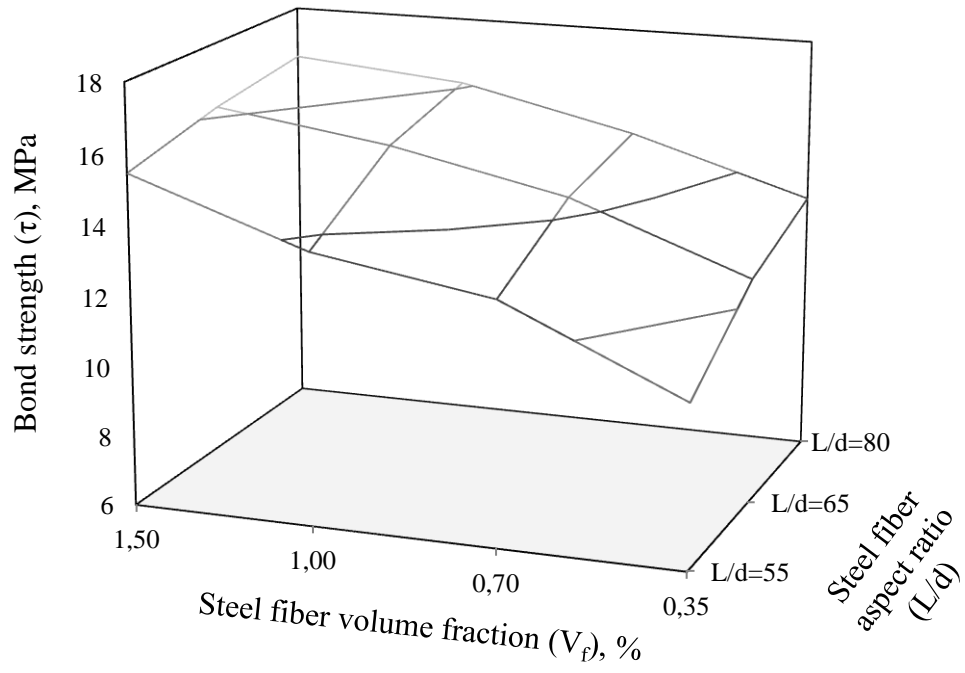
a)
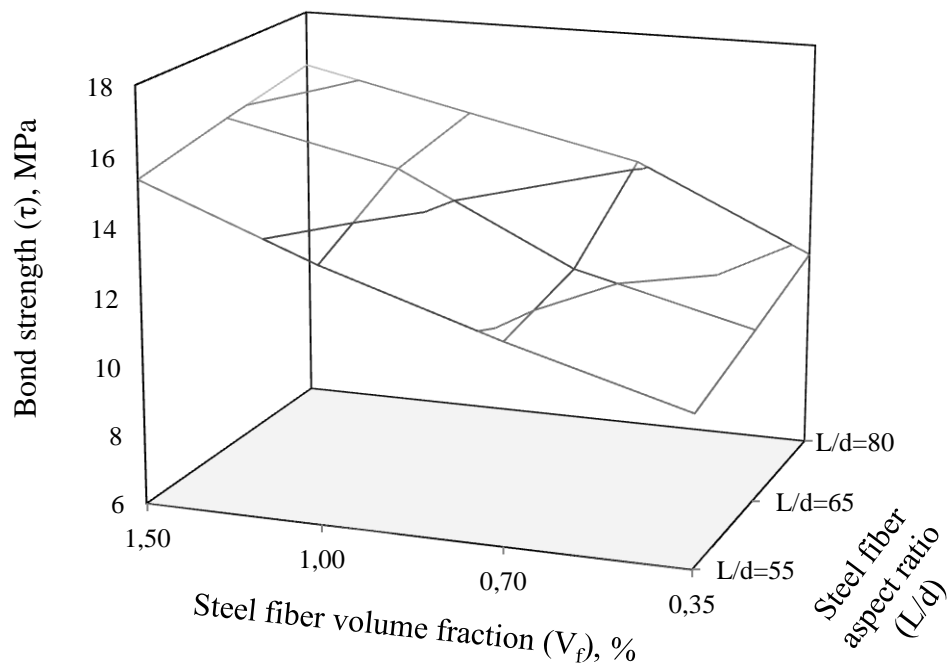
b)

Figure 4.19 Variation of τ with L/d and V_f: a) 45% LWA and b) 60% LWA

CHAPTER 5

5. CONCLUSIONS

Based on the experimental results presented above the following conclusions can be drawn.

- Concrete with compressive strength of approximately 40 MPa can be produced with the cold bonded lightweight fly ash aggregates.

- Decreasing the lightweight fly ash aggregate content from 60% to 45% enhanced the mechanical properties of concrete as well as fracture properties.

- While increasing the steel fiber volume fraction from 0% (plain) to 1.0% into LWAC resulted in increasing the compressive strength by up to almost 10% for concretes with 60% LWA, and by up to almost 5% in concretes with 45%, after 1% using resulted in slightly decreasing of compressive strength in both concrete series.

- The results indicated that the steel fiber usage did not affect the modulus of elasticity.

- Splitting tensile strength of LWAC can be increased by up to more than 50% by increasing the steel fiber volume fraction from 0% (plain) to 1.5%. The best results were obtained at the aspect ratio of 65 in all volume fractions. It may be due to being the cross-section of fiber with aspect ratio of 65 more than aspect ratio of 55 and 80.

- Flexural strength and ultimate load of LWAC subjected to three-point bending test was also increased significantly by increasing volume fraction of fiber from 0% (plain) to 1.5%. The best results for flexural strength and ultimate load were obtained at the aspect ratio of 80 in both concrete series of 45% and 60% LWA. The fiber with aspect ratio of 80 increased the flexural strength and the ultimate load by up to 71% in both concrete series, while this rate was 65% and 68% for aspect ratio of 55 and 65, respectively.

86

- The most efficient results for utilization of steel fiber were obtained in the fracture energy. The best fracture energy values were achieved with the aspect ratio of 80 for the same volume fraction of 55 and 65. It increased the fracture energy more than 250 and 280 times for concrete with 45% and 60% LWA, respectively.

- The characteristic length, which is a measure of ductility of the concrete, was increased significantly by the increasing the steel fiber volume fraction. While the significant improvement was achieved with addition of all steel fiber types, the best value for ductility was obtained with aspect ratio of 80. Moreover it can be inferred that the quasi-brittle concrete was transformed into a ductile composite with addition of steel fibers.

- Decreasing the lightweight fly ash aggregate content from 60% to 45% enhanced the bond between steel bar and concrete, so that increasing in the bond strength is observed. Steel fiber utilization significantly increased the bond strength. As steel fiber volume fraction increased, the bond strength also increased remarkably. The steel fiber with aspect ratio of 80 indicated the best bond strength value when compared with aspect ratio of 55 and 65.

REFERENCES

ACAA. Agreements on Conformity Assessment and Acceptance of Industrial Products. Production and Utilization of Coal Combustion Products (CCPs) in 2006 in Europe. http://www.acaa-usa.org/associations/8003/files/ECOBA_Stat_2006_EU15.pdf. 14/11/2012.

ACAA. Agreements on Conformity Assessment and Acceptance of Industrial Products. 2011 Coal Combustion Product (CCP) Production and Use in United States Survey Report http://www.acaa-usa.org/associations/8003/files/Final2011CCPSurvey.pdf. 14/11/2012.

ACI 544.1R. American Concrete Institute. 1996. State-of-the-art report on fiber reinforced concrete. Farmington Hills, Michigan, USA.

ACI Committee 213. American Concrete Institute. 1987 Guide for Structural Lightweight Aggregate Concrete, (ACI 213R-87). Farmington Hills, Michigan, USA.

ACI Committee 213R. American Concrete Institute. 2003. Guide for Structural Lightweight Aggregate Concrete. Manual of Concrete Practice.

ACI Committee 408. American Concrete Institute. 2003. Bond and development of straight reinforcing bars in tension (ACI408-03). Farmington Hilss, Minchigan, USA, 49 p.

Akçay, B., (2007). Effects of Lightweight Aggregates on Autogenous Deformation and Fracture of High Performance Concrete. PhD Thesis. Istanbul, Istanbul Technical University.

Alexander, M.G., Mindess, S., and Lie Qu. (1992). The Influence of Rock and Cement Types on Fracture Properties of the Interfacial Zone. In Interfaces in Cementitious Composites, Maso, J.C., ed., RILEM, Proceedings 18, Toulouse, E&FN Spon, pp. 129-138.

Altoubat, S.A., and Lange, D.A. (2001). Creep, Shrinkage, and Cracking of Restrained Concrete at Early Age. *ACI Materials Journal*. American Concrete Institute, Farmington Hills, Michigan. 323-331.

Altun, F. (2006). Experimental investigation of lightweight concrete with steel-fiber. *International Journal of Engineering Science*. **12(3)**,333-339.

ASTM C 618-08. American Society for Testing and Materials. 2000. Standard Specification for Coal Fly Ash and Raw or Calcined Natural Pozzolan for Use as a Mineral Admixture in Concrete. *Annual Book of ASTM Standard*. Vol. 04.02.

ASTM C127. American Society for Testing and Materials. 2007. Standard test method for specific gravity and absorption of coarse aggregate. *Annual Book of ASTM Standard*.

ASTM C39/C39M-12. American Society for Testing and Materials. 2012. Standard Test Method for Compressive Strength of Cylindrical Concrete Specimens. *Annual Book of ASTM Standard*. Philadelphia, Vol. 04-02, 7 pages.

ASTM C469/C469M−10. American Society for Testing and Materials. 2010. Standard Test Method for Static Modulus of Elasticity and Poisson's Ratio of Concrete in Compression. *Annual Book of ASTM Standard*. Vol. 04.02, 5 pages.

ASTM C496. American Society for Testing and Materials. 2011 Standard Test Method for Splitting Tensile Strength of Cylindrical Concrete Specimens. *Annual Book of ASTM Standard*. Philadelphia. Vol. 04-02, 5 pages.

ASTM. American Society for Testing and Materials. 2011. Standard Specification for Steel Fibers for Fiber-Reinforced Concrete. ASTM A820. http://enterprise1.astm.org/DOWNLOAD/A820.1181661-1.pdf.

Babbitt, C.W., Linder, A.S. (2005). A life cycle inventory of coal used for electricity production in Florida. *Journal of Cleaner Production.* **13**,903-912.

Balaguru, P., Narahari, R., Patel, M. (1992). Flexural toughness of steel fibre reinforced concrete. *ACI Materials Journal*. **89(6)**:541–546.

Balendran, R.V., Zhou, F.P., Nadeem, A., Leung, A.Y.T. (2002). Influence of steel fibers on strength and ductility of normal and lightweight high strength concrete. *Building and Environment*. **37**,1361-1367.

Baran, E., Akis, T., Yesilmen, S. (2012). Pull-out behavior of prestressing strands in steel fiber reinforced concrete. *Construction and Building Materials*. **28**,362-371.

Barenblatt, G.I. (1959). The formation of equilibrium cracks during brittle fracture. *Journal of Applied Mathematics and Mechanics*. **23**,622-636.

Baykal G., Döven A.G. (2000). Utilization of fly ash by pelletization process; theory, application areas and reseach results. *Resources, Conservation and Recycling*. **30**,59-77.

Baykal, G., Doven, A.G., 2000. Utilization of fly ash by pelletization process: theory, application areas and research results. Resources Conservation and Recycling. **30(1)**, 59–77.

Bayramov, F., Taşdemir, C., and Taşdemir, M.A. (2003). Optimisation of steel fibre reinforced concretes by means of statistical response surface method. *Cement and Concrete Compositess*. **26**,665-675.

Bayulke, N. (1998). Depreme Dayanıklı Betonarme ve Yığma Yapı Tasarımı". İnşaat Mühendisleri Odası İzmir Subesi, Yayın No=27, 245s.

Bažant, Z.P. (1984). Size Effect in Blunt Fracture- Concrete, Rock, Metal, *ASCE Engineering Mechanics*. **110**,518-535.

Bažant, Z.P. and Oh, B.H. (1983). Crack band theory for fracture of concrete, M*aterials and Structures.***16**,155-157.

Bilodeau, A., Kodur, V.K.R., Hoff, G.C. (2004). Optimization of the type and amount of polypropylene fibres for preventing the spalling of lightweight concrete subjected to hydrocarbon fire. Cement and Concrete Compositess. **26**,163-174.

Booya, E.A. (2012). Improving Fresh and Hardened Properties of Self Compacting Cold Bonded Fly Ash Lightweight Aggregate Concretes with Binary and Thernary Blends of Silica Fume and Fly Ash. MSc Thesis. Gaziantep, University of Gaziantep.

Bosfa. Dramix steel fiber seller. http://www.bosfa.com/docs/RC-80_60-BN_groen_GB.pdf. 16/12/2012.

Bremner, T.W., Thomas, M.D.A. (2004). Learning Module on Traditional and Nontraditional Uses of Coal Combustion Products (CCP). http://www.unb.ca/civil/bremner/CIRCA/TextofCourse/TextofCourse.doc. 18/12/2012

BS EN 12350-2. British Standards European Norms. 2009. Testing fresh concrete. Slump test. This replaces BS 1881: Part 102.

BS812, part 110. British Standards. 1990. Methods for determination of aggregate crushing value (ACV).

Büyüköztürk, O., Nilson, A.H., and Slate, F.O. (1971). Stress- Strain Responce and Fracture of a Concrete Model in Biaxial Loading. *ACI Journal*. **68(8)**,590-599.

Campione, G., Cucchiara, C., Mendola, L.L., Papia, M. (2005). Steel-concrete bond in lightweight fiber reinforced concrete under monotonic and cyclic actions. *Engineering Structure*. **105(5)**,553-561.

Campione, G., Miraglia, N., Papia, M. (2001). Mechanical properties of steel fiber reinforced lightweight concrete with pumice stone or expanded clay aggregates. *Materials and Structures*. **34**;201-210.

Chang, T.P., and Shieh, M.M. (1996). Fracture Properties of Lightweight Concrete. *Cement and Concrete Research*. **26(2)**,181-188.

Cheeseman, C.R., Makinde, A., Bethanis, S. (2005). Properties of lightweight aggregate produced by rapid sintering of incinerator bottom ash. *Resources, Conservation and Recycling*. **43(2)**,147-162.

Chen, B., Liu J. (2005). Contribution of hybrid fibers on the properties of the high strength lightweight concrete having good workability. *Cement and Concrete Research*. **35**,913-917.

Chen, B., Liu, J. (2004). Properties of lightweight expanded polystyrene concrete reinforced with steel fiber. *Cement and Concrete Research*. **34**,1259-1263.

Conley, J.E., Wilson, H., Kleinfelter, T.A. (1948). Production of lightweight concrete aggregates from clays, shales, slates and other materials. *Report of Investigation, 4401*. US Bureau of Mines, 121 pp.

Dahab, A.S. (1980). Les argiles expansibles: caracterisation mineralogique et chimique. Expansion statique: application a la culture sans sol. PhD thesis, Laboratoire Paleoge ographie-Substances utiles, ENSG, Nancy, 150 pp.

De' Gennaro, R., Cappelletti, P., Cerri, G., De' Gennaro, M., Dondi, M., Langella, A. (2004). Zeolitic tuffs as raw materials for lightweight aggregates. *Applied Clay Science*. **25(1–2)**,71–81.

Decleer, J., Viaene, W. (1993). Rupelian boom clay as raw material for expanded clay manufacturing. *Applied Clay Science.* **8**,111–128.

Domagala, L. (2011). Modification of properties of structural lightweight concrete with steel fibers. *Journal of Civil Engineering and Management*. **17(1)**,36-44.

Döven, A.G. (1996). Lightweight fly ash aggregate production using cold bonding agglomeration process. PhD Thesis. Istanbul, Boğaziçi University.

Duan, K., Hu, X.Z., Wittmann, F.H. (2003). Boundary effect on concrete fracture and non-constant fracture energy distribution. *Engineering Fracture Mechanics*. **70**, 2257-2268.

Dugdale, D.S. (1960). Yielding of steel sheets containing slits. *Journal of the Mechanics and Physics of Solids*. **8**,100-104.

Düzgün, O.A., Gül, R., Aydın, A.C. (2005). Effect of steel fibers on the mechanical properties of natural lightweight aggregate concrete. *Materials Letters*. **59**,3357-3363.

eHow. How to videos, articles and more. 2012. Uses of steel fiber reinforced concrete. http://www.ehow.com/about_5542383_uses-steel-fiber-reinforced-concrete.html#ixzz2FO8dVzEx. 28/11/2012.

Eligehausen, R., Popov, E.P., and Bertero, V.V. (1983). Local bond stress-slip relationships of deformed bars under generalized excitations. Report No. UCB/EERC-82/ 23, *Earthquake Engineering Research Center*, University of California at Berkeley. California 169 pp.

Gambhir, M.L. 1985. Concrete technology. 2nd Edition. New Delhi, India: TataMcGraw-Hill.

Gao, J., Suqa, W., Morino, K. (1997). Mechanical properties of steel fiber-reinforced, high strength, lightweight concrete. *Cement and Concrete Composites*. **19**,307-313.

Gesoğlu M., Güneyisi E., Öz H.Ö. (2012). Properties of lightweight aggregates produced with col-bonding pelletization of fly ash and ground granulated blast furnace slag. *Materials and Structures*. **45**,1535-1546.

Gesoğlu M., Özturan T., Güneyisi E., (2004). Shrinkage cracking of lightweight concrete made with cold-bonded fly ash aggregates. *Cement and Concrete Research*. **34**,1121-1130.

Gesoğlu, M, Güneyisi, E, Alzeebaree, R, Mermerdaş, K. (2013). Effect of silica fume and steel fiber on the mechanical properties of the concretes produced with cold bonded fly ash aggregates. *Construction and Building Materials*. **40**,982-990.

Gesoğlu, M. (2004). Effects of lightweight aggregate properties on mechanical, fracture, and physical behavior of lightweight concretes. PhD Thesis. Istanbul, Boğaziçi University.

Gikunoo, E. (2004). Effect of fly ash particles on the mechanical properties and microstructure of aluminium casting alloy A534. MSc Thesis. Saskatchewan, Canada, University of Saskatchewan, The College of Graduate Studies and Research.

Gonzalez-Corrochano, B., Alonso-Azcarate, J., Rodas, M. (2009). Production of lightweight aggregates from mining and industrial wastes. *Journal of Environmental Management*. **90**,2801-2812.

Gorhan, G., Kahraman, E., Başpınar, M.S., Demir, İ. (2009). Uçucu Kül Bölüm II: Kimyasal, mineralojik ve morfolojik özellikler. *Yapı Teknolojileri Elektronik Dergisi*. **5(2)**,33-42.

Goto, Y. (1971). Crack formed in concrete around deformed tension bars. *ACI Journal*. **68(4)**,244-251.

Griffith, A.A., (1920). The phenomena of rupture and flow in solids. *Philosophical Transactions of Royal Society of London*. **221**,163-198.

Güler, G., Güler, E., İpekoğlu, U., Mordoğan, H. (2005). Uçuçu küllerin özellikleri ve kullanım alanları. *Turkiye 19. Uluslar arası Madencilik Kongresi ve Fuarı*. 419-423, İzmir.

Güneyisi, E., Gesoğlu, M., Booya, E. (2012). Fresh properties of self-compacting cold bonded fly ash lightweight aggregate concrete with different mineral admixtures. *Materials and Structures*. **45**,1849-1859.

Harajli, M.H., Salloukh, K.A. (1997). Effect of fibers on development/splice strength of reinforcing bars in tension. *ACI Materials Journal.* **94(4),**317–324.

Hillerborg, A. (1985). Theoretical basis of method to determine fracture energy G_F of concrete. *Materials and Structures*. **18**:291296.

Hillerborg, A., Modeer, M. and Peterson, P.E. (1976). Analysis of crack formation and crack growth in concrete by means of fracture mechanics and finite elements. *Cement and Concrete Research*. **6**,773-782.

Hsu, T.T., Slate, F.O., Sturman, G.M., and Winter, G. (1963). Microcracking of plain concrete and the shape of the stress-strain curve. *ACI Journal*. **60(2)**,209-223.

Hu, X.Z., and Wittman, F.H. (2000). Size effect on toughness induced by crack close to free surface. *Engineering Fracture Mechanics*. **65**,209-211.

Irwin, G.R. (1957). Analysis of stresses and strains near the end of a crack transversing a plate. *Journal of Applied Mechanics*. **24**,361-364.

Jenq, Y. and Shah, S.P. (1985). Two parameter fracture model for concrete. *ASCE Journal of Engineering Mechanics*. **11**,1227-1241.

Joseph G., Ramamurthy K. (2009). Influence of fly ash on strength and sorption characteristics of cold-bonded fly ash aggregate concrete. *Construction and Building Materials*. **23**,1862-1870.

Kang, T.H.K., Kim, W., Kwak, Y.K., Hong, S.G. (2011). Shear testing of steel fiber-reinforced lightweight concrete beams without web reinforcement. *ACI Structural Journal*. **108(5)**,553-561.

Kaplan, M.E. (1961). Crack propagation and fracture of concrete. *Journal of American Concrete Institute*. **58**,591-610.

Karihaloo, B.L. 1995. Fracture mechanics and structural concrete. Essex, England: Longman Group Ltd.

Kayali, O., Haque, M.N., Zhu, B. (2003). Some characteristics of high strength fiber reinforced lightweight aggregate concrete. *Cement and Concrete Research*. **25(2)**,207-213

Ke, Y., Beaucour, A.L., Ortola, S., Dumontet, H., and Cabrillac, R. (2009). Influence of volume fraction and characteristics of lightweight aggregates on the mechanical properties of concrete. *Construction and Building Materials*. **23**,2821-2828.

Kim, Y., Kim, J.H., Lee, K.G., Kang, S.G. (2005). Recycling of dust wastes as lightweight aggregates. *Journal of Ceramic Processing Research*. **6(2)**,91–94.

Koçkal, N.U. (2008). Effects of lightweight fly ash aggregate properties on the performance of lightweight concretes. PhD Thesis. Istanbul, Boğaziçi University.

Koçkal, N.U., Özturan, T. (2010). Effects of lightweight fly ash aggregate properties on the behavior of lightweight concretes. *Journal of Journal of Hazardous Materials*. **179**,954-965.

Koçkal, N.U., Özturan, T. (2011). Durability of lightweight concretes with lightweight fly ash aggregates. *Construction and Building*. **25**:1430-1438.

Krstulovic-Opara, N., Watson, K.A., LaFave, J.M. (1994). Effect of increased tensile strength and toughness on reinforcing-bar bond behavior. *Cement and Concrete Composite*. **16(2)**,129–41.

Kumar, V., Sinha, A.K., Prasad, M.M. (2005). Static modulus of elasticity of steel fiber reinforced concrete. In: Proceedings of the international conference on cement combinations for durable concrete, Dundee, Scotland, UK, p.527-36.

Kurt, G. (2006). Lif içeriği ve su/çimento oranının fibrobetonun mekanik davranışına etkileri. MSc Thesis. Istanbul, Istanbul Technical University.

Kurugöl, F., Altun, F., Yiğit, I., Şahin, Y. (2008). Combined effect of silica fume and steel fiber on the mechanical properties of high strength concretes. Construction and Building Materials. **22**,1874-1880.

Kütahya Cement. http://www.kutahyacimento.com/. 01.12.2012.

Kütahya Cement. http://www.kutahyacimento.com/images/pulverize-resimleri/class-f-fly-ash-1-600.jpg. 01.12.2012.

Lee, K.M., and Büyüköztürk, O. (1995). Fracture toughness of mortar-aggregate interface in high strength conctrete. *ACI Materials Journal*. **92(6)**:634-642.

Lee, K.M., Büyüköztürk, O., and Oumera, A. (1992). Fracture Analysis of Mortar-Aggregate Interfaces in Concrete. *ASCE Journal of Engineering Mechanics*. **118(10)**,2031-2047.

Li, Y., Wu, D., Zhang, J, Dhang, L., Wu, D., Fang, Z., et al. (2000). Measurement and statistics of single pellet mechanical strength of differently shaped catalysts. *Powder Technology*. **113(1-2)**,176-84.

Libre, N.A., Shekarchi, M., Mahoutian, M., Soroushian, P. (2011). Mechanical properties of hybrid fiber reinforced lightweight aggregate concrete made with natural pumice. *Construction and Building Materials*. **25(5)**,2458-2464.

Mahmood,, S.F. (2012). Use of cold-bonded blast furnace slag aggregate in the production of self compacting concretes. MSc thesis. Gaziantep, University of Gaziantep.

Mangialardi T. (2001). Sintering of msw fly ash for reuse as a concrete aggregate. *Journal of Hazardous Materials*. **B87**,225-39.

Matsunaga, T., Kim, J.K., Hardcastle, S., Rohatgi, P.K. (2001). Crystallinity and selected properties of fly ash particles. *Materials Science and Engineering*. 333-343.

Matsunaga, T., Kim, J.K., Hardcastle, S., Rohatgi, P.K. (2002). Crystallinity and selected properties of fly ash particles. *Materials Science and Engineering*. 333-343.

Mayfield, B., and Loutai, M. (1990). Properties of pelletized blast furnace slag concrete. *Magazine of Concrete Research*. **150**:29-36.

Mehta, P.K., Monteiro, P.J.M. (2006). Concrete; microstructure, properties, and materials. 3rd edition. New York: McGraw-Hill.

Mindess, S. and Diamond, S. (1982). The cracking and fracture of mortar. *Materials and Structures*. **15**,107-113.

Mor, A. (1992). Steel-concrete bond in high-strength lightweight concrete. *ACI Materials Journal*. 76-82.

MWM. Metal Wire Mesh. http://www.metalmesh.com.cn/news/Do-steel-fibers-affect-the-slump-of-concrete--9.html. 01/12/2012.

Naaman, A.E. (1985). Fibre reinforcement for concretes. *Concrete International, Design and Construction*. **7(3)**,21-25.

Nallathambi, P., and Karihaloo, B.L. (1990). Fracture of concrete: Application of effective crack model. *in 9th International Conference on Experimental Mechanics,* Volume. 4, *Lyngby,* Denmark, 20-24 August, 1413-1422.

Nanni, A. (1998). Splitting-tension test for fiber reinforced concrete. *ACI Material Journal*. **85(4)**,229-233.

Pandey, V.C., Singh, J.S., Singh, R.P., Singh, N., and Yunus M. (2011). Arsenic hazards in coal fly ash and its fate in Indian scenario. *Resources, Conservation and Recycling*. **55**,819-835.

Pietsch W. 1991. Size enlargement by agglomeration. New York: John Wiley and Sons.

Pillai, S.U., Kirk, D.W. 1983. Reinforced concrete design in Canada. 2nd Edition. Canada: McGraw-Hill.

Popovics, S. 1992. Concrete Materials: properties, specifications and testing. 2nd Edition. New Jersey, USA: Park Ridge, Noyes Publications.

Ramachandran, V.S. (1981). Waste and by products as concrete aggregates. Canadian Building Digest CBD-215, National Reseach Council Canada.

Ramadan, K.Z. (1995). Composite and aggregate production using high calciym fly ash. PhD thesis. Istanbul, Boğaziçi University.

RILEM 50-FMC. (1985). Committee of fracture mechanics of concrete. Determination of fracture energy of mortar and concrete by means of three-point bend tests on notched beams. *Materials and Structures*. **18(106)**,285–290.

RILEM RC6. (1996). Recommendations for the testing and use of constructions materials bond test for reinforcement steel. 2. Pull-out test, 3 pages.

Riley, C.M. (1951). Relation of chemical properties to the bloating of clays. *Journal of the American Ceramic Society*. **34**,121–128.

Robins, P.J., and Austin, S.A. (1986). Bond of lightweight aggregate concrete incorporating condensed silica fume, fly ash, silica fume, slag and natural pozzolans. ACI SP-91: 941-958.

Rreil, A., (2007). Fatigue bond behaviour of corroded reinforcement a CFRP confined concrete. PhD thesis. Canada, University of Waterloo.

Satapathy, L.N. (2000). A study on the mechanical, abrasion and microstructural properties of zirconia-fly ash material. *Ceramics International*. **26**,39-45.

Shafigh, P., Mahmud, H., Jumaat, M.Z. (2011). Effect of steel fiber on the mechanical properties pf oil palm shell lightweight concrete. Materials and Design. **28**,95-100.

Shah, S.P., and Winter, G. (1966). Inelastic behavior and fracture of concrete, in causes, mechanism, and control of cracking in concrete. ACI SP-20.

Shah, S.P., Naaman, A.E. (1976). Mechanical properties of glass and steel fibre reinfoced mortar. *ACI Journal*. **73(1)**,50-53.

Shah, S.P., Swartz, S.E., and Ouyang, C. (1995). Fracture mechanics of concrete: applications of fracture mechanics to concrete, rock, and other quasi-brittle materials. John Wiley & Sons, Inc., New York.

Soco, E., Kalembkiewicz, J. (2007). Investigations of sequential leaching behavior of Cu and Zn from coal fly ash and their mobility in environmental conditions. *Journal of Hazardaous Materials*. **145,**482-487.

Taşdemir, C., and Taşdemir, M.A. (1996). Effects of silica fume and aggregate size on the brittleness of concrete. *Cement and Concrete Research*. **26(1)**,63-68.

Taşdemir, C., Taşdemir, M.A., Mills, N., Barr, B.I.G., and Lydon, F.D. (1999). Combined effects of silica fume, aggregate type, and size on post peak responce of concrete in bending. *ACI Materials Journal*. **96(1)**,74-83.

Taşdemir, M.A. and Karihaloo, B.L. (2001). Effect of aggregate volume fraction on the parameters of concrete: A meso-mechanical approach. *Magazine of Concrete Research*. **53**,405-415.

Taşdemir, M.A., Bayramov, F., Ilki, A. ve Yerlikaya, M. (2002). Prefabrik elemanlar icin celik tel donatılı betonlar. *Beton Prefabrikasyon*. **63**,5-12.

Taşdemir, M.A., Lydon F.D., Barr B.I.G. (1996). The tensile strain capacity of concrete. *Magazine of Concrete Research*. **48**,211-218.

Taşdemir, M.A., Taşdemir, C., Akyüz, S., Jefferson, A.D., Lydon, F.D.,and Barr, B.I.G. (1998). Evaluation of strains at peak stresses in concrete: A three phase composite model approach. *Cement and Concrete Composites*. **20**,301-318.

Trende, U., and Büyüköztürk, O. (1998). Size effect and influence of aggregate roughness in interface fracture of concrete composites. *ACI Materials Journal*. **95(4)**,331-338.

Tsai, C.T. Li, L.S., Chang, C.C., Hwang, C.L. (2009). Durability design consideration and application of steel fiber reinforced concrete in Taiwan. *Arab Journal of Science and Engineering*. **34(1B)**,57-79.

Türker, P., Erdoğan, B., Katnas, F., Yeğinobali, A. (2003). Türkiyede uçucu Küllerin sınıflandırılması ve özellikleri. TÇMB, Ankara.

Turkish Standard TS EN 197-1. (2002). Çimento-bölüm 1: genel cimentolar-bilesim, ozellikler ve uygunluk kriterleri.

UM, The University of Memphis.
http://www.ce.memphis.edu/1101/notes/concrete/PCA_manual/Chap03.pdf.
12/12/2012.

UM, The University of Memphis.
http://www.ce.memphis.edu/1101/notes/concrete/PCA_manual/Chap07.pdf.
12/12/2012.

Videla, C., Martinez, P. 2002. Physical, mechanical and microscopic characterization of cold bonded fly ash lightweight aggregates. *Materiales de Construccion*. **52(268)**, 5–18.

Wafa, F.F., Ashour, S.A. (1992). Mechanical properties of high-strength fibre reinforced concrete. *ACI Materials Journal*. **89(5)**,449–455.
Wang, S., and Wu, H. (2006). Enviromental-benign utilization of fly ash as low-cost adosrbents. *Journal of Hazardous Materials*. **136(3)**,482-501.

Wang, Y., Li, V.C., Backer, S. (1990). Experimental determination of tensile behavior of fiber reinforced concrete. *ACI Materials Journal*. **87(5)**,461-468.

Warner, R.F., Rangam, B.V., Hall, A.S., Faulkes, K.A. (1998). Concrete structures, Longman, Australia. *The Open Civil Engineering Journal*. **2**,143-147.

Wasserman, R., Bentur, A. (1997). Effect of lightweight fly ash aggregate microstructure on the strength of concrete. *Cement and Concrete Research*. **27(4)**,525–537.

Weiler, B., Grosse, C. (2010). Pullout behaviour of fibers in steel fiber reinforced concrete. MSc thesis. Malaysia, Universiti Technologi Malaysia.

Xu, A. (1997). Fly ash in concrete, Part-3, waste materials used in concrete manufacturing. Editor: Satish Chandra, Sweden.

Yashima, S., Kanda, Y., Sano, S. (1987). Relationship between particle size and fracture energy or impact velocity required to fracture as estimated from single particle crushing. *Powder Technology*. **51(3)**,227-282.

Yazıcı, H. (2004). Termik santral atığı yapay alçı-uçucu kül-taban külü esaslı yapı malzemesi geliştirilmesi. PhD Thesis. İzmir, Dokuz Eylul Universitesi.

Zhang, M.H., and Gjory, O.E. (1990). Microstucture of the interfacial zone between lightweight aggregate and cement paste. *Cement and Concrete Research*. **20**,610-618.

Zhang, M.H., and Gjory, O.E. (1991). Mechanical properties of high-strength lightweight concrete. *ACI Materials Journal*. **88(3)**,240-247.